AD NUMBER

AD883480

LIMITATION CHANGES

TO:

Approved for public release; distribution is unlimited.

FROM:

**Distribution authorized to U.S. Gov't. agencies and their contractors;
Administrative/Operational Use; 04 JAN 1971.
Other requests shall be referred to Air Force Rocket Propulsion Lab., Edwards AFB, CA.**

AUTHORITY

AFRPL ltr 20 Dec 1971

UNCLASSIFIED

LIMITED

REPORTS

AFRPL-TR-71-18

(2)

CB

STUDY OF MATERIALS FOR HIGH PRESSURE NOZZLES

Volume III - Property Determination of Castable Carbon and Graphite Fiber-Reinforced Pyrolytic Graphite Composite

by
S.G. Bapat, Southern Research Institute
E.L. Olcott, Atlantic Research

FINAL REPORT

Contract F04611-69-C-0070

Atlantic Research
A Division of The Susquehanna Corporation
Alexandria, Virginia 22314

January 4, 1971

161

NOTICES

When U. S. Government drawings, specifications, or other data are used for any purpose other than a definitely related Government procurement operation, the Government thereby incurs no responsibility nor any obligation whatsoever, and the fact that the Government may have formulated, furnished, or in any way supplied the said drawings, specifications, or other data, is not to be regarded by implication or otherwise, or in any manner licensing the holder or any other person or corporation, or conveying any rights or permission to manufacture, use, or sell any patented invention that may in any way be related thereto.

UNCLASSIFIED
Security Classification

DOCUMENT CONTROL DATA - R&D
(Security classification of title, body of abstract and indexing annotation must be entered when the overall report is classified)

1. ORIGINATING ACTIVITY (Corporate author) Atlantic Research A Division of The Susquehanna Corporation Alexandria, Virginia	2a. REPORT SECURITY CLASSIFICATION UNCLASSIFIED 2b. GROUP

3. REPORT TITLE

PROPERTY DETERMINATION OF CASTABLE CARBON AND GRAPHITE FIBER REINFORCED PYROLYTIC GRAPHITE COMPOSITE

4. DESCRIPTIVE NOTES (Type of report and inclusive dates)

Final Report

5. AUTHOR(S) (Last name, first name, initial)

Bapat, S. G., Southern Research Institute
Olcott, E. L., Atlantic Research

6. REPORT DATE	7a. TOTAL NO. OF PAGES	7b. NO. OF REFS
January 8, 1971	149	8

8a. CONTRACT OR GRANT NO.	9a. ORIGINATOR'S REPORT NUMBER(S)
F04611-69-C-0070 b. PROJECT NO.	AFRPL-TR-71-18
c.	9b. OTHER REPORT NO(S) (Any other numbers that may be assigned this report) TR-PL-10025-3
d.	

10. AVAILABILITY/LIMITATION NOTICES

This document is subject to special export controls and each transmittal to foreign governments or foreign nationals may be made only with prior approval of AFRPL (RPORSTINFO), Edwards, California 93523.

11. SUPPLEMENTARY NOTES	12. SPONSORING MILITARY ACTIVITY
	Air Force Rocket Propulsion Laboratory Edwards, California 93523

13. ABSTRACT The thermal conductivity and specific heat of castable carbon (ablative material) and carbon fiber reinforced pyrolytic graphite composite sleeves were determined. Measurements above ambient on castable carbon were conducted on precharred material. Thermal expansion measurements also were made on castable carbon precharred at 4000°F.

The castable carbon virgin material had a low conductivity of about 12 Btu in./hr ft^2°F, the 1500°F prechar had about the same value up to 1500°F and the 4000°F prechar had a value six to ten times higher. The castable carbon in an isotropic material and these values are intermediate between the conductivities in the two directions for molded carbon-phenolic ablatives.

The conductivity values of fibrous PG in the "a-b" direction are lower by a factor of about 7, than the conductivity values of "normal" PG tile, or plate, in the "a-b" direction. The conductivity values of fibrous PG in the "c" direction are of the same order of those found for PG tile in the "c" direction. Thus, the anisotropy ratio (ratio at about 150°F of thermal conductivity in the "a-b" direction to that in the "c" direction) for fibrous PG composite is of the order of 20 compared to about 150 for PG plate.

The thermal expansion data indicated that the castable carbon material is stable up to the precharring temperature. The thermal expansion data fall in between with and across grain expansion values for ATJ-S graphite.

The heat capacity values for castable carbon and fibrous PG composite are about 10 percent higher than the values for polygraphites.

DD FORM 1 JAN 64 1473

UNCLASSIFIED
Security Classification

UNCLASSIFIED

Security Classification

14. KEY WORDS	LINK A		LINK B		LINK C	
	ROLE	WT	ROLE	WT	ROLE	WT
Thermal Property Measurements Ablatives Pyrolytic Graphite Composites						

INSTRUCTIONS

1. **ORIGINATING ACTIVITY:** Enter the name and address of the contractor, subcontractor, grantee, Department of Defense activity or other organization *(corporate author)* issuing the report.

2a. **REPORT SECURITY CLASSIFICATION:** Enter the overall security classification of the report. Indicate whether "Restricted Data" is included. Marking is to be in accordance with appropriate security regulations.

2b. **GROUP:** Automatic downgrading is specified in DoD Directive 5200.10 and Armed Forces Industrial Manual. Enter the group number. Also, when applicable, show that optional markings have been used for Group 3 and Group 4 as authorized.

3. **REPORT TITLE:** Enter the complete report title in all capital letters. Titles in all cases should be unclassified. If a meaningful title cannot be selected without classification, show title classification in all capitals in parenthesis immediately following the title.

4. **DESCRIPTIVE NOTES:** If appropriate, enter the type of report, e.g., interim, progress, summary, annual, or final. Give the inclusive dates when a specific reporting period is covered.

5. **AUTHOR(S):** Enter the name(s) of author(s) as shown on or in the report. Enter last name, first name, middle initial. If military, show rank and branch of service. The name of the principal author is an absolute minimum requirement.

6. **REPORT DATE:** Enter the date of the report as day, month, year; or month, year. If more than one date appears on the report, use date of publication.

7a. **TOTAL NUMBER OF PAGES:** The total page count should follow normal pagination procedures, i.e., enter the number of pages containing information.

7b. **NUMBER OF REFERENCES:** Enter the total number of references cited in the report.

8a. **CONTRACT OR GRANT NUMBER:** If appropriate, enter the applicable number of the contract or grant under which the report was written.

8b, 8c, & 8d. **PROJECT NUMBER:** Enter the appropriate military department identification, such as project number, subproject number, system numbers, task number, etc.

9a. **ORIGINATOR'S REPORT NUMBER(S):** Enter the official report number by which the document will be identified and controlled by the originating activity. This number must be unique to this report.

9b. **OTHER REPORT NUMBER(S):** If the report has been assigned any other report numbers *(either by the originator or by the sponsor)*, also enter this number(s).

10. **AVAILABILITY/LIMITATION NOTICES:** Enter any limitations on further dissemination of the report, other than those imposed by security classification, using standard statements such as:

(1) "Qualified requesters may obtain copies of this report from DDC."

(2) "Foreign announcement and dissemination of this report by DDC is not authorized."

(3) "U. S. Government agencies may obtain copies of this report directly from DDC. Other qualified DDC users shall request through

_____."

(4) "U. S. military agencies may obtain copies of this report directly from DDC. Other qualified users shall request through

_____."

(5) "All distribution of this report is controlled. Qualified DDC users shall request through

_____."

If the report has been furnished to the Office of Technical Services, Department of Commerce, for sale to the public, indicate this fact and enter the price, if known.

11. **SUPPLEMENTARY NOTES:** Use for additional explanatory notes.

12. **SPONSORING MILITARY ACTIVITY:** Enter the name of the departmental project office or laboratory sponsoring *(paying for)* the research and development. Include address.

13. **ABSTRACT:** Enter an abstract giving a brief and factual summary of the document indicative of the report, even though it may also appear elsewhere in the body of the technical report. If additional space is required, a continuation sheet shall be attached.

It is highly desirable that the abstract of classified reports be unclassified. Each paragraph of the abstract shall end with an indication of the military security classification of the information in the paragraph, represented as *(TS)*, *(S)*, *(C)* or *(U)*.

There is no limitation on the length of the abstract. However, the suggested length is from 150 to 225 words.

14. **KEY WORDS:** Key words are technically meaningful terms or short phrases that characterize a report and may be used as index entries for cataloging the report. Key words must be selected so that no security classification is required. Identifiers, such as equipment model designation, trade name, military project code name, geographic location, may be used as key words but will be followed by an indication of technical context. The assignment of links, rules, and weights is optional.

Security Classification

AFRPL-TR-71-18

STUDY OF MATERIALS FOR HIGH PRESSURE NOZZLES

Volume III - Property Determination of Castable Carbon and Graphite Fiber-Reinforced Pyrolytic Graphite Composite

by

S.G. Bapat, Southern Research Institute

E.L. Olcott, Atlantic Research

FINAL REPORT

Contract FO4611-69-C-0070

FOREWORD

This report was jointly prepared by Southern Research Institute and Atlantic Research to document work performed under Air Force Contract F04611-69-C-0070. The work under this contract is presented in a series of three volumes which cover the technical work (Volume I), the nondestructive testing (Volume II), and the materials characterization which is in this Volume III. The work described in Volume III was conducted under Subcontract No. P03583 over the period of July 24, 1970, to December 31, 1970. The prime contract was administered under the direction of the Air Force Rocket Propulsion Laboratory, Edwards, California, with Captain John Ellison as the Project Officer. This report was submitted 4 January 1970.

Mr. Eugene Olcott served as the Project Director of the prime contract. Mr. S.G. Bapat conducted the experimental work at Southern Research. The helpful suggestions and guidance of Mr. C.D. Pears of Southern Research Institute are acknowledged.

This technical report has been reviewed and is approved.

CHARLES R. COOKE
Chief, Solid Rocket Division

ABSTRACT

The thermal conductivity and specific heat of castable carbon (ablative material) and carbon fiber reinforced pyrolytic graphite composite sleeves were determined. Measurements above ambient on castable carbon were conducted on precharred material. Thermal expansion measurements also were made on castable carbon precharred at 4000°F.

The castable carbon virgin material had a low conductivity of about 12 Btu in./hr ft^2 °F, the 1500°F prechar had about the same value up to 1500°F and the 4000°F prechar had a value six to ten times higher. The castable carbon is an isotropic material and these values are intermediate between the conductivities in the two directions for molded carbon-phenolic ablatives.

The conductivity values of fibrous PG in the ''a-b'' direction are lower by a factor of about 7, than the conductivity values of ''normal'' PG tile, or plate, in the ''a-b'' direction. This probably results from the combination of circumferential layers of carbon fibers and PG infiltration in between. The conductivity values of fibrous PG in the ''c'' direction are of the same order of those found for PG tile in the ''c'' direction. Thus, the anisotropy ratio (ratio at about 150°F of thermal conductivity in the ''a-b'' direction to that in the ''c'' direction) for fibre reinforced PG is of the order of 20 compared to about 150 for PG tile.

The thermal expansion data indicated that the castable carbon material is stable up to the precharring temperature. The thermal expansion data fall in between with and across grain expansion values for ATJ-S graphite.

The heat capacity values for castable carbon and fibrous PG sleeve are about 10 percent higher than the values for polygraphites.

TABLE OF CONTENTS

TABLE OF CONTENTS (continued)

LIST OF ILLUSTRATIONS

LIST OF ILLUSTRATIONS - CONTINUED

LIST OF ILLUSTRATIONS - CONCLUDED

LIST OF TABLES

LIST OF TABLES - CONCLUDED

I. INTRODUCTION

Under Contract F04611-69-C-0070, Atlantic Research conducted a study of materials for high pressure solid rocket motor nozzles. Volume I of this Final Report describes program tasks, test procedures, and program results. Volume II describes the nondestructive testing applied to the graphite components of the high pressure nozzles.

One of the program objectives was to identify new or improved materials which would be useful in high pressure solid rocket motor nozzles. Further, in the event that these promising new materials were not adequately characterized as to thermal or other properties, the program provided for such characterization. Particularly desired for these new materials were those properties over a temperature range which serve as input to the computer programs used to conduct thermal analyses and predict chemical erosion. The thermal conductivity and specific heats are necessary for these calculations.

During the course of the program, two such materials were identified. One was castable carbon, a furane resin bonded dense coke filler, which is of low cost and was found to be a good performer in the converging and diverging section of the high pressure nozzles. The second was a carbon fiber reinforced pyrolytic graphite composite (PYROSTRAND*) which is attractive for throat inserts and blast tubes for high pressure nozzles.

Southern Research Institute was selected as a subcontractor to determine the required properties. Southern Research is fully experienced in conducting such measurements at temperatures up to 5000° F and has the equipment and staff available for such work. In addition, because of their knowledge of behavior of similar materials and the comparative data they have generated on other Air Force sponsored programs, they can authoritatively interpret the data measured. This Volume III of the Final Report presents the data measured by Southern Research along with a description of the test materials.

---

*Trademark, The Susquehanna Corporation

II. SUMMARY

During the conduct of the program to study high pressure nozzle materials, two recently developed materials were identified as having promise for nozzle application. Thermal properties required for design and performance predictions for these materials were not available, and so a materials characterization task was included in the program. These studies were conducted at Southern Research Institute on subcontract.

The materials identified as promising for high pressure applications were castable carbon, a low cost ablative, and a carbon fiber reinforced pyrolytic graphite (Pyrostrand). Castable carbon is a furane resin bonded dense coke filled material, the raw materials of which cost 11 cents per pound. It is fabricated by casting in open molds and curing. The erosion resistance approaches that of pressure molded carbon-phenolic material. Pyrostrand graphite composite is a carbon fiber reinforced pyrolytic graphite fabricated by depositing pyrolytic graphite on a removable substrate which also serves to position the filamentary reinforcements. It differs from other carbon-carbon composites in that it is fabricated at a high temperature (3,650°F), contains no carbon char constituent, and is impermeable.

The thermal conductivity of an ablative material such as castable carbon is difficult to determine because the process of ablation is rather violent, the char is in a transient state, and the heat conductance is a combination of several modes of heat transfer, difficult to simulate. Because of these difficulties, precharred materials are used for measurements at temperatures above the decomposition temperature. The ablative is heated in a furnace and converted to a char at some temperature above that at which the measurements will be made. This technique represents an estimate of the thermal conductivity when the virgin material first reaches that prechar temperature in the ablation process but does have some limitations in analysis of time effects.

The castable carbon virgin material had a low conductivity of about 12 Btu in/hr ft^2 °F, the 1,500° F prechar had about the same value up to 1,500° F and the 4,000° F prechar had a value six to ten times higher. The castable carbon is an isotropic material and these values are intermediate between the conductivities in the two directions for molded carbon-phenolic ablatives.

The thermal expansion for 4,000° F precharred castable carbon increased from 1.65×10^{-3} in/in from 75 to 980° F to 11.10×10^{-3} in/in from 75 to 4,496° F. The thermal expansion data

indicated that the castable carbon material is stable up to the precharring temperature. The thermal expansion data fall in between with and across grain expansion values for ATJ-S graphite.

For measurements on the fiber reinforced pyrolytic graphite, a standard specimen size used for determination of properties on other composites was selected. This is a cylinder 1 inch in O.D., 0.850 inch in I.D., and 2 inches long. Techniques previously developed at Southern Research Institute to measure conductivity in both the thickness direction (principally c direction orientation) and in the axial direction (principally a-b orientation) were employed. Conductivities measured in the c direction were 9.59 at 2,069 °F, 11.79 at 3,106°F, 16.02 at 3,804 °F, all in Btu inch/hr ft^2 °F. Conductivities in the a-b direction were measured at 271 at 544 °F, 281 at 994 °F, and 289 at 1,529 °F, all being in units of Btu in/hr ft^2 °F. The conductivity values of fibrous PG in the ''a-b'' direction are lower by a factor of about 7, than the conductivity values of PG tile, or plate, in the ''a-b'' direction. This probably results from the combination of circumferential layers of carbon fibers and PG infiltration in between. The conductivity values of fibrous PG in the ''c'' direction are of the same order of those found for PG tile in the ''c'' direction. Thus, the anisotropy ratio (ratio at 150°F of thermal conductivity in the ''a-b'' direction to that in the ''c'' direction) for fibrous PG sleeve is of the order of 20 compared to about 150 for PG tile.

The slightly increasing thermal conductivity (a-b direction) with increasing temperature as shown by the fiber PG composite is unusual in that other refractories, including PG plate, show decreasing conductivity with increasing temperature.

The electrical resistivity of fiber reinforced PG composite (a-b direction) decreased from 1,650 μohm-cm at ambient to 1,550 μohm-cm at 1,000°F. This is approximately four times the electrical resistivities of PG plate, and the composite shows less resistance decrease with temperature than does PG plate.

The heat capacity of castable carbon increased from 0.31 Btu/lb °F at 500°F to 0.56 Btu/lb°F at 4,500°F. The heat capacity of Pyrostrand graphite composite increased from 0.28 Btu/lb°F at 500°F to 0.60 Btu/lb°F at 3,500°F. The heat capacity values for castable carbon and the fibrous PG composite are about 10 percent higher than the values for polygraphites.

III. MATERIAL DESCRIPTION

A description of the two materials, castable carbon and graphite fiber reinforced pyrolytic graphite, is presented to familiarize the reader with these relatively new materials.

CASTABLE CARBON

Resin-bonded carbon-filled ablative materials have generally been found useful as rocket nozzle components. The Atlantic Research castable carbon material is a 20 weight percent furane resin binder and a balance of dense coke filler. The average raw material cost in these proportions is 11 cents per pound which makes it an attractive low-cost ablative. Performance-wise, it is competitive with pressure-molded carbon-phenolic materials which have a raw material cost of over $20 per pound. The material is fabricated by mixing the liquid resin binder with the filler, casting in open molds without pressure, and slowly curing to 340°F. The dense coke filler is not graphitized and, therefore, contributes to a low thermal conductivity. It is also characterized by relatively low chemical reactivity and so contributes resistance to chemical erosion. Additional information on this material may be found in Reference 1.

FIBER-REINFORCED PYROLYTIC GRAPHITE

Carbon fiber-reinforced pyrolytic graphite (Pyrostrand) composite was recently developed at Atlantic Research to take advantage of the desirable properties of pyrolytic graphite and, at the same time, to reduce the anisotropy and thereby make a material more suited to structural applications. This composite differs from the carbon-carbon composites under development for reentry applications in that those materials contain a pyrolytic carbon deposited at a relatively low temperature (1,800 to 2,400°F), are permeable, or at least contain predominantly connected pores, and may or may not contain carbon from a charred resin. The Pyrostrand graphite composite contains only pyrolytic graphite deposited at a temperature of 3,650°F and a carbon filament reinforcement. There are some disconnected pores which exist between the graphite filament turns. A dense pyrolytic graphite layer between each yarn layer also contributes to the impermeable nature of the structure.

The pyrolytic graphite is formed by passing methane over a heated mandrel which also supports the positioned graphite filaments. Deposition conditions are 3,650 °F temperature and 26 inches of mercury vacuum. The nature of the composite can be varied by the use of different graphite filament reinforcements and in different quantities. Union Carbide WYB 85, Thornel, and Kureha KC-100 are typical reinforcements. They are generally used in quantities of 5 to 15 volume percent. Higher fiber content promotes strength, whereas higher PG matrix content favors greater erosion resistance in reactive environments. Density varies from 1.75 to 2.0 depending principally on the yarn content. Potential applications for this composite are rocket nozzles, thrust chambers, blast tubes, biomedical, and reentry heat shields or nose cones. Additional information on this composite may be obtained in References 2 through 5.

IV. SAMPLE PREPARATION

The castable carbon material was supplied in various shapes and sizes and in three different conditions by Atlantic Research and was machined into the desired specimen shape by Southern Research Institute. The Pyrostrand graphite composite, on the other hand, was fabricated and machined to size prior to submittal to SRI.

The castable carbon was furnished in three different conditions: (1) cast and cured, (2) cast, cured, and pyrolyzed at 1,500°F, (3) cast, cured, and pyrolyzed at 4,000°F. All pyrolyzing operations were conducted in furnaces. The characteristics of furnace chars have been found to be quite similar to those formed in rocket motor nozzles (Reference 6), the furnace chars showing slightly higher density because they are free to contract during pyrolysis. Furnace charring at 1,500 degrees was accomplished by packing the material in a stainless steel box filled with carbon powders, placing the box in a resistance heated muffle furnace and utilizing the thermal lag of the box charge to provide a moderately slow heating rate through the resin pyrolysis region. A 24-hour period was provided for heat-up, hold, and cooling. Some of the 1,500°F char material was then placed in a graphite susceptor induction heating furnace and heated to 4,000°F where it was held for 1 hour and cooled.

The castable carbon starting material was taken from a number of different castings which were originally made for other purposes, such as for components of test nozzles. Generally, for one or two test pieces, the practice has been to cast a solid billet and machine the component from this billet. Material cut from the end or cored from cylinders is retained for other purposes. Also, some of the material was cut from the sound portion of a billet which had been rejected for a crack. The formulations were the same for all of the various billets used, and it was believed that the random selection of materials from different castings gave a more representative material sample.

The test sample size for the graphite composite was determined by the standard specimen size previously used at SRI for other carbon-carbon composites. This is a cylinder 1 inch in O.D., 0.850 inch in I.D. and 2 inches long. Originally, seven test pieces were required; but since it was anticipated that the thermal testing cycle would not affect the specimens, this number was reduced to four which required some specimen reuse.

Two fabrication runs were made with substrates 0.850 inch in I.D. by 4-1/4 inches in length. Fabrication was at 3,650°F and 26 inches of mercury vacuum. Each piece was cut at midpoint, trimmed at the ends, and the outside surface was machined to provide a 1.0 inch O.D. For the fiber reinforcement, Kureha KC-100 single-ply carbon yarn was used. This material is made from a pitch precursor and has 500 filaments per ply. The maximum thermal exposure during manufacture is probably around 2,200°F, considerably lower than that incurred during the composite fabrication process. The single-ply yarn is approximately 10 mils in diameter. There was approximately 20 mils spacing between turns, and four layers of yarn were used for each fabrication run. Portions of the fourth and outer layer were partly removed during machining of the outside surface to give a constant wall thickness. The sleeves were identified by numbers from 2 to 5. These identifications are maintained with the data. About 1/8-inch-long rings from one of the ends of each sleeve were cut and used for NDT evaluations at SRI.

Typical nomenclature utilized to identify the specimen was as follows:

CR - 1 - 70

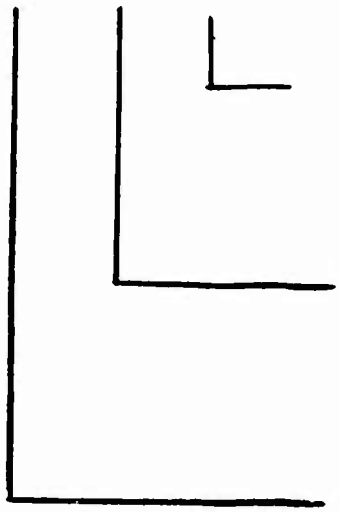

Temperature of heat treatment

70 - for uncharred (really 340°F)
1,500 - 1,500°F precharred
4,000 - 4,000°F precharred

Number of the specimen (note this number is followed when necessary by ''a'' or ''c'' where ''a'' is for the axial direction, ''c'' is for the thickness or radial direction)

Type of specimen - CR - comparative rod, RI - radial inflow, HC - heat capacity, CTE - thermal expansion

MATERIALS INSPECTION

Castable Carbon

Various NDT/monitor inspections were performed on the castable carbon materials: visual, radiography, bulk density, ultrasonic velocity, electrical resistivity, and porosity by liquid absorption. Inspections were performed on bulk shapes and specimen configurations. Visual and radiographic inspections were performed on bulk shapes to select specimen sites from the best material. After final machining, the test specimens were inspected for flaws and by the monitors. The NDT work was conducted at SRI.

Upon receipt of initial material, a charred bulk shape was selected and radiographed to select specimen sites. However, because the outer surface of the material contained several large voids and material separations (striations or cracks) it was concluded that the bulk shapes would have to be machined to a regular configuration before radiography could be an effective selector. The bulk shapes were then machined and radiographed.

The radiograph (radial direction) of one of the 1500°F precharred samples (machined bulk shape) is given in Figure 1. In the axial view, no materials separations were revealed. However, in the radial view, several large ones were apparent indicating, of course, that the major dimensions of the separations were aligned in diametrical planes.

A photomicrograph of the 4000°F precharred material is presented in Figure 2.

From the radiographs on the machined bulk shapes, specimen sites were selected and the test specimens were removed and machined. A comprehensive visual inspection was performed on each test specimen. No apparent anomalies were observed for Specimens CR-2-70 and CTE-3-70. For the other specimens, however, large voids and material separations occurred frequently. Photographs selected to depict material background are given in Figures 3 through 12. Some selected radiographs are given in Figures 13 through 17.

One result of the visual and radiographic inspections was that the uncharred material (cured at 340°F) was relatively free of material separations and large voids; however, for material

precharred to 1500°F and above, material separations and large voids occurred frequently. For example, a photograph and radiograph of an uncharred specimen (CR-1-70) are shown in Figures 3 and 13. Relatively speaking, this material was sound when compared with photographs and radiographs of the other chars (1500°F char - Specimen CR-1-1500 photograph shown in Figure 4, radiograph shown in Figure 14; 4000°F char - Specimen RI-2-4000, photograph shown in Figure 9 and radiograph shown in Figure 15). Further, as shown in the selected photographs and radiographs, some of the specimens contained some gross material delaminations: CR-1-1500, visual, refer to Figure 4; CR-2-1500, visual, refer to Figure 5; CR-1-4000, visual, refer to Figure 7; CR-2-4000, visual, refer to Figure 8; RI-2-4000, radiography in 0° and 90° views, refer to Figure 15; RI-3-4000, radiography in 0°, 90°, 180° and 270° views, refer to Figure 16.

The results of inspections by monitors (bulk density, velocity, electrical resistivity, and porosity by absorption) are given in Table 1. The density for the uncharred specimens was about 1.53 gm/cm^3, for the 1500°F precharred specimens about 1.34 gm/cm^3, and for the 4000°F precharred specimens about 1.29 gm/cm^3. Velocity for the uncharred material was 0.1067 and 0.1082 in./μsec; however, velocity could not be measured for the charred specimens because of signal attenuation. Electrical resistivity for uncharred and 4000°F specimens measured in the ranges of 426,000 - 431,000 μohm cm and 12,000 - 12,400 μohm cm, respectively. This result indicated that the uncharred resin had a very high resistance which decreased with the heat treatment. Open and closed porosities determined by liquid absorption measurements for 4000°F charred material were 25 percent and 12 percent. It should be noted here, that the closed porosity measurement was based on a total porosity assuming the true density of graphite of 2.22 gm/cm^3. The true density of the dense coke filler is actually less than 2.22 gm/cc, and so the porosities calculated by this method are above actual.

For comparison purposes, some typical values measured at Southern for some polygraphites are given below:

Material	Density gm/cm^3	With Grain Velocity in./μsec	With Grain Resistivity μohm cm	Open Porosity %	Closed Porosity %
ATJ-S medium grain	1.82	0.1030	801	9	9.2
G-90 coarse grain	1.90	0.1130	850	6	9.3
AXF-5Q fine grain	1.83	0.1200	1300	14	3

Fibrous PG

NDT/monitor inspections of fibrous PG were not as exhaustive as those on the castable carbon primarily because of the bulk specimen configuration (1" O.D. x 0.85" I.D. x 2" long). Successful NDT inspections consisted of visual and radiographic inspections. A filtered particle inspection using Partek P-1A in alcohol was also used on the bulk sleeves, but no new material anomalies were revealed. Monitor evaluations consisted of bulk density (gravimetric) and porosity (by liquid absorption) measurements.

Photomicrographs (35X and 80X) made in the axial direction showing the cross-section in the material are presented in Figure 18.

Visual inspection of the as-received bulk sleeves revealed a background of residual porosity (aligned circumferentially) in the outer surface. A photomicrograph (10X) of the outer surface of Sleeve 2, which typified this background porosity, is shown in Figure 19. Partek P-1A penetrant was used here to gain further insight into the smaller voids; however, the structure of the material was such that the results were confounded resulting in no new information on the material.

The as-received bulk sleeves were inspected for flaws by radiography using a "sidewall" technique. This technique, which has been used quite successfully here at Southern on large carbon/carbon cylinders, consists of merely radiographing the specimen (sleeves) radially for the correct exposure of the sidewall. This technique causes circumferentially aligned anomalies to be aligned in their most advantageous orientation to require the least sensitivity for disclosure. Using this technique, a background of uniformly spaced low-absorptive spots was revealed in all four sleeves. The spots were somewhat spherically shaped and about 0.02 inch in diameter. The radiograph (photographically reproduced) showing these low-absorptive spots in Sleeves 2 and 3 is shown in Figure 20.

In addition to the "sidewall" radiographs, some 0.125 inch high rings were removed from the as-received sleeves (for absorption measurements and photomicrographs) and were radiographed in the axial direction for material background information. This radiograph clearly showed the Kureha C-100 carbon material as either one or two low-absorptive rings. This radiograph (photographically reproduced) is shown in Figure 21.

The results of inspections by monitors (bulk density, velocity, electrical resistivity, and porosity by absorption) are given in Table 2. Bulk density (gravimetric) of the four "as-received" sleeves ranged from 1.766 gm/cm^3 to 1.800 gm/cm^3. Velocity and electrical resistivity measurements were not made because of the geometrical shape of the specimens (1.0 inch O.D. x 0.85 inch I.D. x 2 inches long). Open and closed porosities by liquid absorption ranged from 1.9 to 3.2 percent and from 15.4 to 16.5 percent, respectively. This result (high closed and low open porosity) indicated that the background of 0.02 inch voids revealed in the sidewall radiographs and the low-absorptive circumferential rings revealed in the axial radiographs on the 0.125 inch high rings constitute part of the closed porosity system. The theoretical density used in the calculations (2.22 gm/cc is above the actual because the yarn component (spun from pitch and pyrolyzed) has a significantly lower density. Thus the calculated porosities are high.

V. PROPERTY DETERMINATIONS

APPARATUSES AND PROCEDURES

Several apparatuses were used in this program to evaluate thermal conductivity, specific heat, thermal expansion and NDT/monitors on the castable carbon and fibrous PG sleeves. Each apparatus is briefly described under the proper heading and detailed descriptions of these apparatuses are included in the appendices.

Thermal Conductivity

Comparative Rod Apparatus

Thermal conductivities of a wide variety of materials are determined from about -160°F to 2,000°F utilizing a cylindrical specimen stacked in series with two cylindrical references of known thermal conductivity. Temperature gradients are measured when axial steady-state heat flow is obtained. A comparison of the temperature gradients in the specimen and references is used to compute the specimen thermal conductivity. For a standard specimen configuration 2 inch in diameter X 1 inch long, the uncertainty in measurements is estimated, from error analysis at ±5 percent.

With castable carbon (uncharred and 1,500°F precharred) Code 9606 Pyroceram references were used. For 4,000°F precharred material one specimen each was evaluated with Code 9606 Pyroceram and 316 Stainless Steel references. A standard specimen size was utilized for all measurements.

For thermal conductivity measurements on fibrous PG sleeve in the axial ("a-b") direction, additional experimental work was necessary before actual measurements could continue. This was necessary due to the thin wall (~0.070 inch) of the sleeve. For sufficient wall thickness, we usually either glue pieces with graphite glue (National No. 14 Cement) to create a normal configuration or prepare one of the surfaces of the references with a curvature so as to mate at the interfaces of the cured specimen. Neither of the above approaches was practicable due to the thin wall of this material. It was therefore necessary to make measurements on the sleeve in the cylindrical configuration and check calibrations on a similarly configurated sleeve made of material of known thermal conductivity, prior to the actual runs.

For calibration, two sleeves from 316 Stainless Steel were machined to the same configuration as that of fibrous PG sleeve. The schematic for the calibration buildup is shown in Figure 22. Chromel/Alumel thermocouples were placed in the 316 Stainless Steel adaptors on both sides of the sleeve and a thin Grafoil ring (0.010 thick) was placed at each interface of the sleeve and the adaptors. The Grafoil ring provided good thermal contact between the sleeve and the adaptors. Corrections were made to the temperature drop across the Grafoil ring from the known in-house thermal conductivity data on Grafoil. The inside of the sleeve was filled with thermatomic carbon.

The system was analyzed for the heat bypass through thermatomic carbon. Calculations indicated that the heat bypass through the thermatomic carbon was less than ±1 percent of the total heat flux through the specimen for the temperature range covered (500°F to 1500°F).

The calibration data on 316 Stainless Steel sleeves are shown in Figure 23 and in Table 3. Excellent agreements were obtained at 500, 1000 and 1500°F with the thermal conductivity curve established for 316 Stainless Steel references.

After calibration runs were completed, identical procedures were used for fibrous PG sleeve and measurements in the axial ("a-b") direction were made at 500°F, 1000°F and 1500°F.

The uncertainty in measurements on fibrous PG sleeve in the axial ("a-b") direction is conservatively estimated at ±10 percent.

Radial Inflow Apparatus

Measurements are made from 1500°F to 5500°F in furnaces resistively heated with graphite heaters utilizing a water calorimeter to measure the heat flow through the specimen. A standard specimen of size 1-1/16 inches in diameter x 1 inch long plus two 1/2 inch long guards is utilized with this apparatus. Thermal conductivity is determined by measuring the heat inflow to the calorimeter and the temperature drop across the gage section of the specimen. The uncertainty in measurements using a standard specimen configuration is estimated, based on error analysis, at ±7 percent.

Measurements on castable carbon (4000°F precharred) were made from 1500°F to 4500°F. A standard specimen size was used. To check any anisotropy in the material, a pair of cold and hot holes were drilled to the specimen. Two values of thermal conductivity were generated at each temperature level using one pair of temperature measurements for the front to back direction and the other pair of temperature measurements for the side to side direction. Figure 24 is self-explanatory.

To measure thermal conductivity of fibrous PG sleeve in the "c" direction from 2000°F to 4000°F an optical method and the water calorimeter were employed. The configuration for this method is shown in Figure 25. The technique involves measuring inside and outside specimen surface temperatures with an optical pyrometer. The sleeve is centered on a calorimeter by means of ATJ graphite specimens support cylinder fitted into the top and bottom CS graphite guards. In order to view the inner walls of the specimen, no packing is used in the annulus. The calorimeter is painted with a flat black enamel. Heat transfer takes place from the specimen to the calorimeter by gas conduction and radiation. A 0.100 inch diameter hole is drilled in a surrounding cylinder to measure the face temperature of the specimen. This hole provides a blackbody cavity with a length to diameter ratio of about 2.5:1. A similar hole 0.100 inch in diameter is drilled through both the specimen support cylinder and the specimen. This hole is offset 0.130 inch from the centerline so that the view of the inner wall is not obstructed by the calorimeter.

Thermal Expansion

Graphite Dilatometer

Thermal expansion measurements are made from 70°F to 5500°F utilizing graphite tube dilatometer with a dial gage. The specimen is radiantly heated in graphite tube furnaces.

Thermal expansion measurements on castable carbon (4000°F precharred) were made to 5000°F. A 3 inch long specimen was used for the measurements.

Enthalpy and Heat Capacity (Specific Heat)

Adiabatic Calorimeter

A specimen, either cooled (dry ice or liquid nitrogen) or heated in an electric furnace to temperatures up to 1000°F is dropped into copper calorimeter cup which is thermally guarded so that all the heat loss by the specimen is sensed as a change in temperature of the calorimeter cup from which enthalpy at temperature is calculated.

The uncertainty in measurements is estimated, based on error analysis, at ±3 percent.

Ice Calorimeter

A specimen, heated in a tube-type graphite furnace to temperatures from 1000°F to 5500°F, is dropped into an ice calorimeter. The enthalpy of the specimen is determined from the amount of ice melted in the ice mantle.

The uncertainty in measurements is estimated, by error analysis, at ±5 percent.

From the enthalpy versus temperature curve obtained experimentally by the above apparatuses, the heat capacity is computed by two methods, a graphical solution and an analytical or least squares curve fit solution.

Ultrasonic Velocity

Ultrasonic velocity measurements and flaw detection by pulse-echo are accomplished using a Sperry UM721 reflectoscope. Acoustic velocity is measured using the through-transmission, elapsed-time technique. The Sperry UM721 is used as the pulser, and a Tektronix 564 oscilloscope complete with a 3B3 time base (precision of 1 percent) and a 3A3 vertical amplifier is used as the signal measuring device. The detection of macro flaws is accomplished using the pulse-echo, reflection technique. Frequently used test specimens are the tensile blank specimen having dimensions of 1/2 inch diameter by 4 to 6 inches long and the 1/4 inch long segment from gage section of a fractured tensile specimen which is removed and machined after the tensile test has been performed. Ultrasonic inspection is performed on specimens having machined, flat surfaces normal to the longitudinal axis of the specimen.

In using the through-transmission, elapsed-time technique for measuring acoustic velocity, a short pulse of longitudinal-mode sound is transmitted through the specimen. An electrical pulse originates in a pulse generator and is applied to a ceramic piezoelectric crystal (SFZ). The pulse generated by this crystal is transmitted through a short delay line and inserted into the specimen. The time of insertion of the leading edge of this sound beam is the reference point on the time base of the oscilloscope which is used as a high-speed stop watch. When the leading edge of this pulse of energy reaches the other end of the specimen, it is displayed on the oscilloscope. The difference between the entrance and exit times is used with the specimen length in calculating ultrasonic velocity. A short lucite delay line is used to allow time isolation of the sound wave from electrostatic coupling and to facilitate clear presentation of the leading edge of the entrant wave resulting in a more accurate "zero" for time. Alcohol is used as the couplant to reduce errors incurred by solid couplants. The precision of measurement for tensile test blanks is ±0.002 inch per microsecond; for the 1/4 inch removed section, ±0.010 inch per microsecond.

In using the pulse-echo, reflection technique of ultrasonics to detect macro flaws, test blocks from a similar material are used as calibration references for estimating the location, depth and size of discontinuities. These blocks are normally about 5/8 inch square by 2, 3 and 4 inches long. At one end, a single hole is drilled along the longitudinal axis to a depth of 1 inch. For a

polygraphite such as ATJ-S, the hole sizes range from 1/32 to 1/4 inch in 1/32 inch increments and an ultrasonic frequency of 1 MHz is used. At 1 MHz, propagation of acoustical energy is limited by attenuation to distances on the order of 12 inches. When using pulse-echo, this means a specimen 6 inches long is within test range. Alcohol is used as the couplant between the transducer and the specimen. Instrument settings are duplicated as much as possible for evaluations on similar material.

Using a Tektronix Oscilloscope C-12 camera, two techniques are used in recording pulse-echo signals from specimen blanks. The first technique involves taking photographs of the signal as transmitted from one or both ends of the specimen to determine "standing signals". The second technique involves recording a multiple trace (smear) of the signal. This is done by revolving the specimen on the face of the transducer on about a 1/8 inch radius with the camera shutter open. This technique tends to randomize the background noise and to define the more repetitive "standing signals".

Radiography

Radiography of graphite materials is performed using state-of-the-art X-ray techniques for low-absorptive materials. The radiographic unit is a Radifluor 360 manufactured by Torr X-ray Corporation, a division of Phillips Electronics. This unit is rated for operation from 0 to 120 kv at either 3 or 5 ma, making it ideal for carbon and graphite materials having thicknesses up to about 2 inches. It incorporates certain basic characteristics which are necessary for examining low-absorptive materials with high resolution and sensitivity. For example, the X-ray tube has a 0.015 inch thick beryllium window with a focal spot size of 0.35 mm. The beryllium window provides low inherent filtration for low energy rays permitting them to exit the tube for utilization. The small focal spot provides distortion-free imaging of small discontinuities. The radiographic sensitivity using extra-fine grain film is less than 2 percent.

Operational and film development procedures used are consistent with conventional good radiographic practices. For example, lower power settings are used by extending development time in order to enhance image contrast. Extra-fine grain film (such as Eastman Type M) is used to ensure sharp imaging. Further, when

specimen geometry will permit, image unsharpness is reduced by using a focus-to-film-distance of 42 inches. Image quality is checked using a penetrameter made from a similar material. Drilled holes indicate 2 and 4 percent sensitivities. No intensifying screens, filters or masks are used to affect imaging for graphite thicknesses up to 2 inches. Film processing is consistent with good standard practices. Examination of radiographs is made using a variable, high intensity spot illuminator.

Electrical Resistivity

Electrical resistivity is measured using the potentiometer method. The test specimen may be either a specimen blank or a finished specimen configuration having a uniform gage length of 1 inch or more. The attachment taps to the specimen are spring-loaded graphite discs. Potential taps which have a gage length of 1 inch are normally clipped to the specimen.

The procedure used in the potentiometer method involves comparing the voltages for a standard resistor with a specimen of unknown resistance when a common, known current flows through both. For example, with 1 amp flowing through the specimen and a standard 5000 μ ohm resistor, the potentiometer leads are connected across the standard 5000 μ ohm resistor, the potentiometer set on 5000 μV, and the rheostat adjusted until there is no current flow through the galvanometer. Then, the potentiometer leads are switched to the specimen. The potentiometer is adjusted for zero current flow through the galvanometer, and the voltage across the specimen is read.

From the relation

$$R = \frac{E}{I} \qquad (1)$$

the relationship between the standard resistance, the unknown resistance and the associated voltages can be expressed as

$$\frac{R_x}{R_s} = \frac{E_x}{E_s} \quad \text{or} \quad R_x = R_s \frac{E_x}{E_s} \tag{2}$$

where

R_x = Resistance of specimen
R_s = Resistance of standard resistor (5000 μohm in this case)
E_x = Voltage drop across specimen
E_s = Voltage drop across standard resistor

A full-wave rectified DC power supply operated by an AC regulated power source is used to induce current flow through the specimen. A galvanometer having a sensitivity of 0.8 μV per millimeter with a 1000 ohm series resistor is used with a potentiometer having a dial graduation of 0.0005 μV to measure voltage.

Using the measured voltage drop across the specimen, the known current flow, and the dimension measurements from the specimen, the volume electrical resistivity is calculated using the equation

$$\rho = \frac{A}{L} \frac{V_x}{I} \tag{3}$$

where

ρ = Volume elctrical resistivity
A = Cross-sectional area of specimen
V_x = Voltage drop across gage length of specimen (corrected for open-circuit voltage)
I = Current flow through specimen
L = Gage length of specimen

The normal uncertainty for the value of electrical resistivity determined from this apparatus is ±2 percent.

Open and Closed Porosity by Liquid Absorption

Liquid absorption measurements are made to further characterize the nature of a material. A vacuum-impregnation technique using mineral spirits (s.g. about 0.77) as the impregnant is used.

Using this technique, the three weights - dry weight, suspended weight and saturated weight are determined for evaluating the absorption, density and porosity of a material. This technique is used frequently to characterize material near the fracture zone of tensile specimens. For such evaluations, 1/4 inch segment or segments from the long and/or short halves of the tensile specimens are used. A 1/4 inch "fracture" section is a 1/4 inch long section including the fracture face. A 1/4 inch "removed" section is a section behind the 1/4 inch "fracture" section; that is, a section from 1/4 to 1/2 inch behind the fracture face.

The normal procedure used in making liquid absorption measurements involves first of all thorough drying and then precise weighing of specimens to determine dry, suspended and saturated weights (recorded to nearest 0.0001 gram). First, the specimens are oven dried at 300°F for two hours to drive out absorbed moisture and then weighed to determine dry weight. Individual specimens are then placed in small beakers which are placed on their sides in a desiccator. After the desiccator is sealed off, a vacuum of 50 microns of Hg is pulled and held for two hours to remove entrapped air from the specimens. The desiccator is then purged with mineral spirits until the beakers containing the specimens are submerged. The desiccator is then vented, and the specimens are left in the desiccator for 20 minutes to allow vapor inside the specimens to condense.

The suspended weight is obtained by weighing the saturated specimen while suspended in the mineral spirits. The specimens are kept submerged by righting the beakers in the desiccator to maintain the mineral spirits level above the specimen. Figure 26 illustrates the procedure used for suspending the specimen in mineral spirits from a balanced beam. The tare weight of the basket, which is subtracted from the total suspended weight to determine the suspended weight of the specimen, is determined by weighing the suspended basket submerged in mineral spirits to the same depth that the specimen is weighed. Care is exercised to ensure that no air bubbles cling to the basket and that a clearance between the basket and sides of the beaker is maintained.

For determining saturated weight, the specimens are removed from the mineral spirits and wiped carefully to remove excessive surface mineral spirits. The specimens are then weighed immediately to determine the saturated weight.

From the three weights taken for each specimen (dry weight, suspended weight and saturated weight) percent water absorption, open porosity, bulk density and apparent density are determined. The total porosity can be determined also when the true density of the material is known. The equations used for these calculations are:

$$W_a = \left(\frac{W_{sa}-W_d}{W_d}\right) \frac{\rho_w}{\rho_m} \times 100 \text{ percent} \quad (4)$$

$$P_o = \left(\frac{W_{sa}-W_d}{W_{sa}-W_{su}}\right) \times 100 \text{ percent} \quad (5)$$

$$\rho_b = \left(\frac{W_d}{W_{sa}-W_{su}}\right) \times \rho_m \quad (6)$$

$$\rho_a = \left(\frac{W_d}{W_d-W_{su}}\right) \times \rho_m \quad (7)$$

$$P_t = \frac{\left(\frac{W_{sa}-W_{su}}{\rho_m} - \frac{W_d}{\rho_t}\right)}{\left(\frac{W_{sa}-W_{su}}{\rho_m}\right)} \times 100 \text{ percent} \quad (8)$$

where

W_a = Water absorption
W_{sa} = Weight of sample when saturated with liquid m
W_d = Dry weight of sample
W_{su} = Weight of sample when suspended in liquid m
ρ_m = Density of liquid m (about 0.77 gm/cm^3 for mineral spirits - s.g. checked after each run)
ρ_w = Density of liquid water
ρ_t = True density of sample
ρ_b = Bulk density of sample
ρ_a = Apparent density of sample
P_o = Open porosity
P_t = Total porosity

Weights for this evaluation are determined using an analytical balance sensitive to 0.0001 gram. Instrument precision for measuring absorption is ±0.10, bulk density is ±0.002 gm/cm^3, open porosity is ±0.15 and total porosity is ±0.05.

Gravimetric Bulk Density

Each specimen is initially machined to a predetermined blank size and the bulk density of each blank is determined from direct measurements of weight and dimensions. Weight measurements are made on an analytical balance having a sensitivity of 0.0001 gram. Dimensional measurements are made to the nearest 0.0005 inch using micrometers.

Filtered-Particle Inspection

For inspecting porous materials whose particle size is 100 mesh or smaller, the filtered-particle inspection method is applicable. The filtered-particle system consists of a fluid (suspending medium) containing a dispersion of properly sized and shaped particles. Differential liquid absorption between an area containing a crack and one that does not is the phenomena which causes the particles to congregate about a surface discontinuity. For example, when the filtered-particle penetrant is applied, more liquid is absorbed at the site of a crack than in flaw-free material because of the extra absorptive area within the defect. As the liquid enters the defect, the suspended particles are filtered out at the surface causing a higher concentration of particles along the defect.

The procedure for using the filtered-particle system consists first of all in applying the system to materials which are applicable to the system. Partek P-1A used on materials such as some polygraphites reveal minute cracks which measure about 0.002 to 0.003 inch wide on the surface. Application is by hand using an eye dropper. Inspection is done under black light. Results are recorded photographically using a Polaroid NP-3 camera with a Polaroid No. HNCP 37 x 0.030 inch filter and black light illumination.

The filtered-particle system used at Southern for polygraphite type material is Partek P-1A, manufactured by Magnoflux Corporation. This system can be obtained with either an oil or alcohol base with a fluorescent particle which becomes clearly visible under black light.

DATA AND RESULTS

Thermal Conductivity

Castable Carbon

The thermal conductivity data for the castable carbon on virgin (cured at 340°F), 1500°F precharred and 4000°F precharred materials are shown in Figure 27 and in Tables 4 through 8. The conductivity values were 12.5 Btu in./hr ft^2°F at 150°F for virgin materials (cured at 340°F), 11.0 Btu in./hr ft^2°F at 1450°F for 1500°F precharred material and 70 Btu in./hr ft^2°F at 4000°F for 4000°F precharred material.

In order to check any anisotropy in the material, the comparative rod specimens were machined in such a way that the direction of heat flows was mutually perpendicular for two specimens during conductivity measurements on the virgin and 1500°F precharred materials. For 4000°F precharred material two mutually perpendicular directions of heat flow were covered during the radial inflow conductivity measurements and the third direction was covered during the conductivity measurements in the comparative rod apparatus. From the conductivity data, it was concluded that the material is isotropic for the thermal conductivity.

The comparison of the data at 1500°F indicates that the thermal conductivity for 4000°F precharred material is about 7 times the conductivity for 1500°F precharred material at about the same temperature. This increase in conductivity for 4000°F percharred material undoubtedly is due to ordering of the structure (graphitization) of the material.

The "boxed" values of conductivity are shown in Figure 28. In this technique the materials are precharred to certain temperature levels. Thermal conductivities of the precharred materials are determined at a steady-state up to precharring temperatures, thus providing conductivity values for each precharring temperature level and permitting a "boxing" of the best probable conductivity value within the temperature intervals selected. Thus, the "boxing" technique represents an estimate of the thermal conductivity when the material first reaches that temperature, during ablation process.

To make the point clear, suppose the virgin material reaches 1500°F in the ablation process. Figure 27 predicts that the thermal conductivity value should be 12 Btu in./hr ft^2°F when the material first reaches 1500°F in the ablation process. This is opposed to the value of 85 Btu in./hr ft^2°F observed at 1500°F for the 4000°F prechar. Similarly, the virgin material would have a value of about 70 Btu in./hr ft^2°F when it first reached 4000°F. Figure 28 includes a plot of the probable "boxed" value of conductivity as a function of temperature. Observe that one would expect a conductivity of 39 Btu in./hr ft^2°F at 3000°F when the virgin material first reached 3000°F.

Fibrous PG Sleeve

The thermal conductivity data in the axial ("a-b") direction for the sleeves are shown in Figure 29 and in Table 9. The conductivity increased linearly from 273 Btu in./hr ft^2°F at 500°F to 295 Btu in./hr ft^2°F. It was expected that the conductivity values should decrease initially with temperature, a behavior similar to PG in the "a" direction. An additional rerun was made using Armco-Iron references. The data agreed with previously obtained data using the 316 Stainless Steel references. To understand this result electrical resistivity measurements were made from 70°F to 1000°F. The data are shown in Figure 30 and in Table 10. The electrical resistivity slightly dropped from 1600 μohm cm at 70°F to 1500 μ ohm cm at 1000°F.

A composite plot of electrical resistivities, thermal conductivities of PG, fibrous PG and glassy carbon is shown in Figure 30. The behavior of electrical resistivity and thermal conductivity on fibrous PG are somewhat similar to glassy carbon.

The thermal conductivity data on fibrous PG in the ''c'' direction are shown in Figure 31 and in Table 11. The determinations at the three different temperature levels were all made on the same test sleeve. Thermal conductivity values were slightly higher (about 10 percent) for the second run compared to the first exposure. The conductivity increased from 10 Btu in./hr ft^2·F at 2,000·F to 18 Btu in./hr ft^2·F at 4,000·F. Increased conductivity above 3,000·F in helium may be due to the presence of delaminations. Also the 4,000·F test temperature is above the original fabrication temperature of the material and some further graphitization of the fiber and the matrix may occur.

The measured thermal conductivity of fibrous PG has been plotted for comparison with that of other refractories in Figure 32.

Data at about 2000°F were also obtained in vacuum and in helium during the rerun. These data were obtained to provide a direct comparison between the data in vacuum and in helium and permit a feel for the extent of the delaminations. Vacuum data at above 2000°F were lower by about 2.0 Btu in./hr ft^2°F when compared to helium data at about the same temperature. This shift is relatively small and detailed calculations probably would indicate that the delaminations are not continuous. SRI data on PG tile in the "c" direction are also shown in Figure 31 for comparison.

The thermal conductivity of the fibrous PG sleeve in the "c" direction will depend upon several factors such as (1) number and locations of delaminations, (2) width of the delaminations and (3) gases present in the delaminations. These factors were not analyzed in this program; however, they have been analyzed for PG sleeves, and may be found in "The Effective Thermal Conductivity of Pyrolytic Graphite Cylinders in Various Gas Environments", a paper presented at the Thermal Conductivity Conference, Iowa State University, October, 1969.

Thermal Expansion

Castable Carbon

The thermal expansion data obtained on 4000°F precharred material are presented in Figure 33 and in Table 12. The expansion increased linearly from the reference point of 70°F to 10.6×10^{-3} in./in. at 4000°F which indicated that the material was stable up to the precharring temperature. Above 4000°F, the material started shrinking and the data at 5000°F were obtained while the dial gage was moving.

The specimen contraction (zero return at 70°F) observed by the dial gage and micrometer were in excellent agreement.

The thermal expansion data were compared with typical SRI data on ATJ-S graphite in the with and across grain directions. The thermal expansion data for castable carbon are higher than the with grain but lower than the across grain expansion of ATJ-S graphite.

Enthalpy and Heat Capacity

Castable Carbon

The enthalpy and heat capacity data are shown in Figure 34 and in Tables 13 through 16. The heat capacity increased from 0.31 Btu/lb°F at 500°F to 0.56 Btu/lb°F at 4500°F.

The least squares treatment of the enthalpy data resulted in the following equation for enthalpy:

$$h_{32} = 0.395T + 0.161 \times 10^{-4}T^2 + 0.769 \times 10^{5}T^{-1} - 356$$

where the temperature (T) is in degrees Rankine.

The derivative of the enthalpy equation resulted in the following equation for heat capacity after the equation was adjusted to agree with graphical solution for heat capacity at 500°F.

$$HC = 0.395 + 0.322 \times 10^{-4}T + 0.107 \times 10^{6}T^{-2}$$

Good agreement existed between the analytical solution and the graphical solution both for heat capacity and enthalpy. The plots for heat capacity and enthalpy as shown in Figure 34, represent the best fit of the values determined by both methods.

Fibrous PG Sleeve

The enthalpy and heat capacity data are presented in Figure 35 and in Tables 17 and 18. The heat capacity increased from 0.28 Btu/lb°F at 500°F to 0.61 Btu/lb°F at 3500°F. Heat capacity values are about 6 percent higher than those of pyrolytic graphite.

The least squares treatment of the enthalpy data resulted in the following equation:

$$h_{32} = 0.280T + 0.431 \times 10^{-4}T^2 + 0.544 \times 10^{5}T^{-1} - 259$$

where the temperature (T) is in degrees Rankine.

The derivative of the enthalpy equation was adjusted to agree with graphical solution at 500°F to establish the following equation for heat capacity:

$$HC = 0.280 + 0.862 \times 10^{-4}T - 0.766 \times 10^{5}T^{-2}$$

Good agreement is found between analytical solution (least squares fit) and the graphical solution both for heat capacity and enthalpy. The curves for heat capacity and enthalpy as shown in Figure 35, present the best fit of the values determined by both methods.

A composite plot for heat capacities of castable carbon, fibrous PG sleeve, pyrolytic graphite and polygraphite is shown in Figure 36. In general, heat capacity values for both the materials evaluated for Atlantic Research are higher than those found in literature for polygraphites.

VI. OTHER CASTABLE CARBON DATA

In addition to the properties measured by SRI and described previously, the Atlantic Research castable carbon has been included in an Aerojet-NASA program for large motor ablatives; and some property determinations were made at Aerojet (Reference 7). The TGA of this material is shown along with several elastomeric materials in Figure 37. These data, measured at a heating rate of 20°C/min., show far less weight loss for the castable carbon than the other elastomeric materials. Since the furane resin system yields a high char content on pyrolysis, the weight loss of the binder is relatively low. Thus 50 percent carbon char formed from the binder, which was originally 20 percent, gives a 10 percent weight loss. From the same reference are reported thermal conductivity, diffusivity, and heat capacity for the virgin material and are shown in Table 19. The Aerojet determined values for the conductivity of the virgin material are approximately 30 percent higher than the SRI values. This is explained by the Aerojet samples being of slightly higher density and also by the calculation of conductivity from diffusivity measurements. Conductivity data calculated from the diffusivity are generally higher than the values obtained by direct measurement.

Erosion data also determined by Aerojet are shown in Figure 38 (Reference 8) and, as determined in the high pressure nozzle studies at Atlantic Research (Volume I of this Final Report), show that it performs similarly to the pressure molded carbon cloth-phenolic materials.

Typical mechanical properties, as reported in Reference 1, are 2,000 psi modulus of rupture and 5,000 psi compressive strength. Some versions of castable carbon contain from 3 to 5 weight percent chopped carbon fibers which tend to enhance the structural characteristics of the material.

VII. CONCLUSIONS AND RECOMMENDATIONS

For castable carbon it was found that the material is isotropic, and the thermal conductivity is intermediate between the two different directions of molded carbon-phenolic. The heat capacity is approximately 10 percent higher than bulk graphites. The thermal expansion data of castable carbon show that the material is stable up to precharring temperature. The thermal expansion data fall in between the with grain and the across grain expansion values for ATJ-S graphite.

The thermal expansion of castable carbon increases linearly from ambient to 10.6×10^{-3} inches per inch at 4,000°F which indicates that the material is stable up to the precharring temperature. The thermal expansion of castable carbon is higher than the with grain, but lower than the across grain expansion of ATJ-S graphite.

The conductivity values of fibrous PG in the ''a-b'' direction are lower by a factor of about 7, than the conductivity values of ''normal'' PG tile, or plate, in the ''a-b'' direction. The conductivity values of fibrous PG in the ''c'' direction are of the same order of those found for PG tile in the ''c'' direction. Thus, the anisotropy ratio (ratio at 150°F of thermal conductivity in the ''a-b'' direction to that in the ''c'' direction) for fibrous PG composite is of the order of 20 compared to about 150 for PG plate. This reduced anisotropy, along with the retention of good insulating properties in the ''c'' direction, should facilitate the use of the composite material in lieu of pyrolytic graphite shapes which suffer from extreme anisotropy.

The heat capacity for the fiber reinforced PG is about 10 percent higher than the values for bulk graphite.

Now that the measured data on castable carbon and the fiber reinforced PG are available, it is recommended that they be used for design and performance predictions. It is also recommended that thermal expansion data be measured on the fiber reinforced PG. Also, in the future, it may be desirable to measure the thermal conductivity of the fiber reinforced PG containing several different levels of fiber reinforcement, both above and below that of the specimens measured in this program.

REFERENCES

1. Atlantic Research, Castable Carbon for Nozzle Application, AFRPL-TR-66-111 under Contract AF 04(611)-9718, November 1965.

2. Olcott, E. L., Development of High Temperature Resistant Materials for Use in Naval Ordnance (U), Summary Report, Prepared by Atlantic Research under Contract N00017-68-C-2403, Naval Ordnance Systems Command, July 1968. UNCLASSIFIED.

3. Olcott, E. L., Study of Graphite Filament Reinforced Pyrolytic Graphite Rocket Nozzle Throat Inserts, Final Report, Prepared by Atlantic Research under Contract No. NAS-7-700, National Aeronautics and Space Administration (RPM), March 1969. UNCLASSIFIED.

4. Olcott, E. L., Norton, H., and Hayman, H., Development of High Temperature Resistant Materials for Use in Naval Ordnance (U), Final Report, Prepared by Atlantic Research under Contract N00017-69-C-4404, Naval Ordnance Systems Command, August 1969. UNCLASSIFIED.

5. Olcott, E. L., Development of High Temperature Resistant Materials for Use in Naval Ordnance (U), Summary Report, Prepared by Atlantic Research under Contract No. N00017-70-C-4401, Naval Ordnance Systems Command, August 1970. CONFIDENTIAL.

6. Clayton, W. A., Kennedy, P. B., Evans, R. J., Cotton, J. E., Francisco, A. C., Thermal Properties of Ablative Chars, Technical Report AFML-TR-67-413, Prepared by The Boeing Company Aerospace Group, Air Force Materials Laboratory, Air Force Systems Command, Wright-Patterson Air Force Base, Ohio, January 1968. UNCLASSIFIED.

7. Simmons, Dr. B. A., and Nachbar, D. L., Development of Cost-Optimized Insulation System for Use in Large Solid Rocket Motors, Volume I: Task I - Survey and Screening, prepared for NASA Lewis Research Center, Contract NAS3-11224, by Aerojet-General Corporation. August 1969.

8. Warga, J. J., et al, Evaluation of Low-Cost Materials and Manufacturing Processes for Large Solid Rocket Nozzles, AFRPL-TR-67-310, Aerojet-General Corporation, December 1967.

T

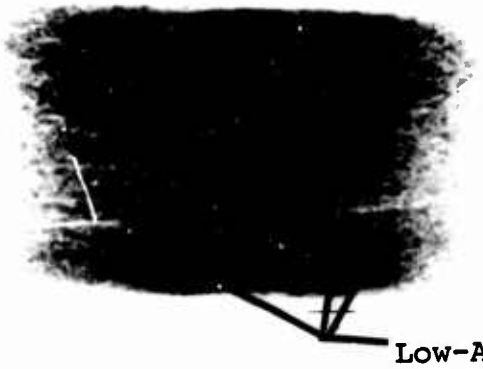

90

Figure 1. Radiograph (Photographically Reproduced) of a 1500°F Heat Treated Castable Carbon Material (Machined Bulk Shape) - Radial View

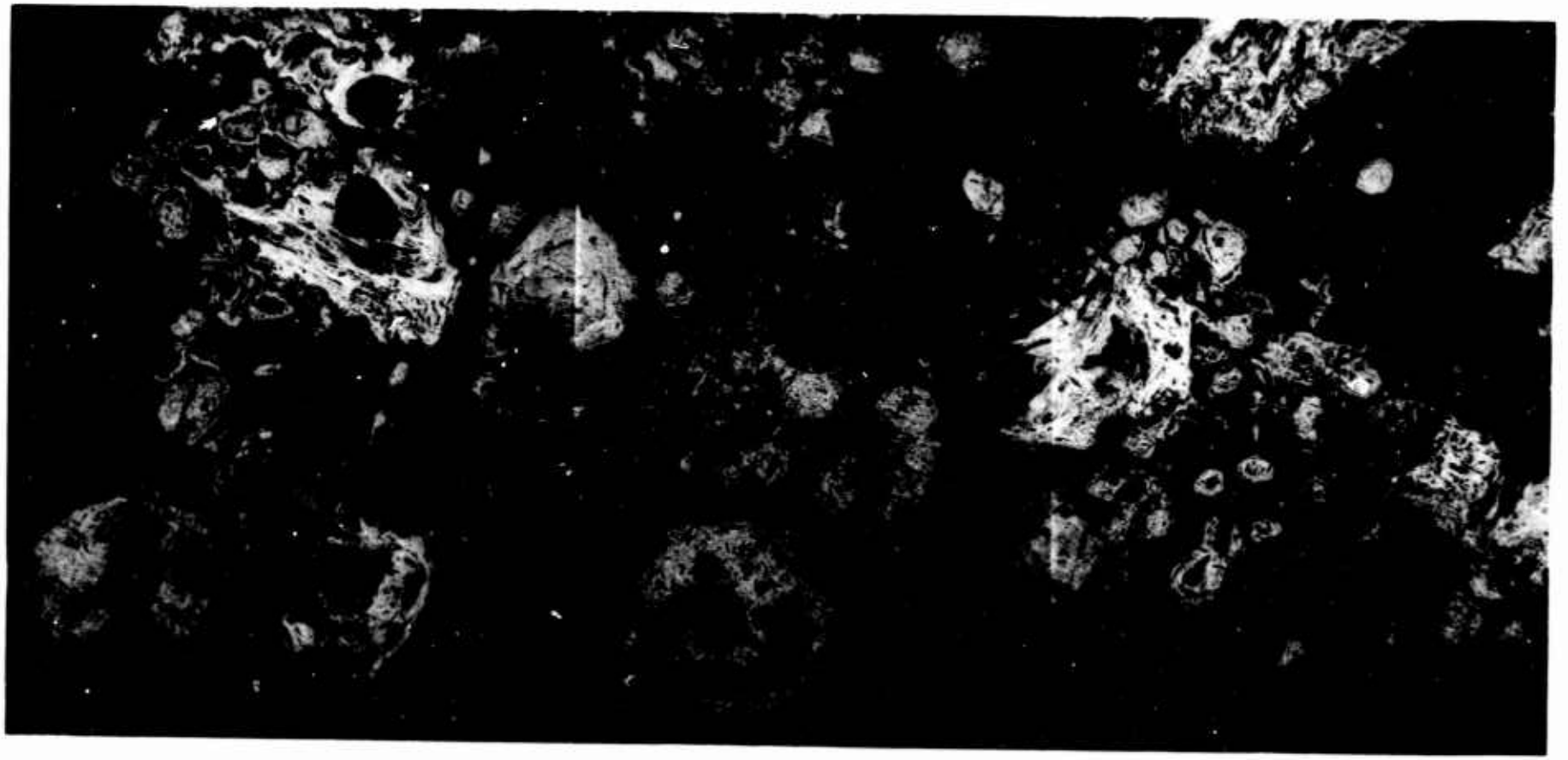

(Actual Size)

Figure 2. Photomicrograph (40X) of 4000°F Charred Castable Carbon

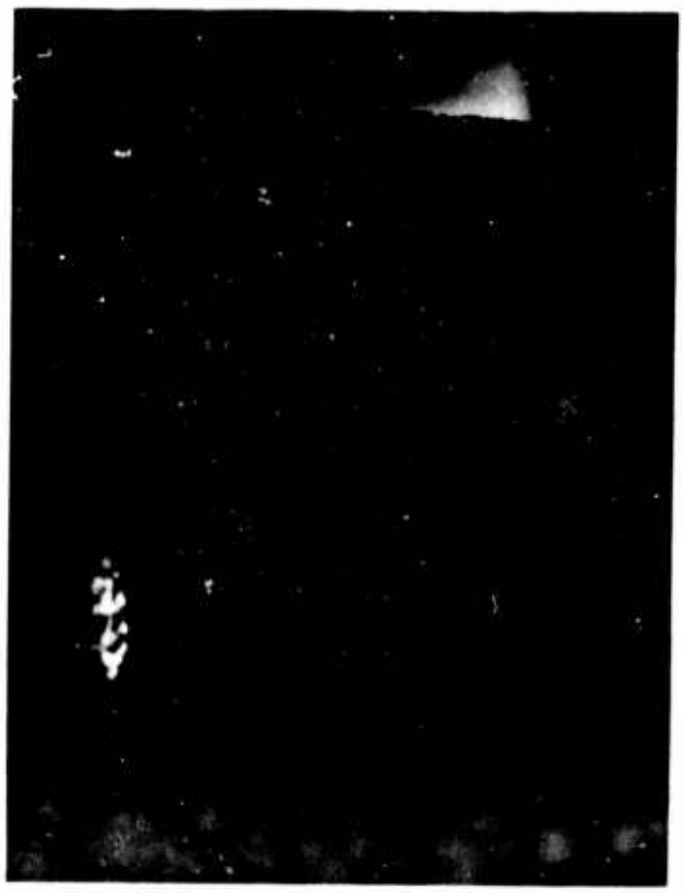

Figure 3. Photograph (3.3X) of Specimen CR-1-70 (50° Orientation) from a Castable Carbon Material

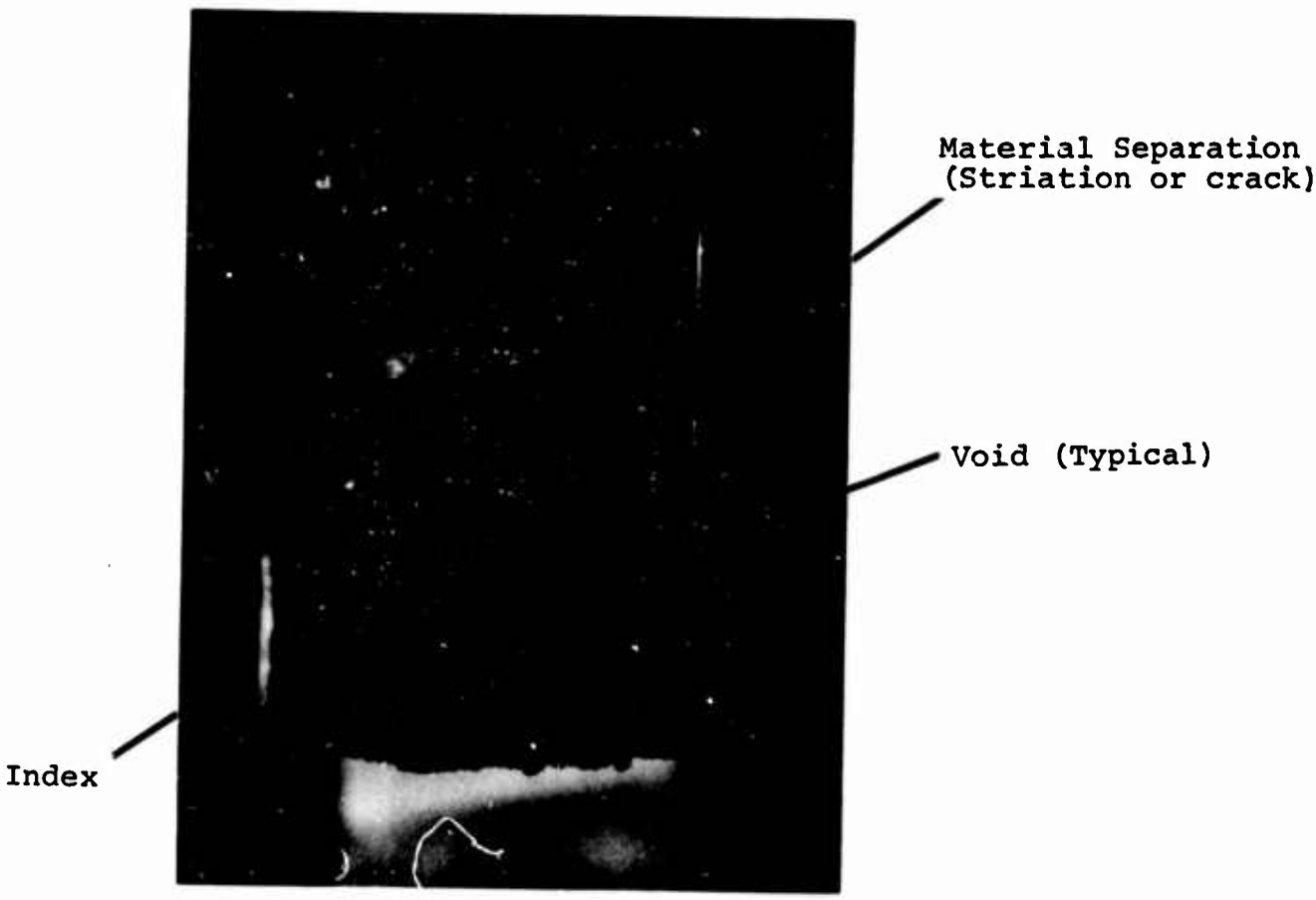

Figure 4. Photograph (3.3X) of Specimen CR-1-1500 (90° Orientation) from a Castable Carbon Material

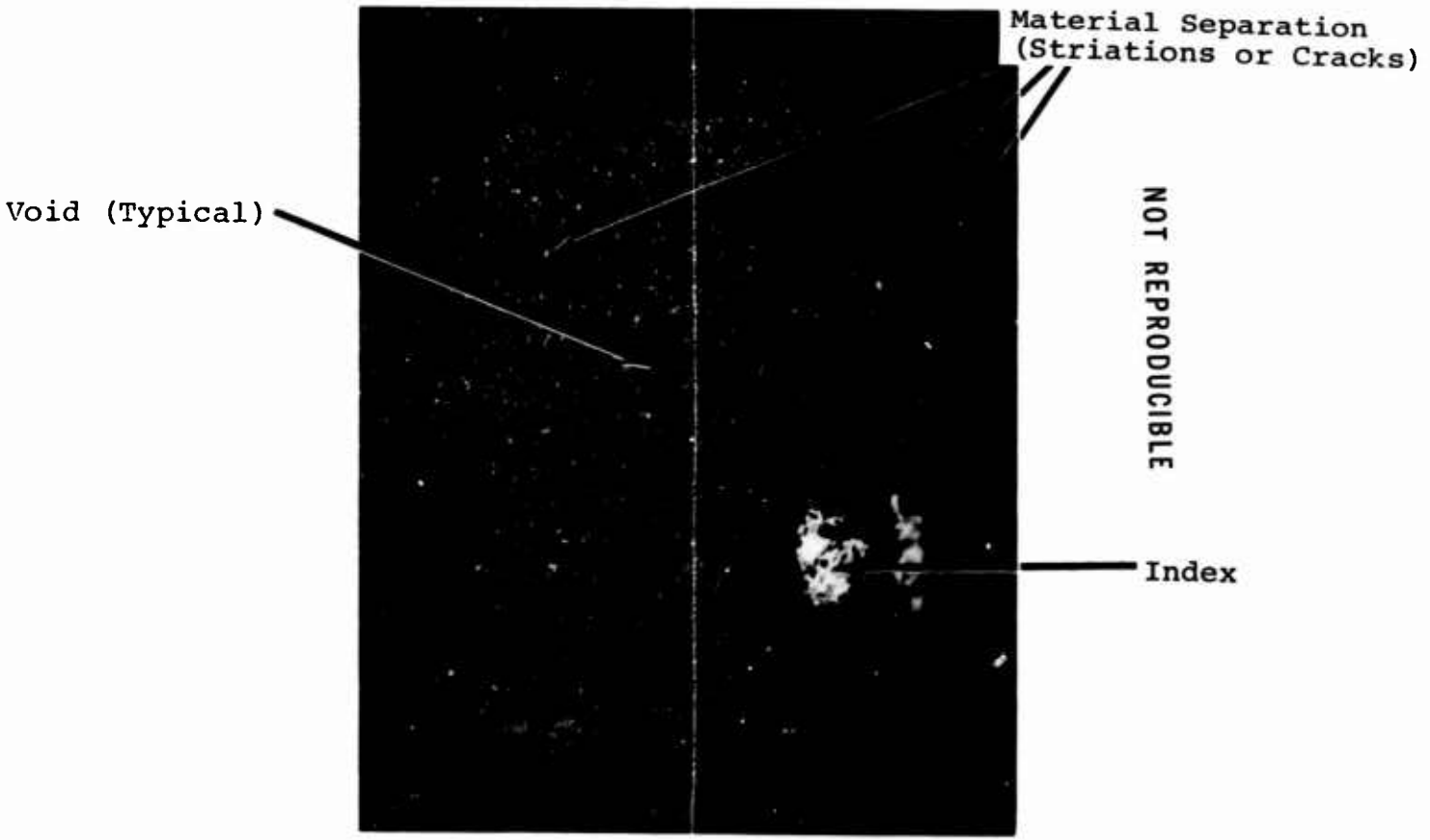

Figure 5. Photograph (3.3X) of Specimen CR-2-1500 (340° Orientation) from a Castable Carbon Material

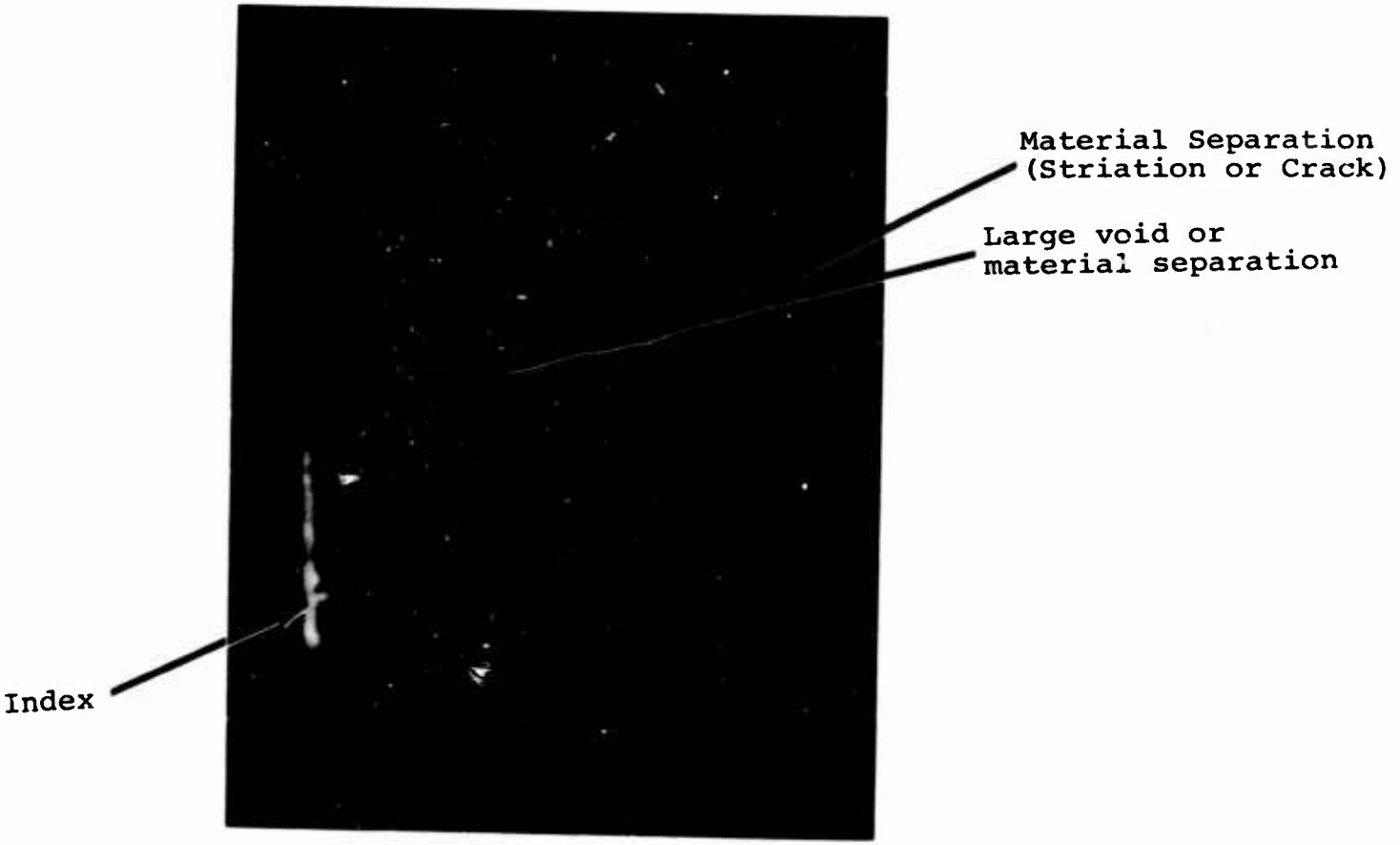

Figure 6. Photograph (3.3X) of Specimen CR-1-4000 (90° Orientation) from a Castable Carbon Material

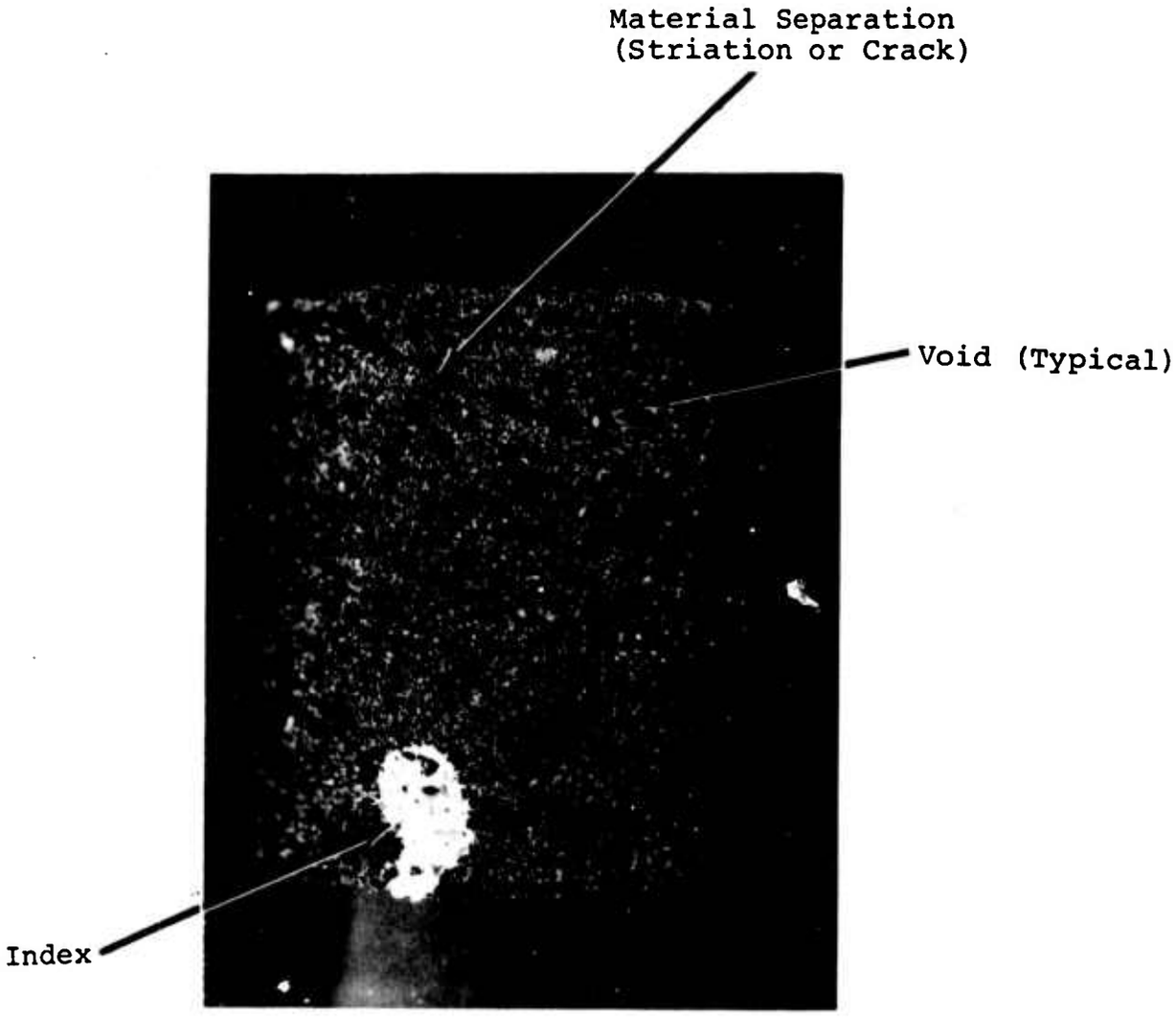

Figure 7. Photograph (3.3X) of Specimen CR-1-4000 (15° Orientation) from a Castable Carbon Material

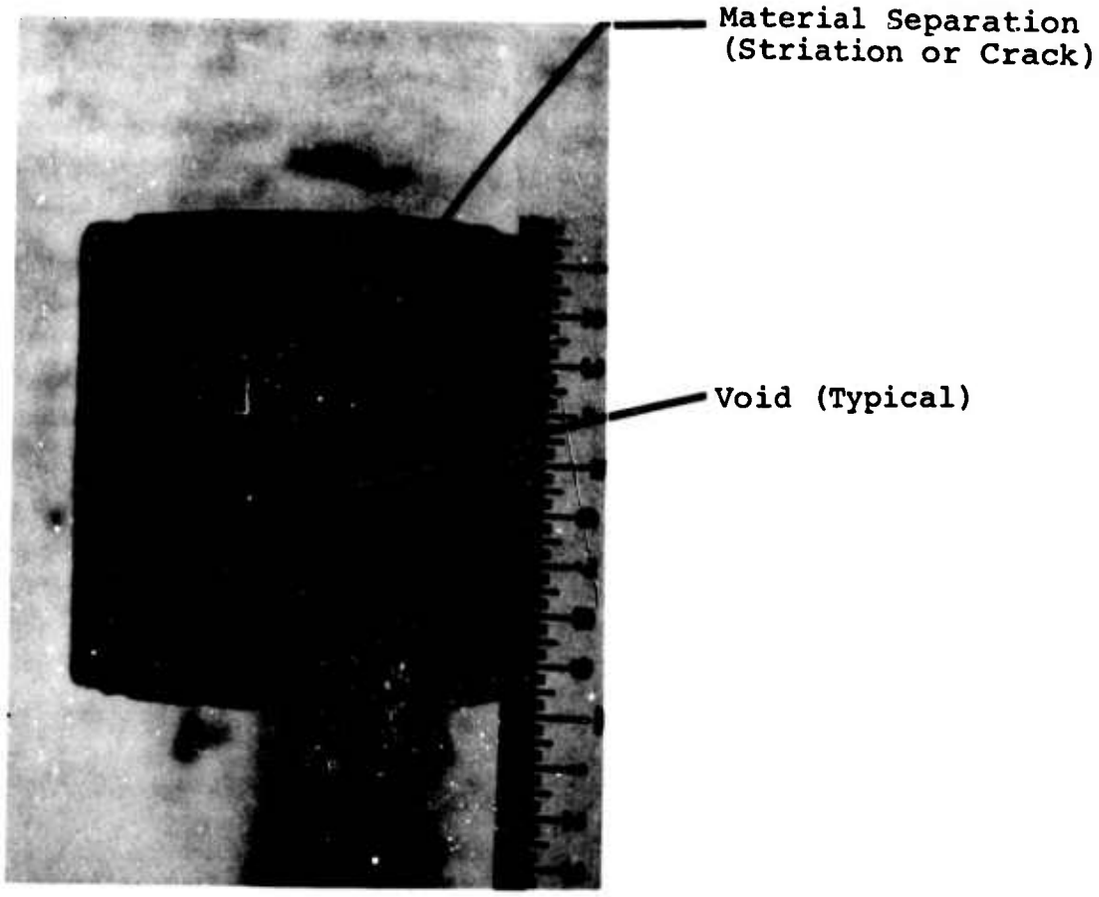

Figure 8. Photograph (2.5X) of Specimen CR-2-4000 from a Castable Carbon

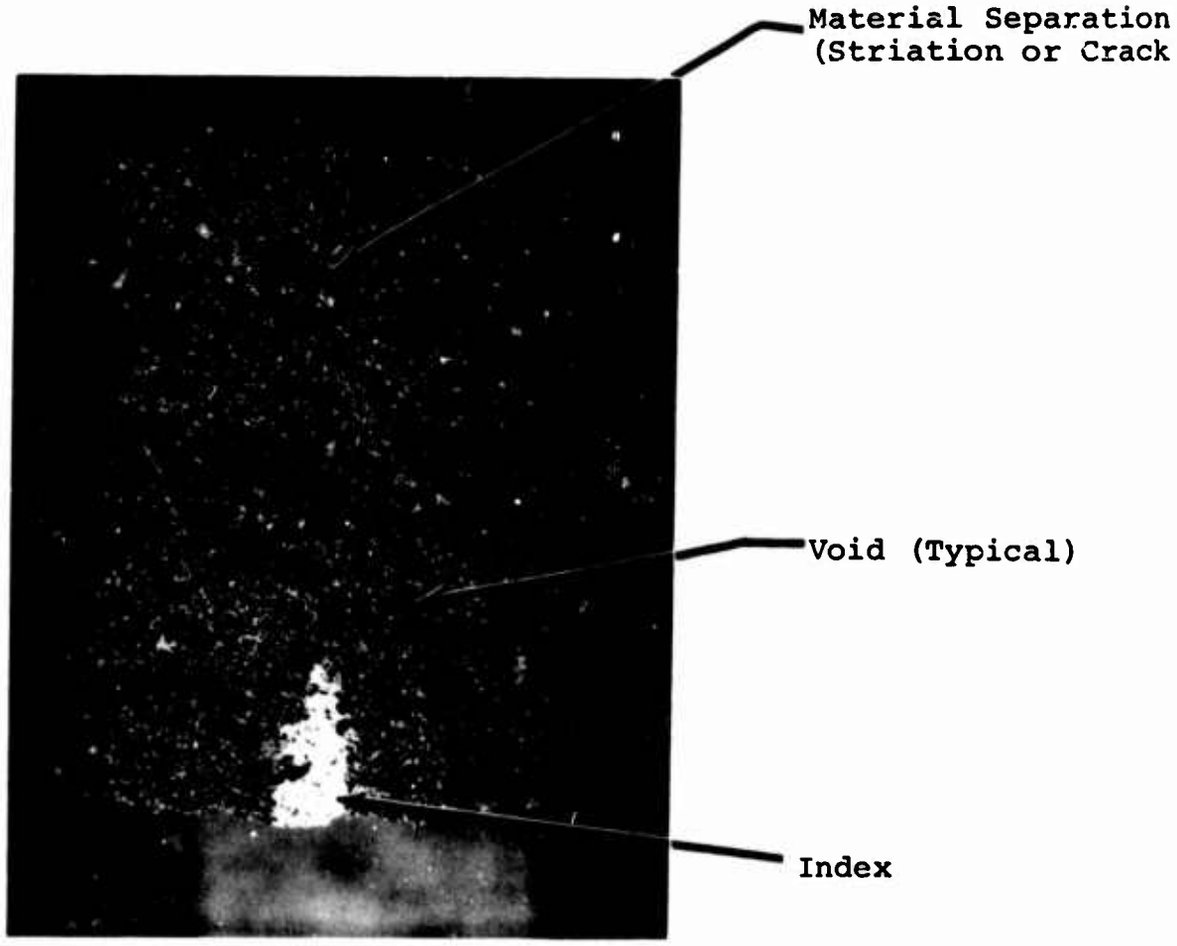

Figure 9. Photograph (4X) of Specimen RI-2-4000 (0° Orientation) from a Castable Carbon Material

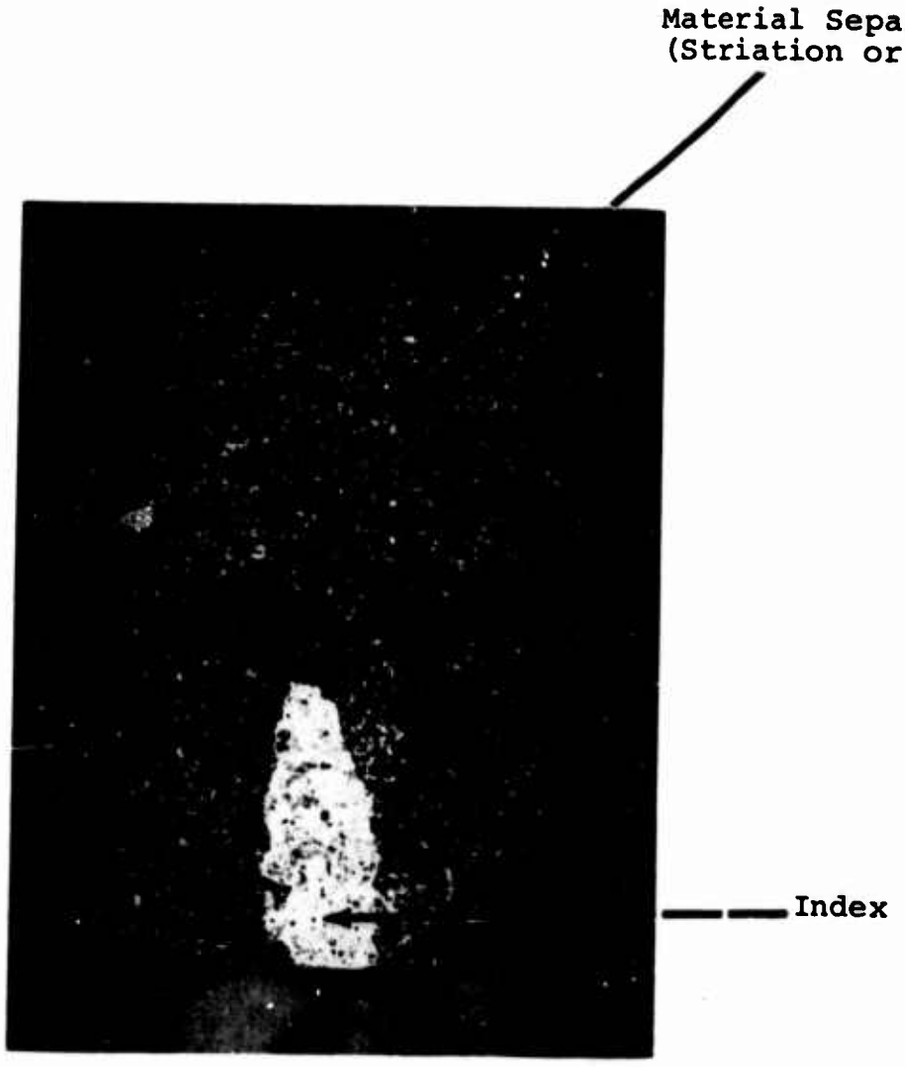

Figure 10. Photograph (4X) of Specimen RI-3-4000 (0° Orientation) from a Castable Carbon Material

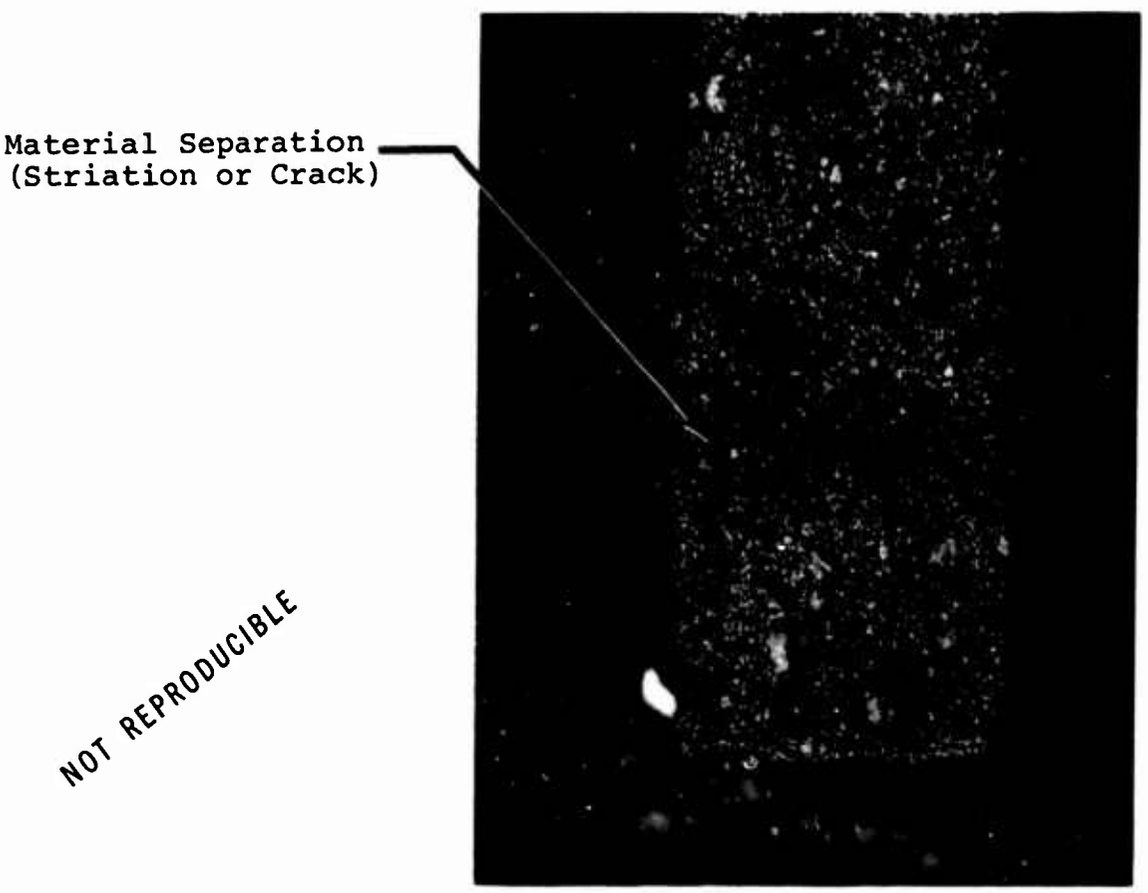

Figure 11. Photograph (3.6X) of Specimen CTE-1-4000 from a Castable Carbon Material

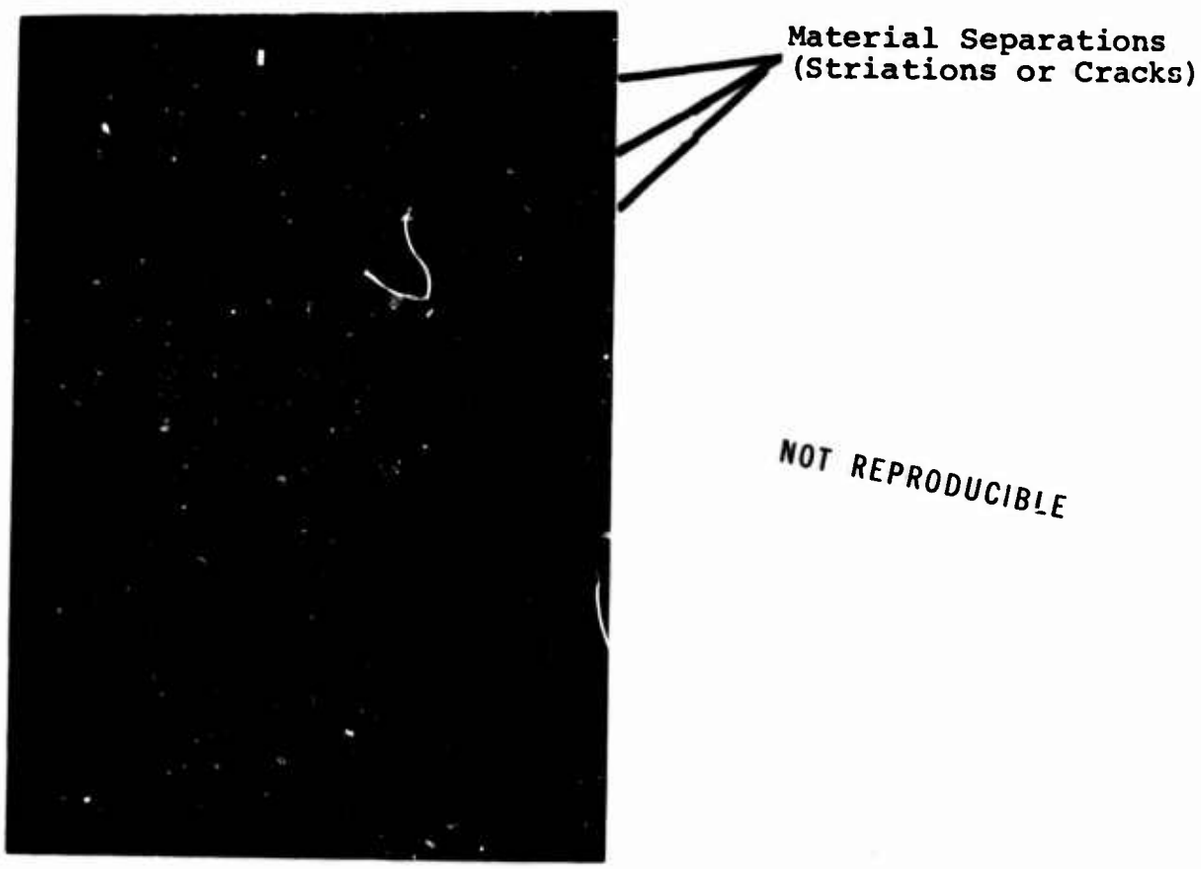

Figure 12. Photograph (3.6X) of Specimen CTE-2-4000 from a Castable Carbon Material

225

CR 1 70

Figure 13. Radiograph (Photographically Reproduced) of Specimen CR-1-70 from a Castable Carbon Material

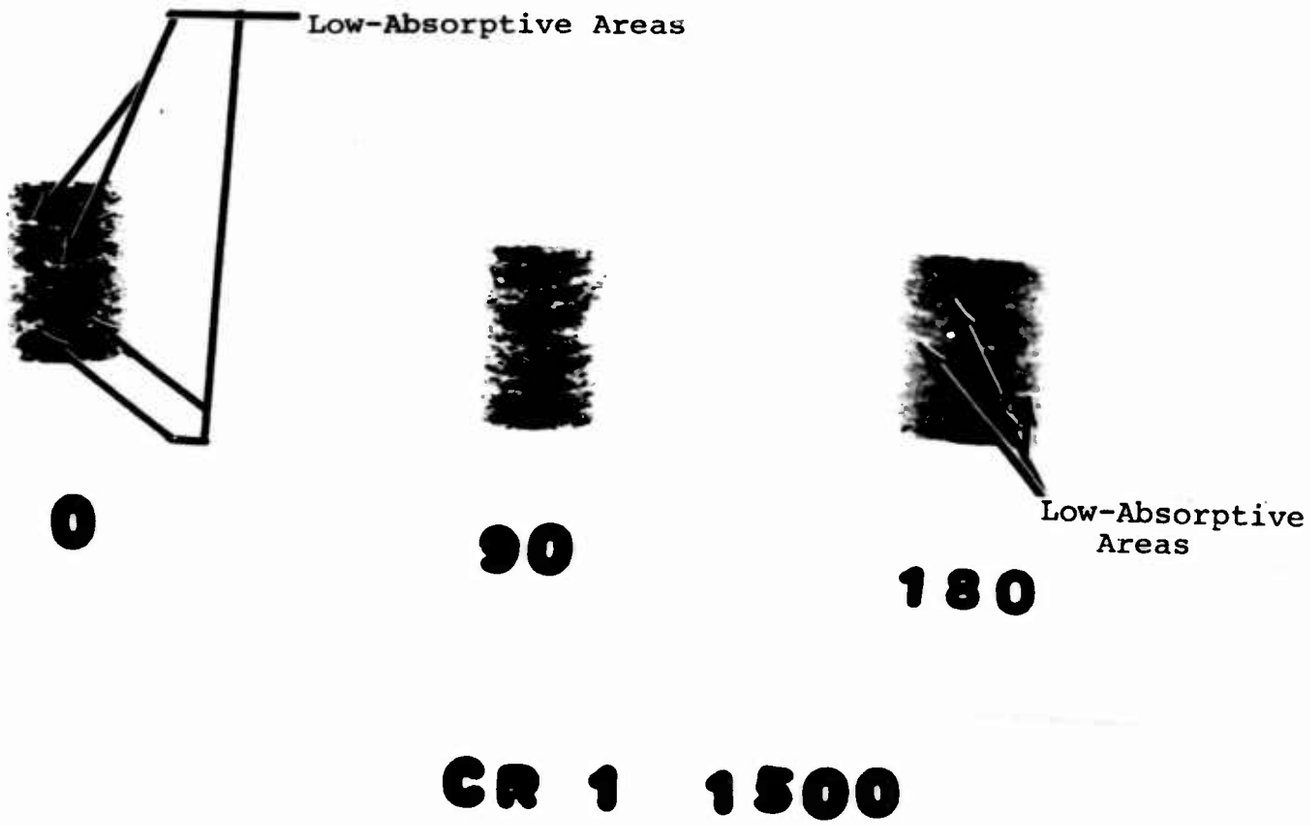

Figure 14. Radiograph (Photographically Reproduced) of Specimen CR-1-1500 from a Castable Carbon Material

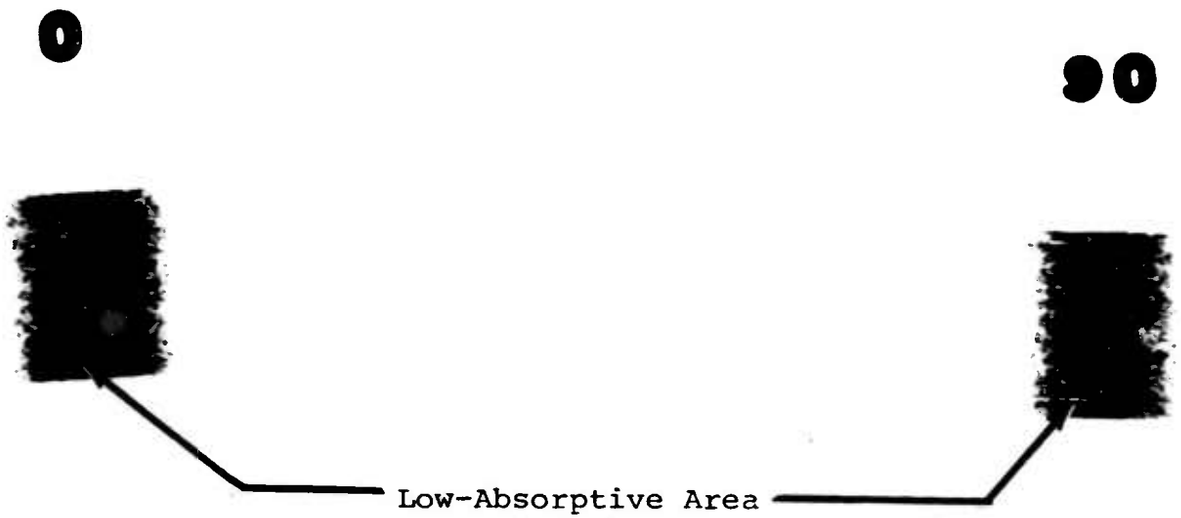

(Actual Size)

Figure 15. Radiograph (Photographically Reproduced) of Specimen RI-2-4000 from a Castable Carbon Material

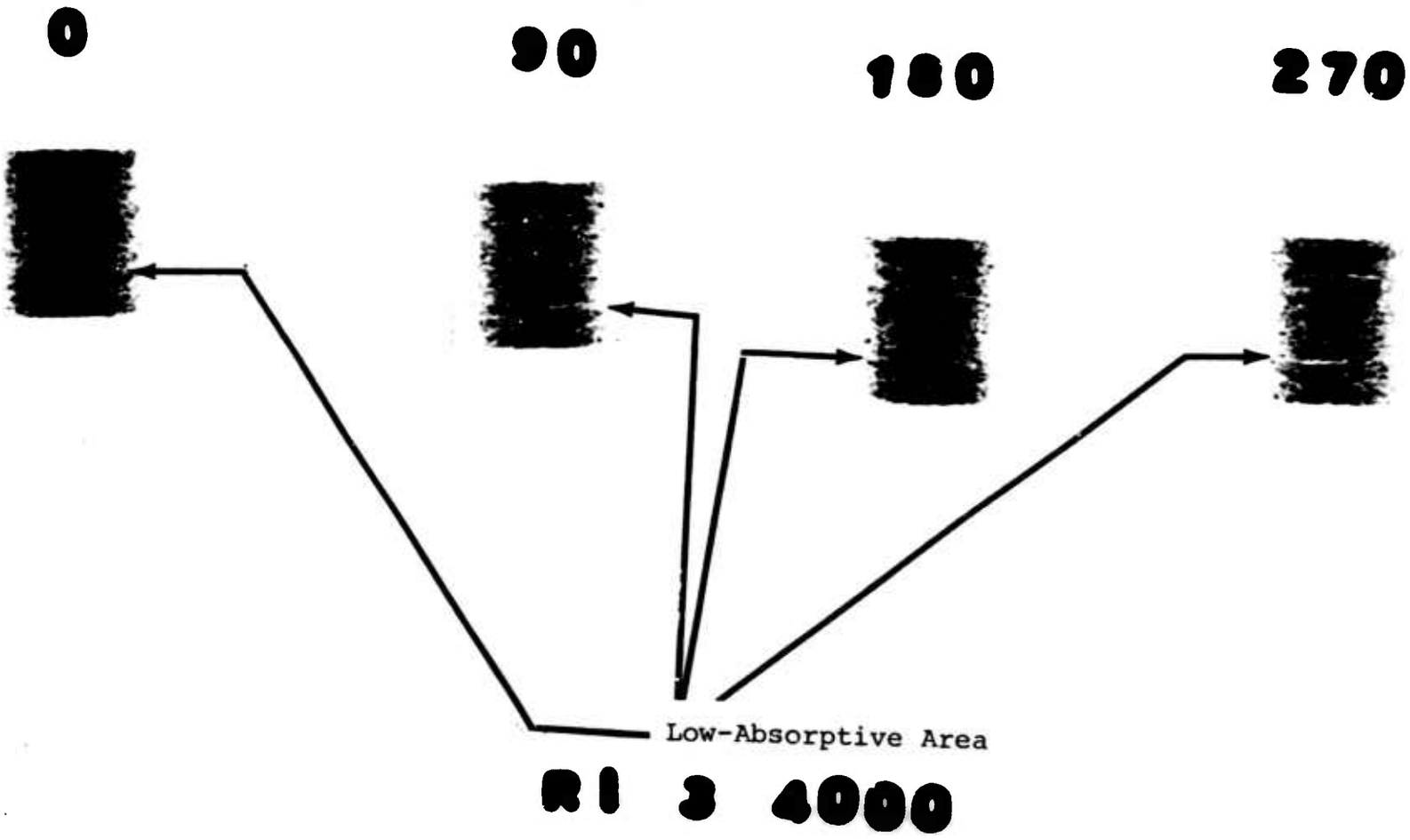

(Actual Size)

Figure 16. Radiograph (Photographically Reproduced) of Specimen RI-3-4000 from a Castable Carbon Material

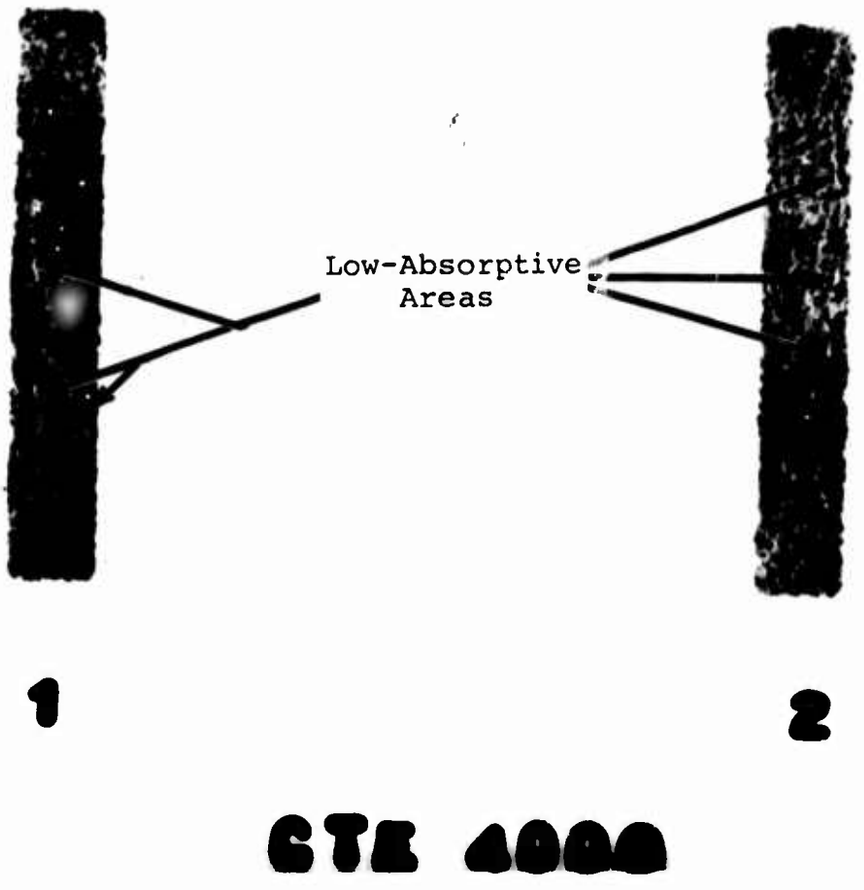

Figure 17. Radiograph (Photographically Reproduced) of Specimen CTE-1-4000 and CTE-2-4000 from a Castable Carbon Material

INNER SURFACE
35X - ACTUAL SIZE

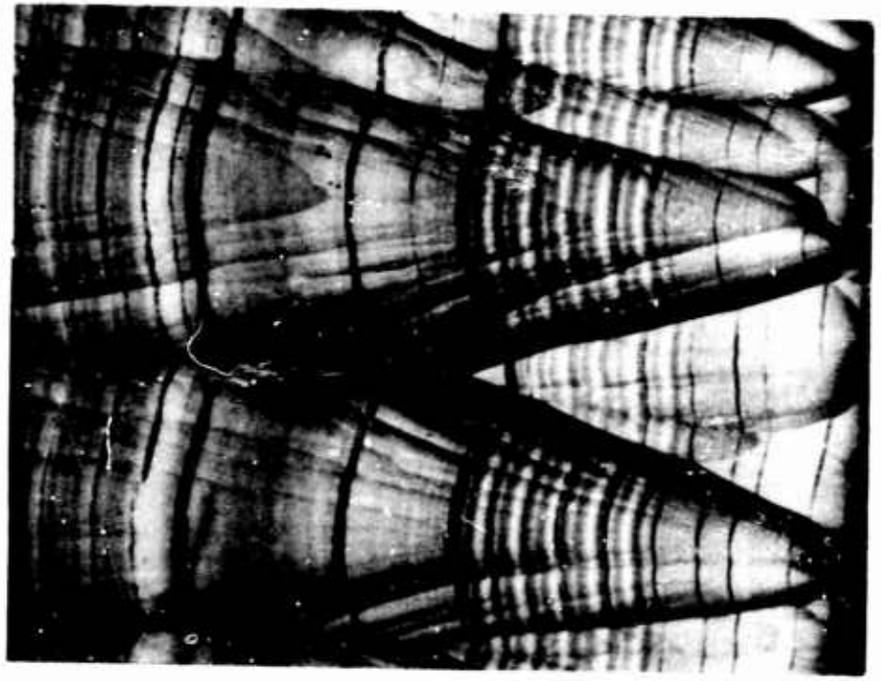

INNER SURFACE
100X - ACTUAL SIZE

NOTE: TWO INCH LONG SLEEVE WAS CUT INTO TWO HALVES AFTER RUN COMPLETED
(Exposed - 4,000°F) AND PHOTOMICROGRAPHS WERE TAKEN .

Figure 18. Photomicrographs (35X and 100X) in the Axial Direction Made on Fibrous PG Sleeve (Ring No. 3).

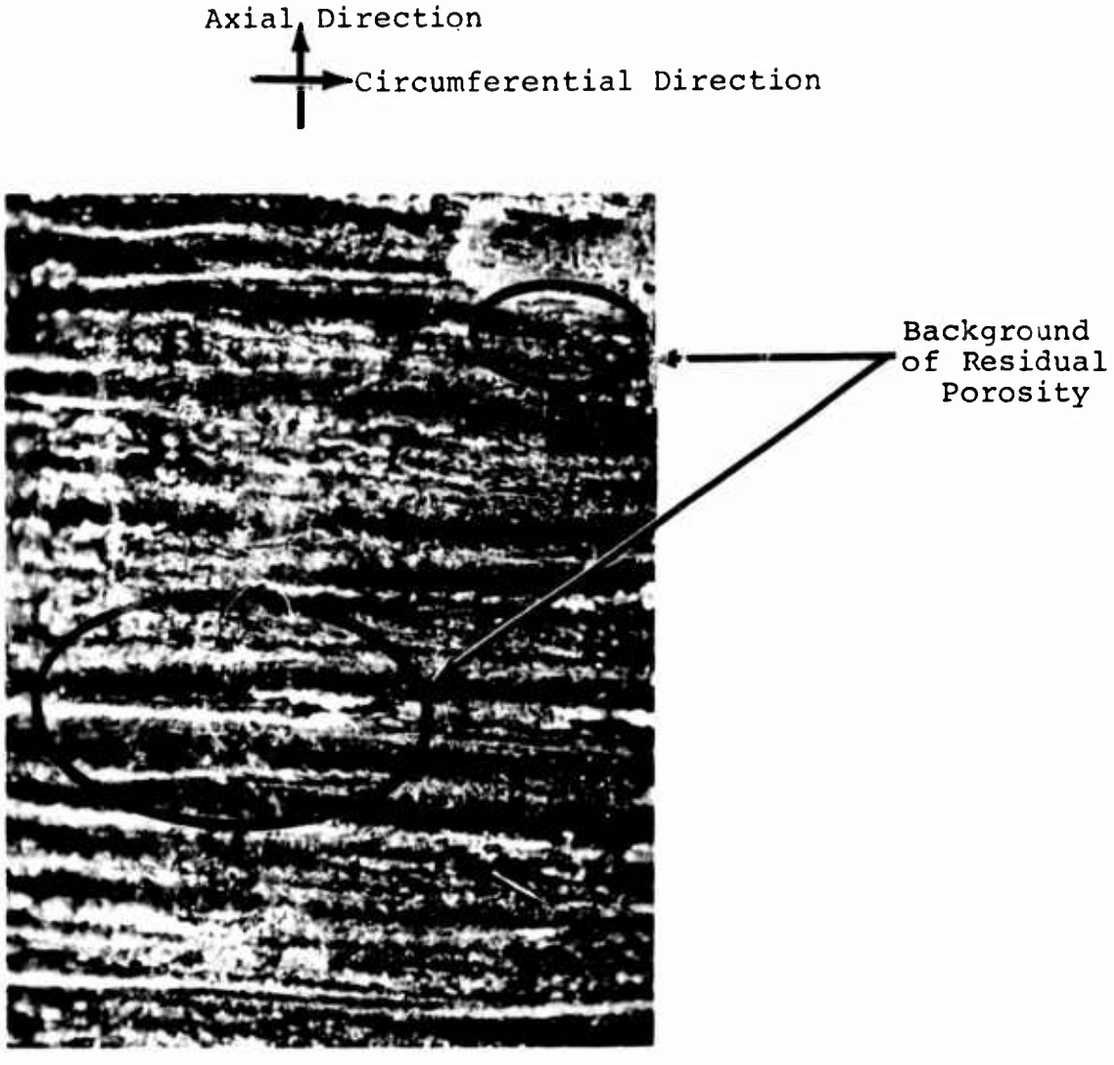

Figure 19. Photomicrograph (10X) of Outer Surface of an As-Received Fibrous PG Sleeve Showing Residual Porosity Background

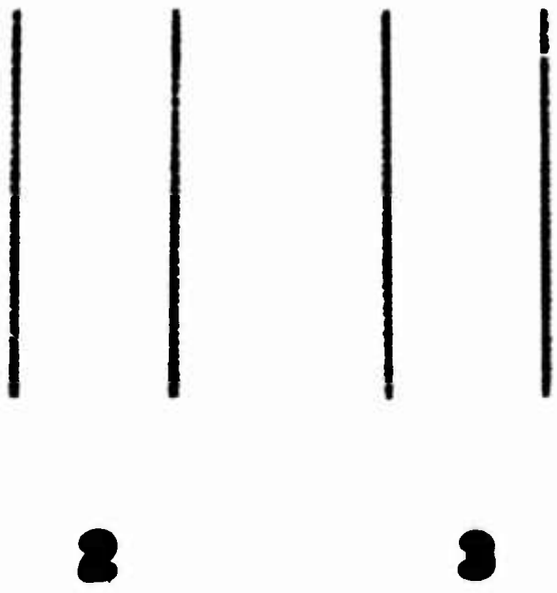

Note: White spots in walls are ~0.02 inch low-absorptive spots.

Figure 20. Radiograph (Photographically Reproduced) Showing Typical Sidewall of Fibrous PG Sleeves - 0° View

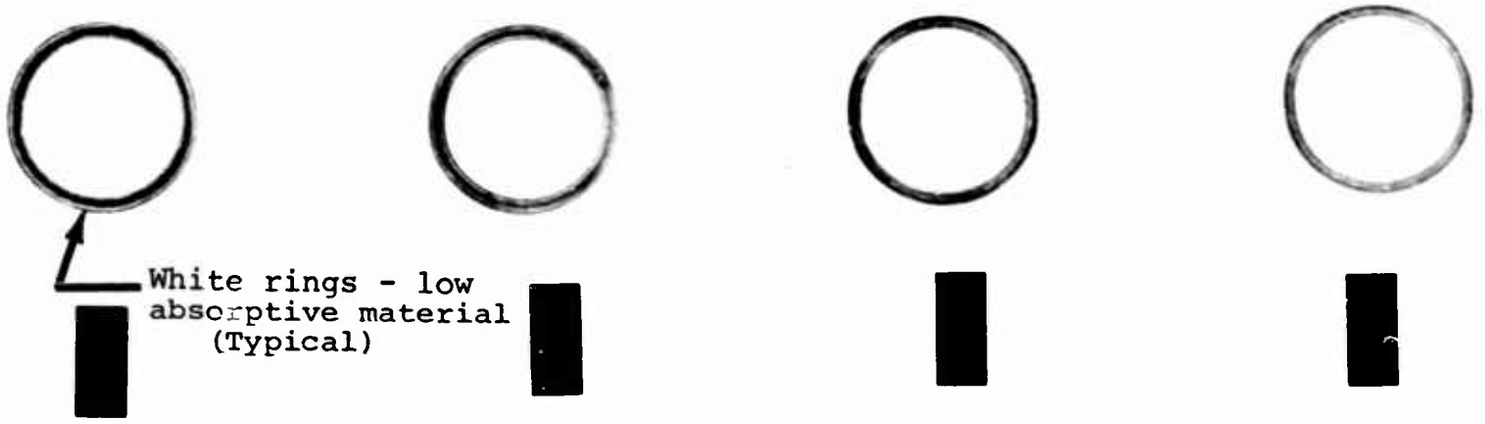

Figure 21. Radiograph (Photographically Reproduced) in Axial Direction on 0.125-Inch High Rings Removed from As-Received Fibrous PG Sleeve

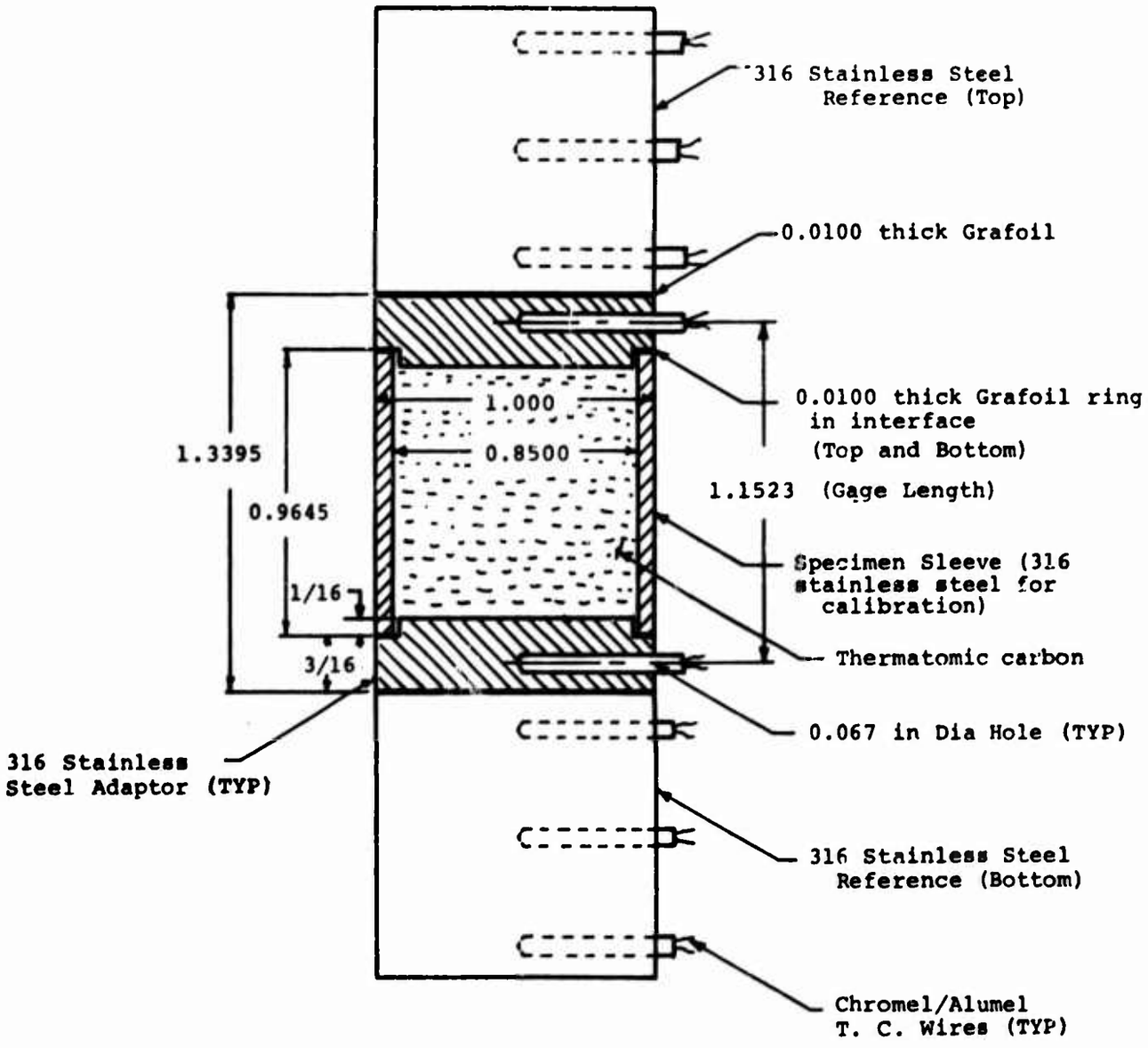

Figure 22. Schematic of Calibration Buildup for 316 Stainless Steel Sleeve used in the Comparative Rod Apparatus

Note: The same buildup was used during evaluationn on Fibrous PG Sleeve in the axial (a-b) Direction

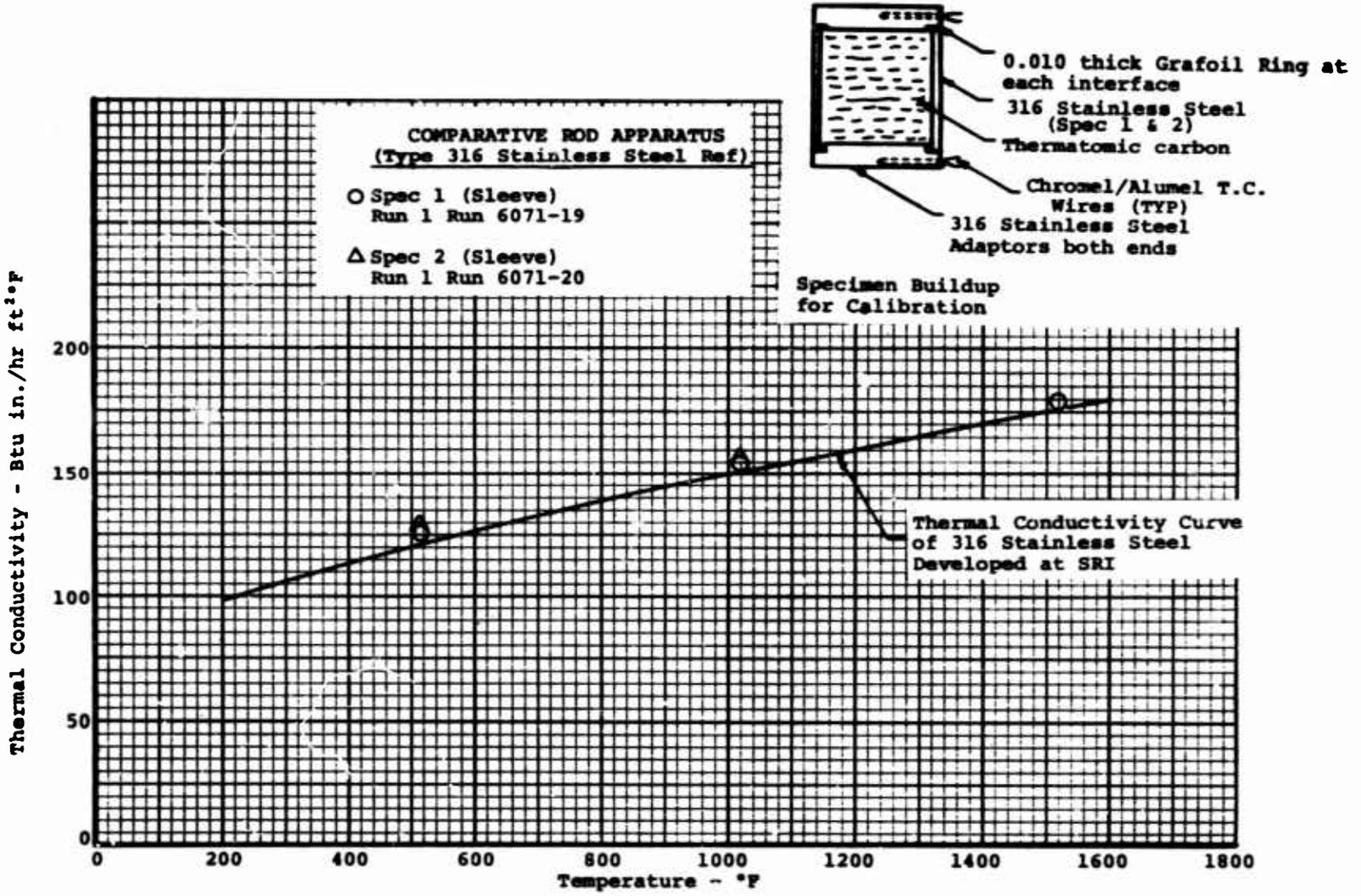

Figure 23. Calibration of Type 316 Stainless Steel Sleeve Using Adaptors

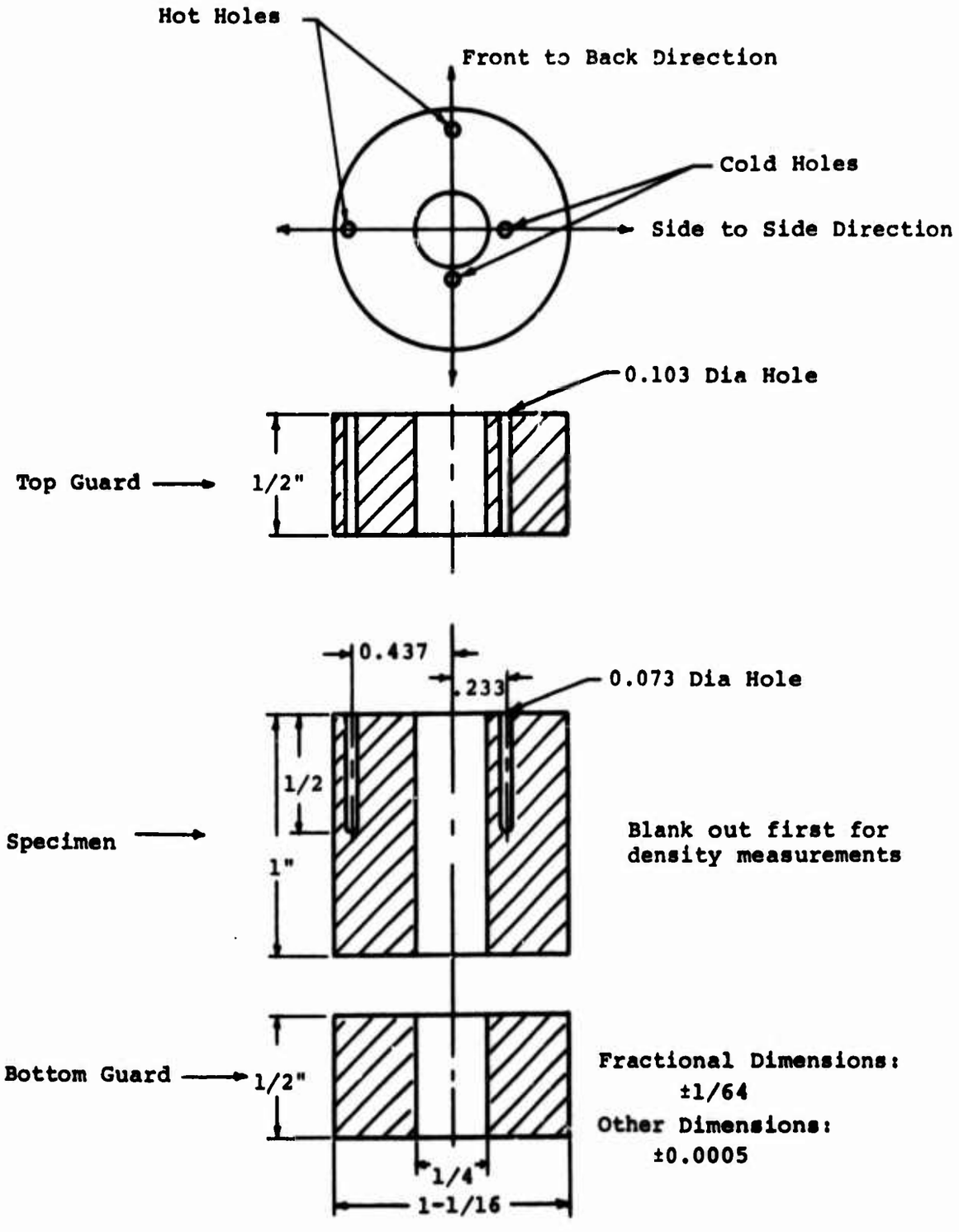

Figure 24. Configuration of the Cylindrical Thermal Conductivity Specimen for the Radial Inflow Apparatus

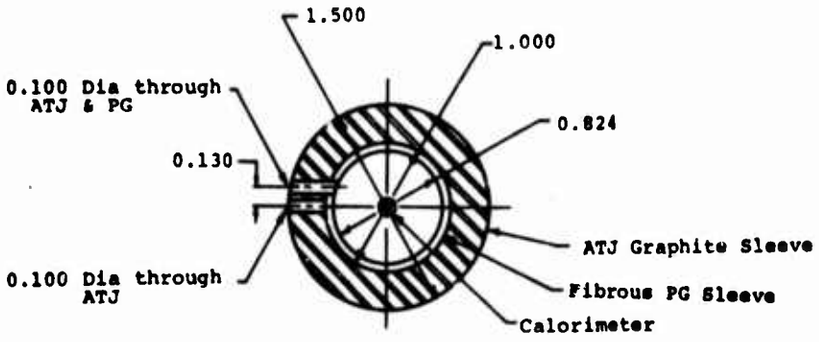

Section A-A
Detail of Sight Hole

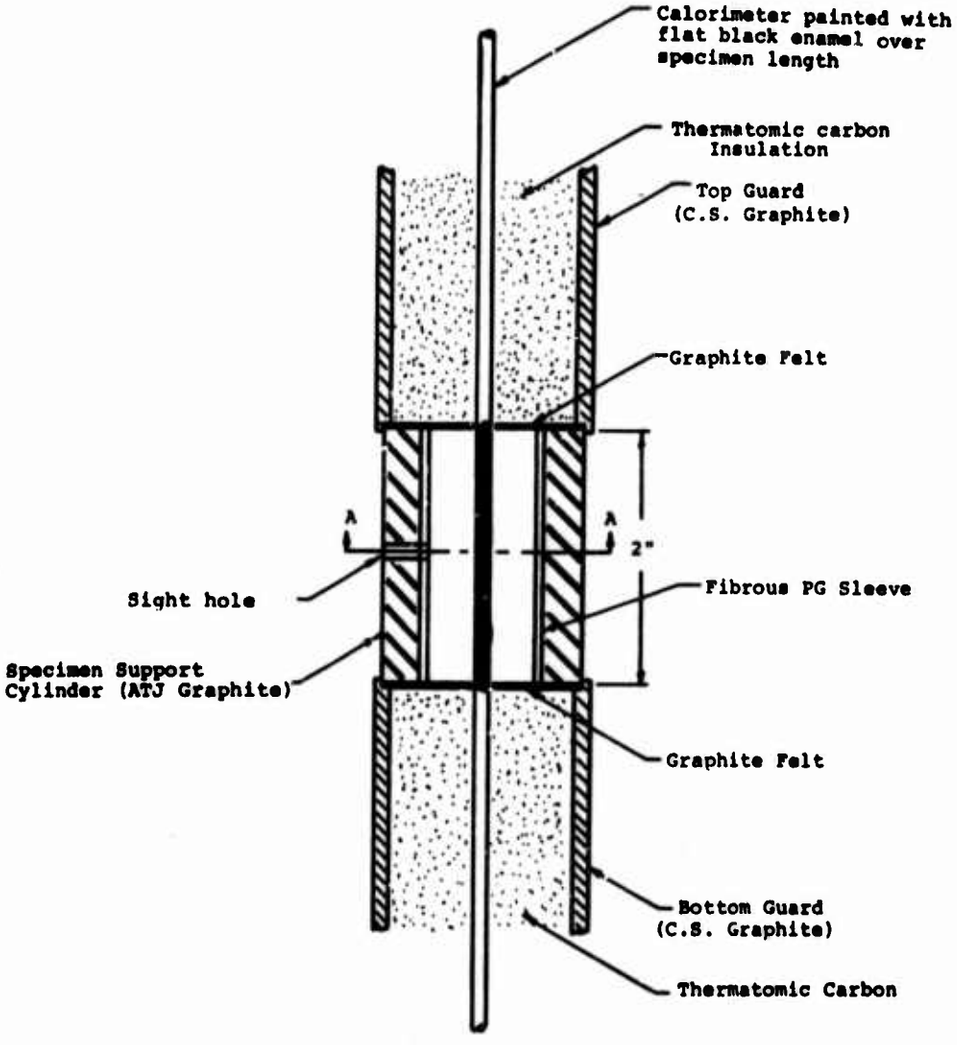

Figure 25. Buildup for Optical Measurements of Inside Surface Temperature of Fibrous PG Sleeve during thermal conductivity measurements in the "c" Direction using the Radial Inflow Apparatus

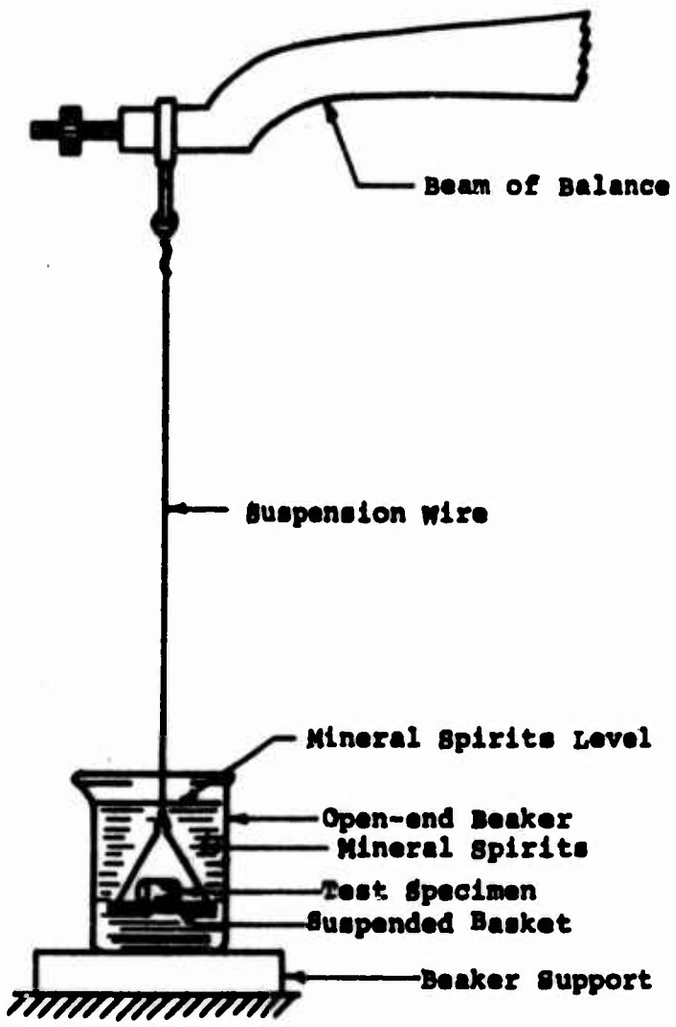

Figure 26. Setup for Determining Suspended Weight of Saturated Specimen for Liquid Absorption Evaluation

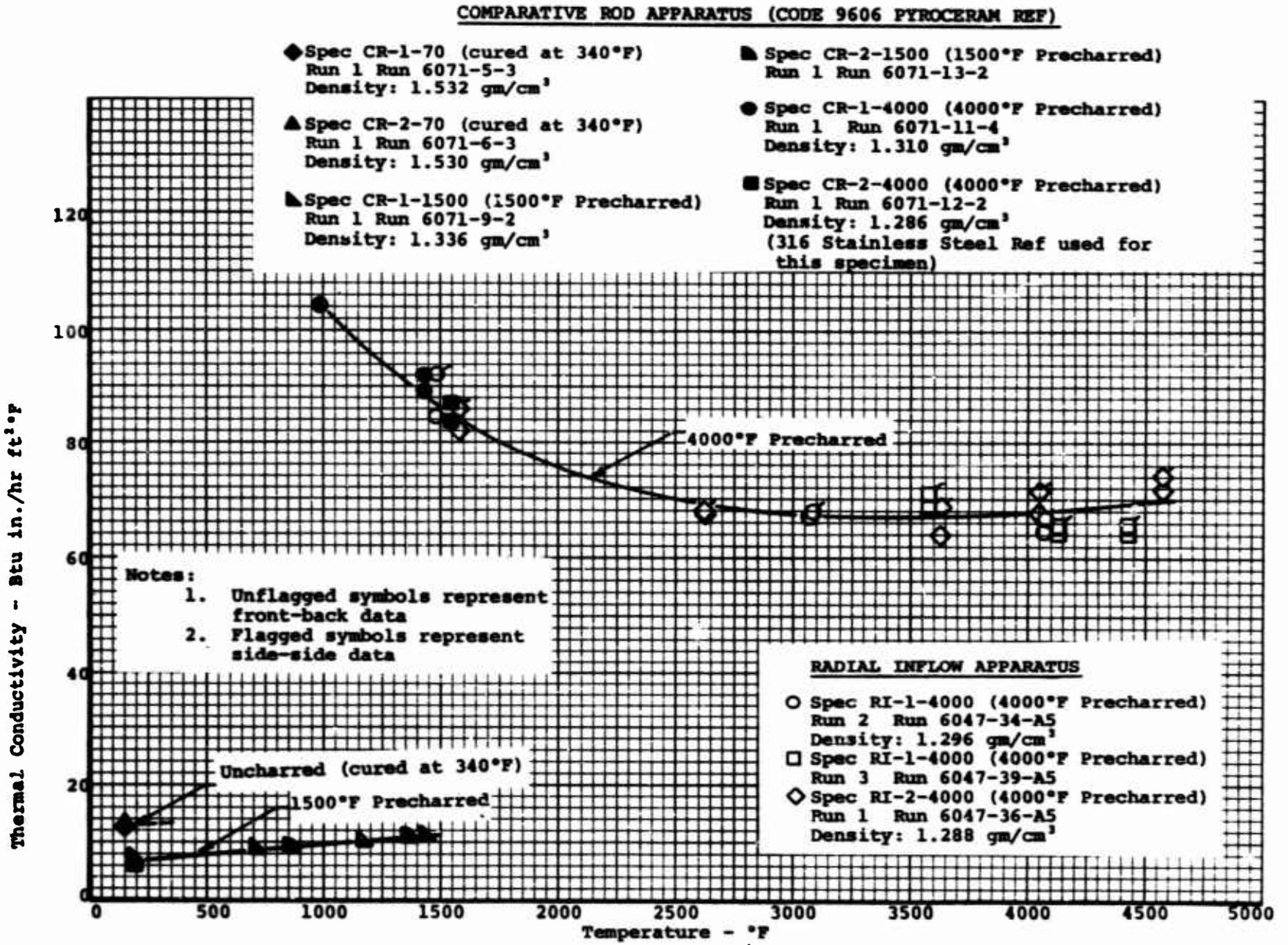

Figure 27. Thermal Conductivity of Castable Carbon

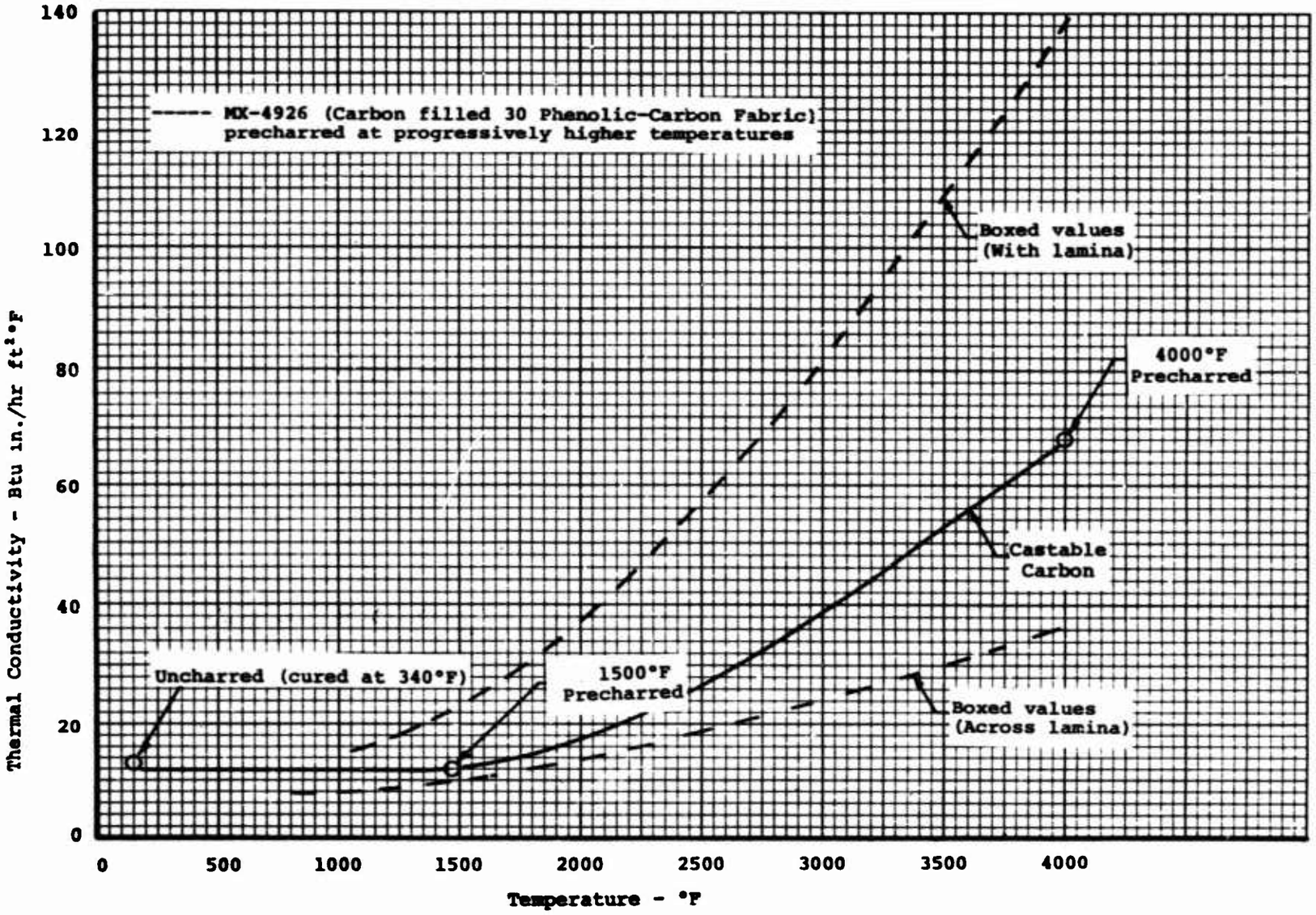

Figure 28. Thermal Conductivity of Castable Carbon (Virgin (340°F), 1500°F Precharred and 4000°F Precharred)

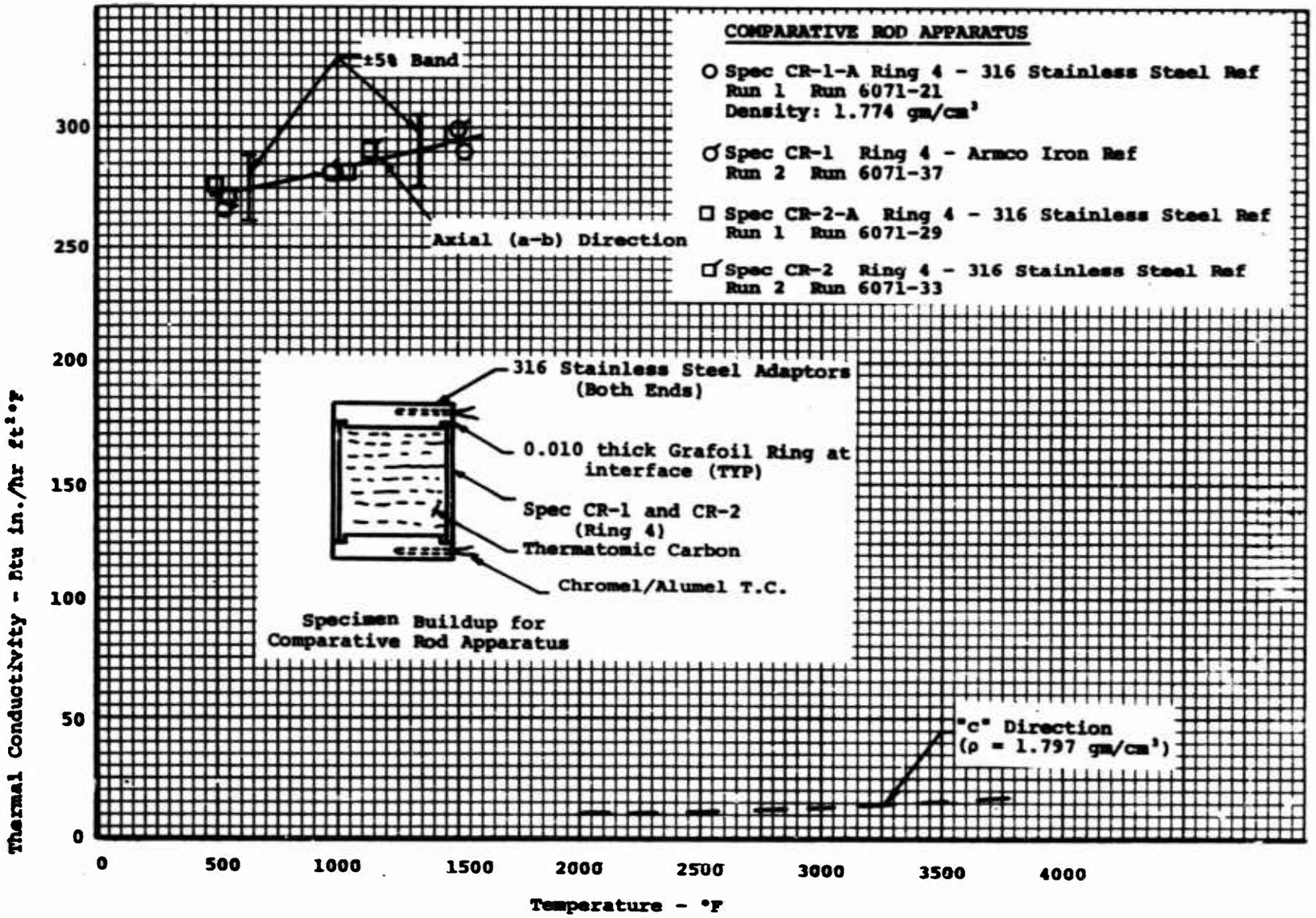

Figure 29. Thermal Conductivity of Fibrous PG Sleeve in the Axial (a-b) Direction

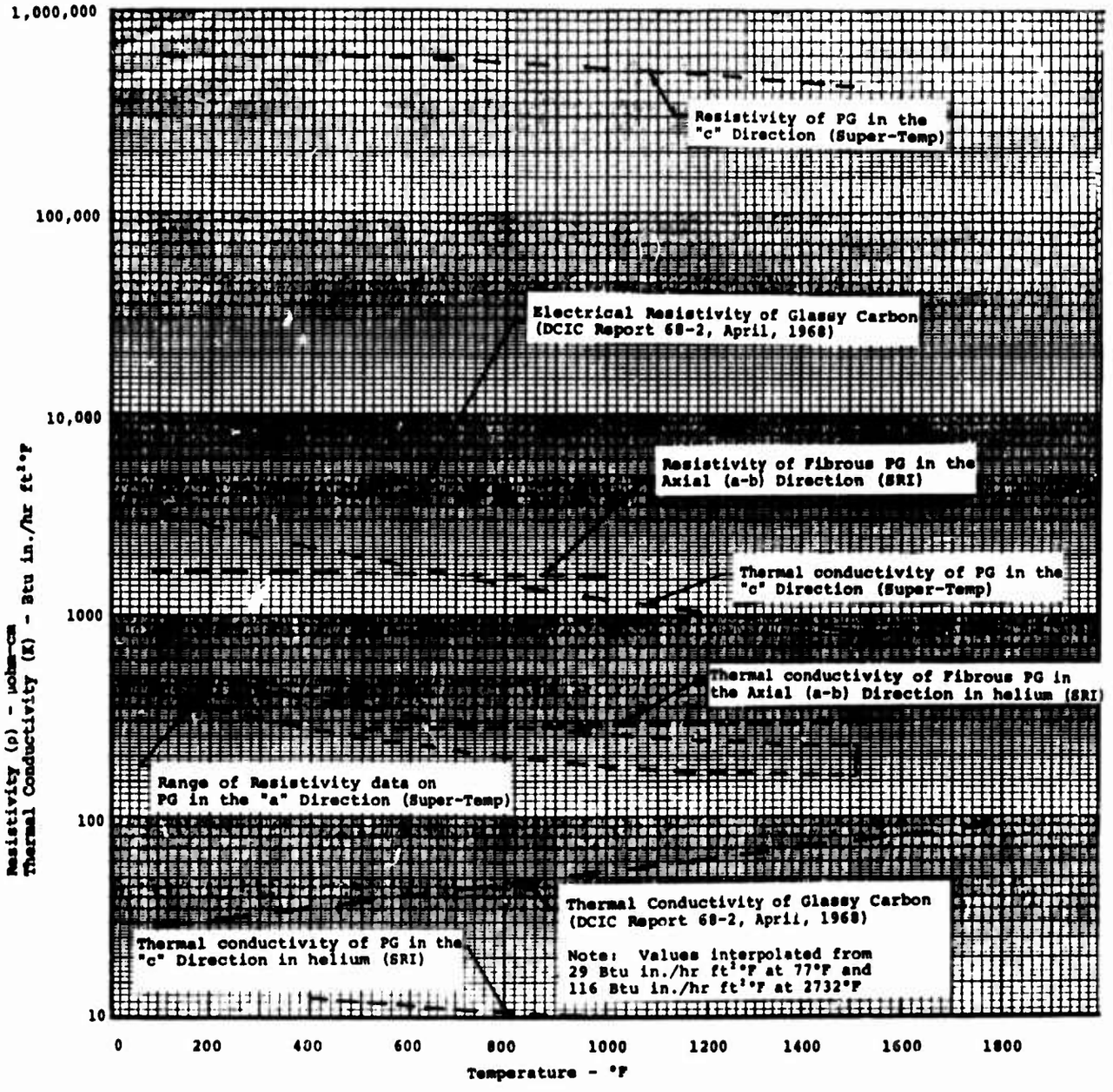

Figure 30. Composite Plots of Electrical Resistivities and Thermal Conductivities for PG, Fibrous PG and Glassy Carbon

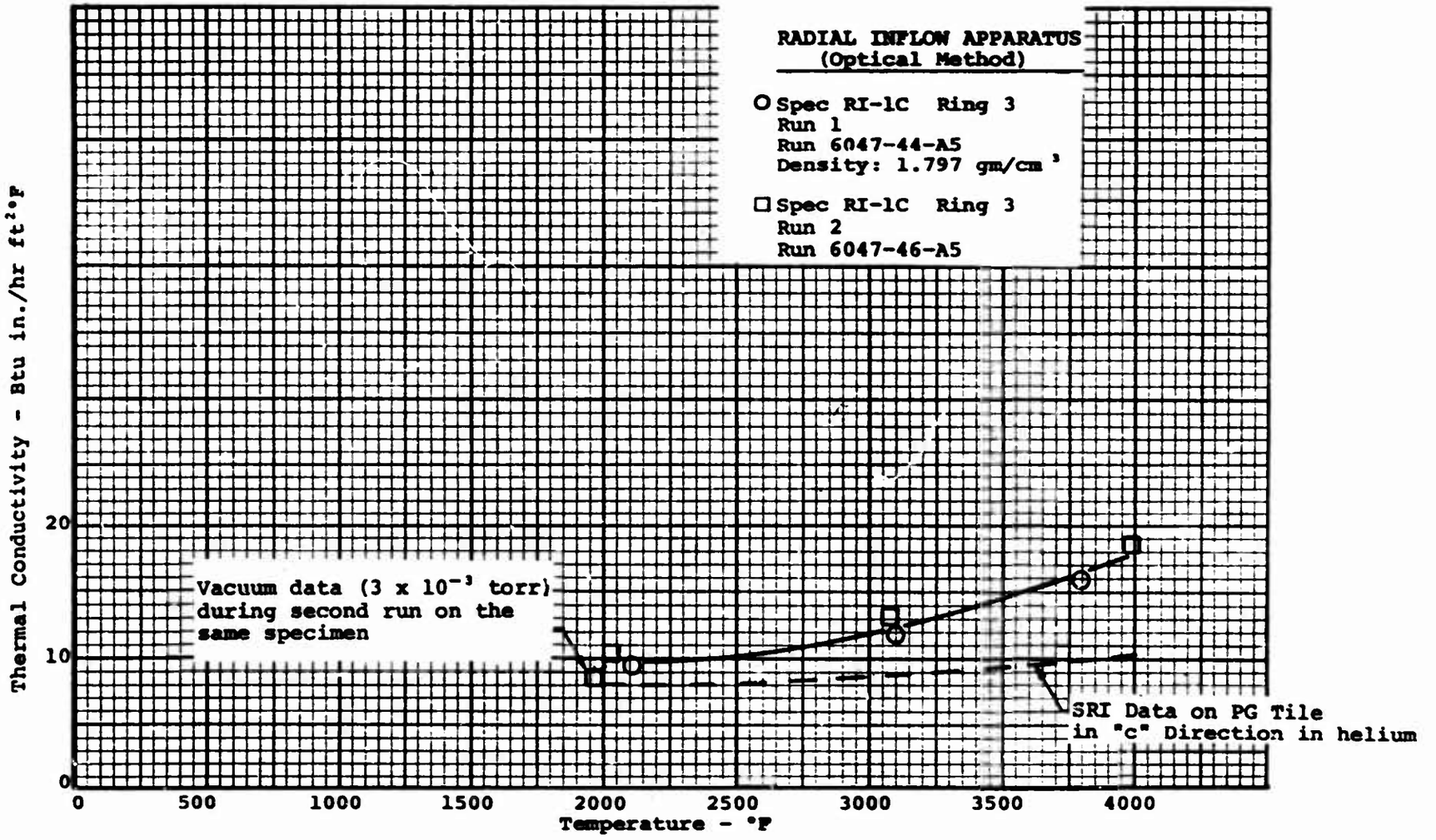

Figure 31. Thermal Conductivity of Fibrous PG Sleeve in the "c" Direction

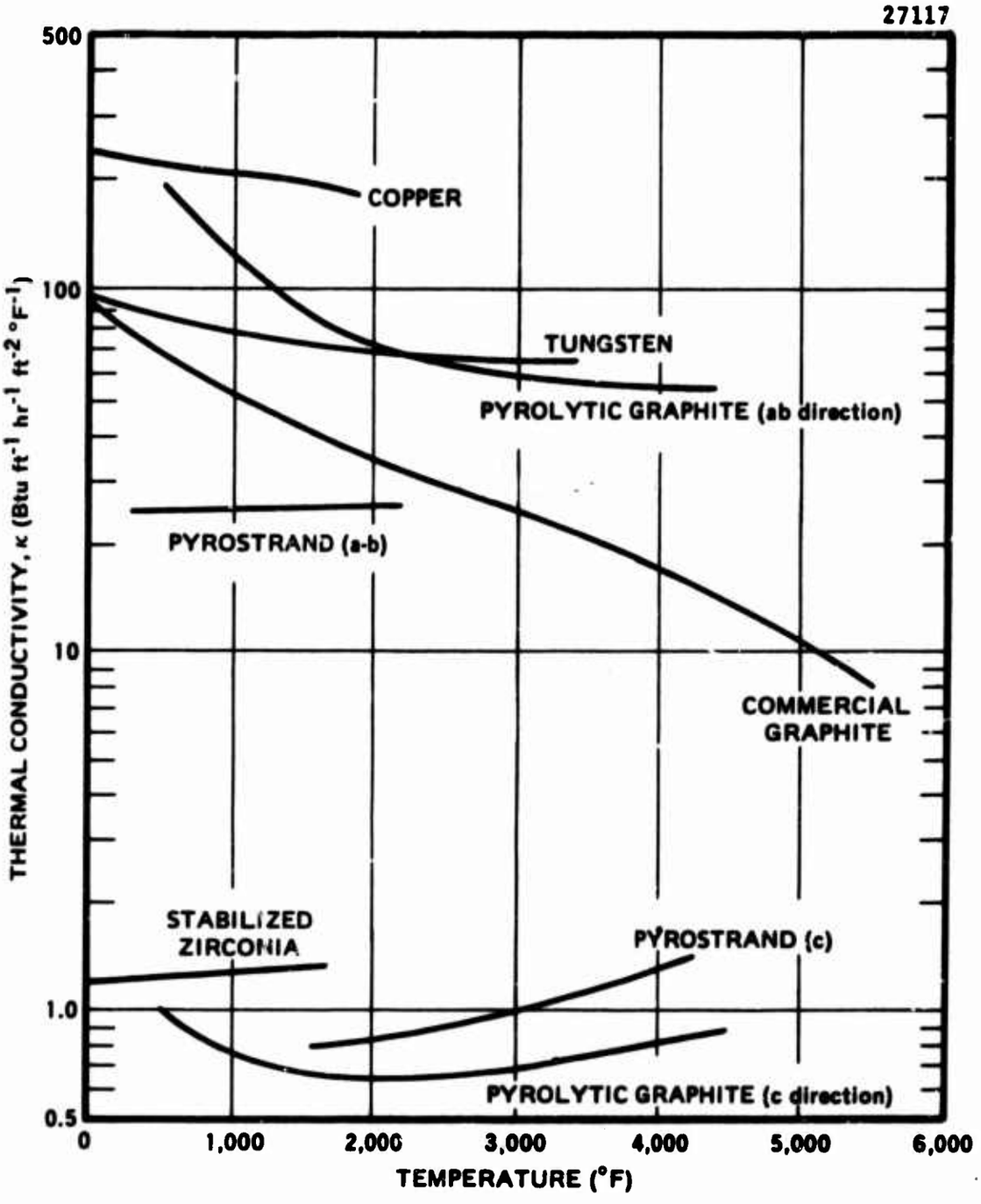

Figure 32. Thermal Conductivity of Materials.

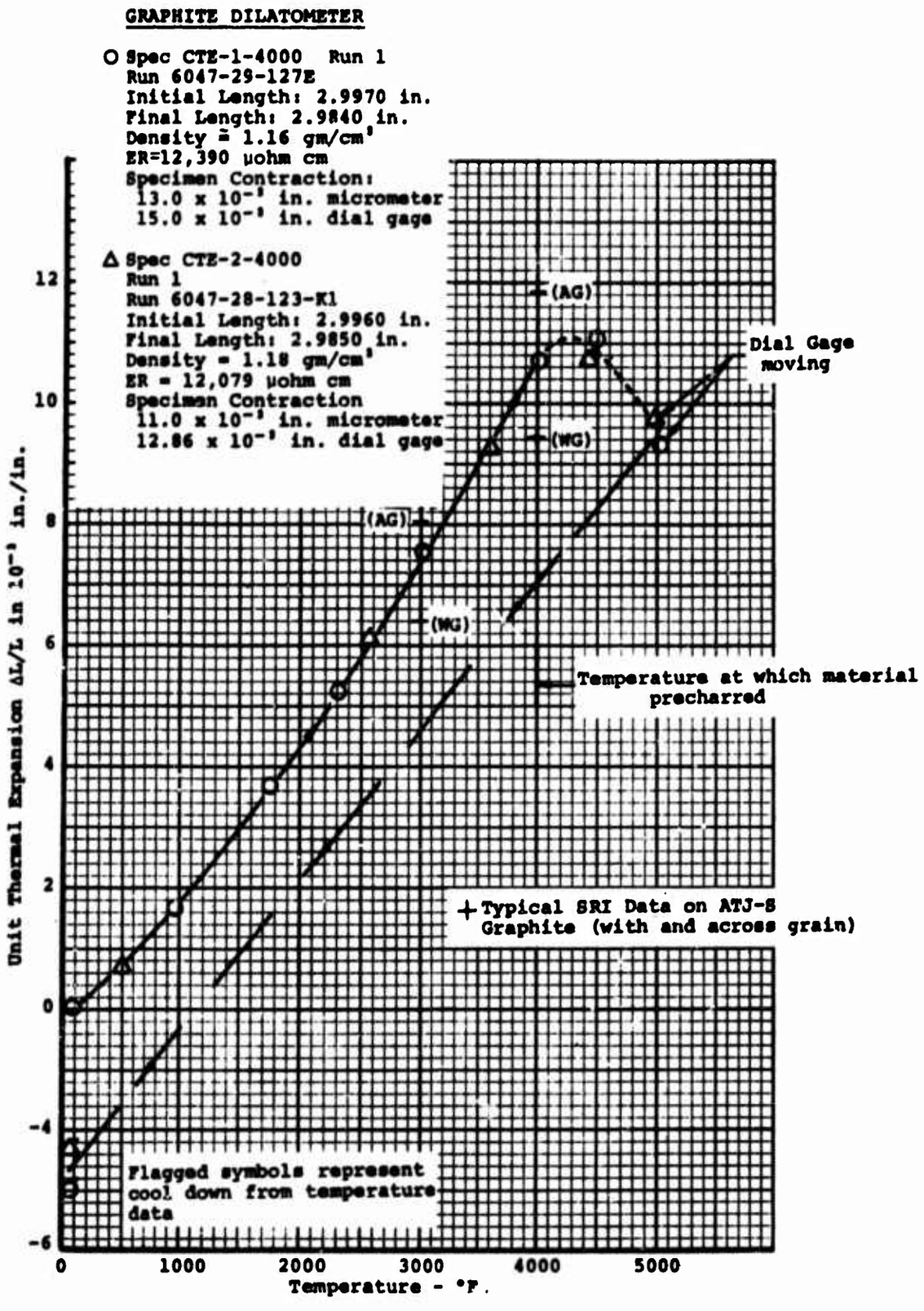

Figure 33. Thermal Expansion of Castable Carbon — 4000°F Precharred

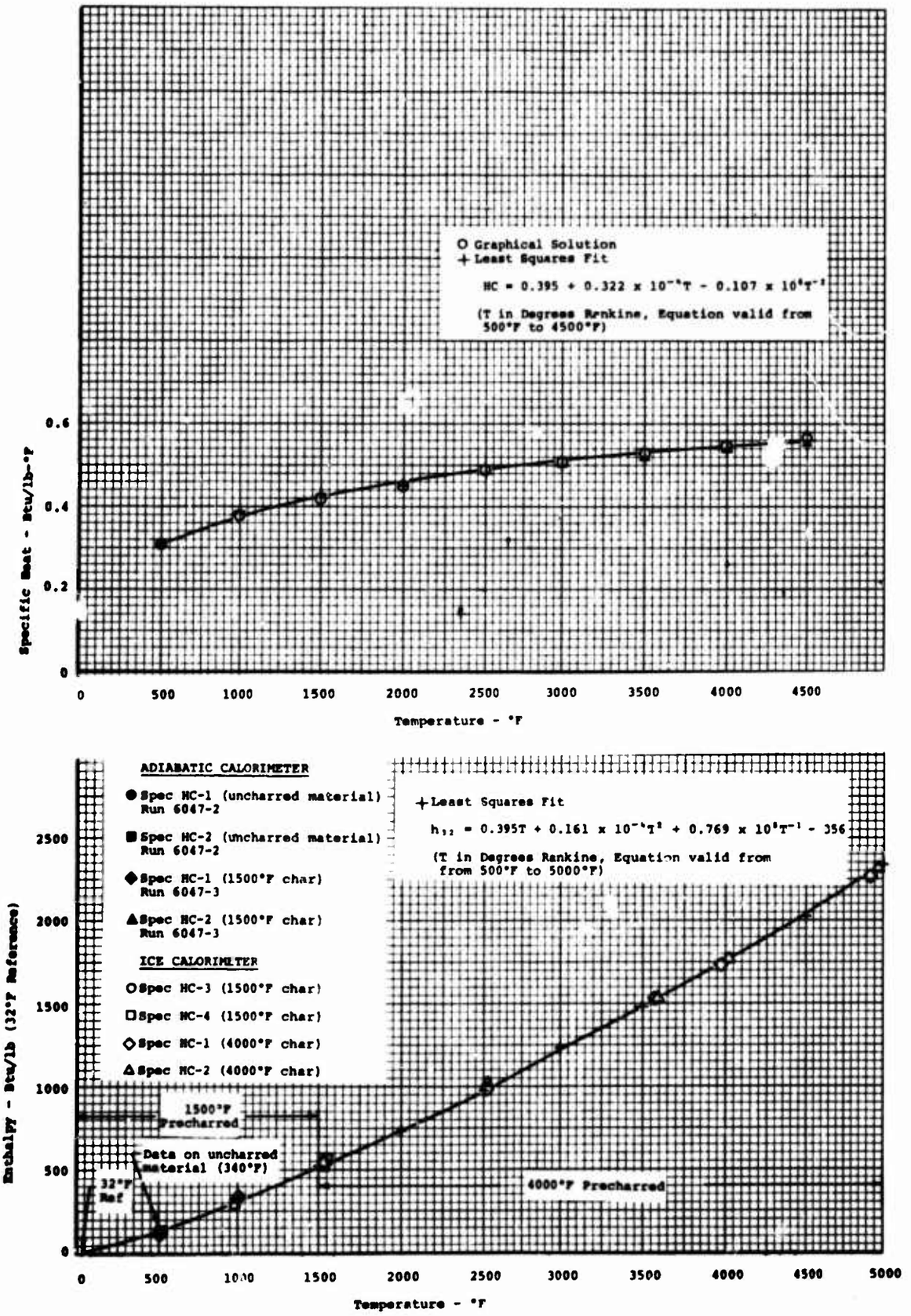

Figure 34. Enthalpy and Specific Heat of Castable Carbon

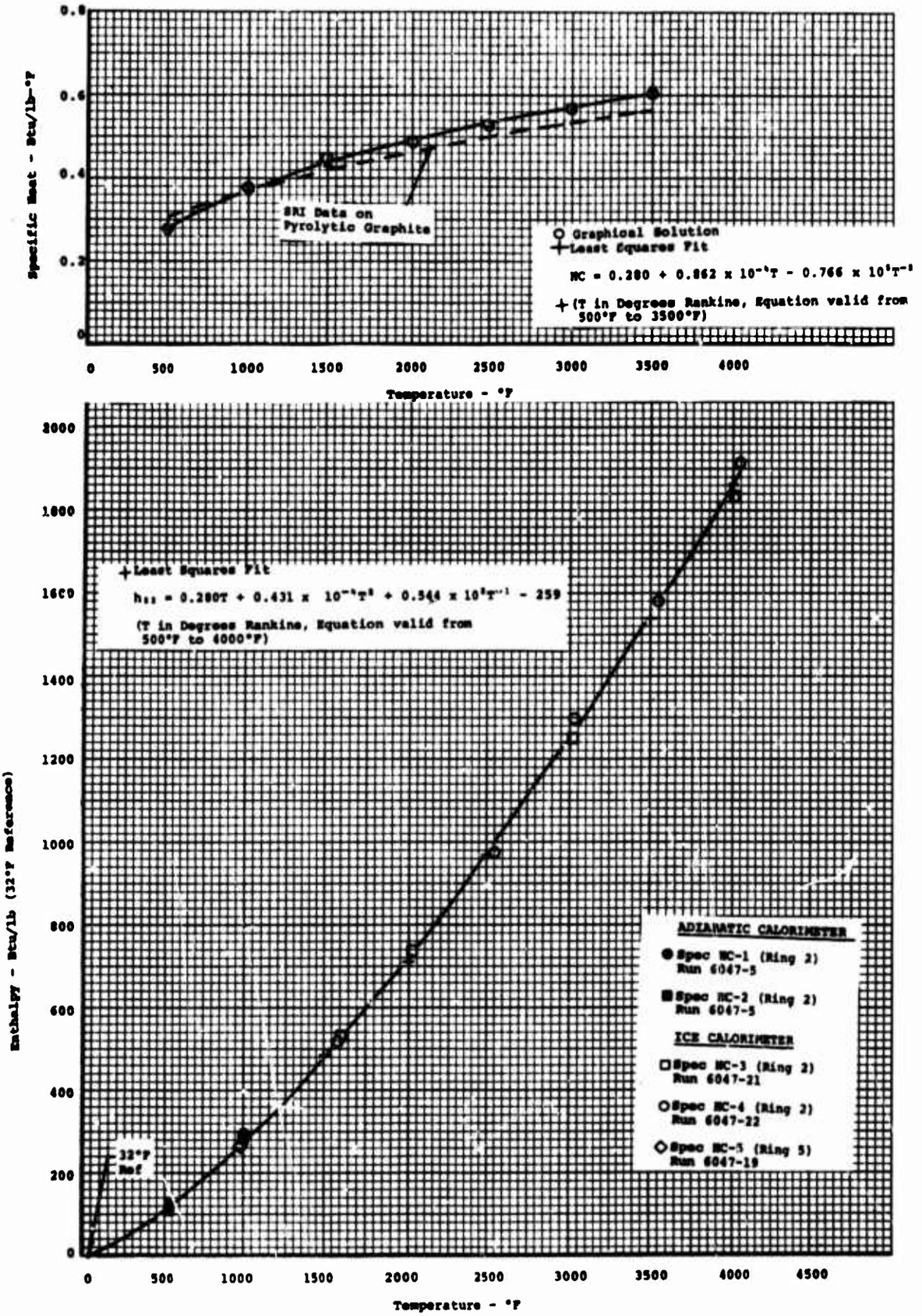

Figure 35. Enthalpy and Specific Heat of Fibrous PG Sleeve

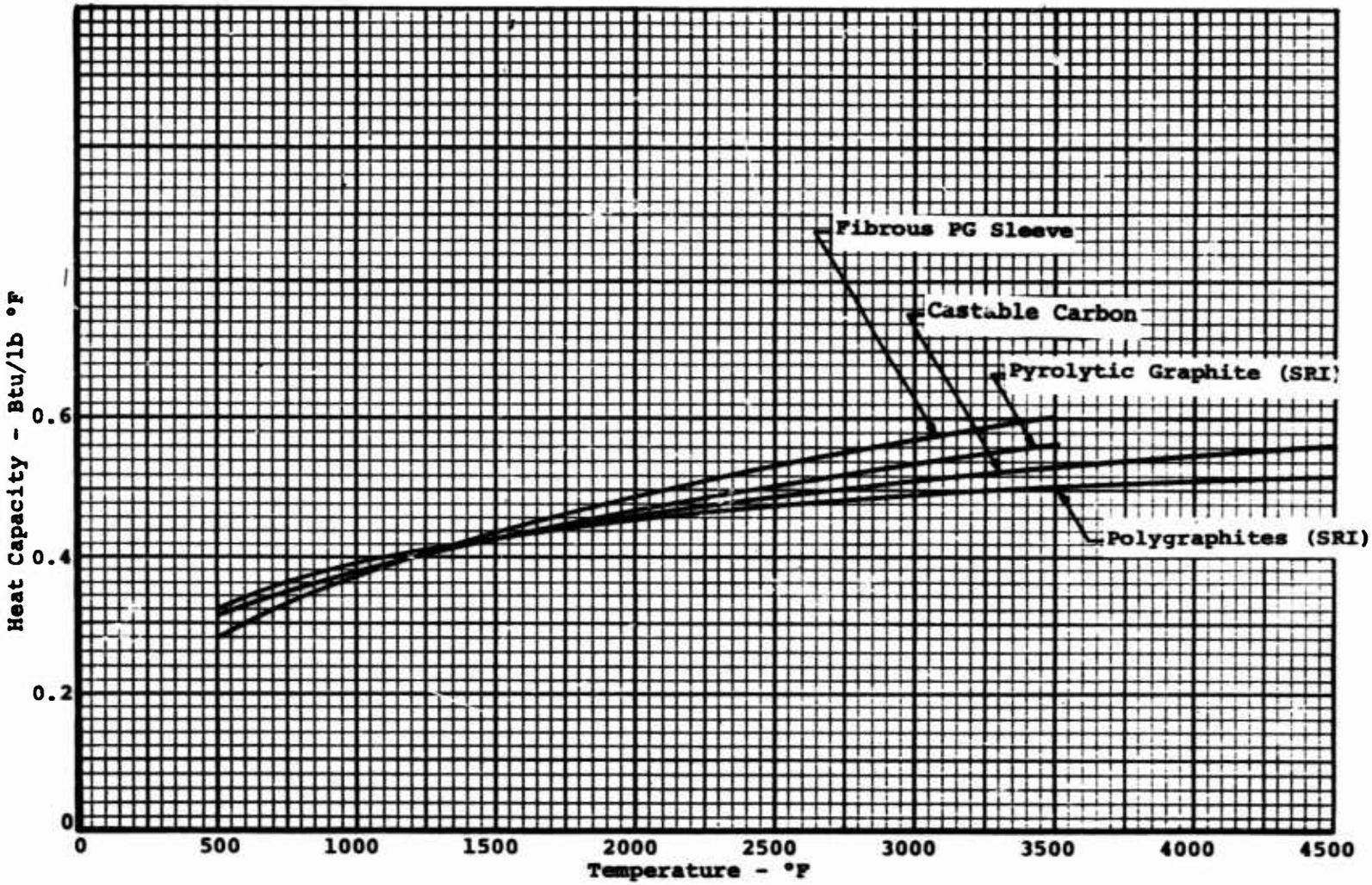

Figure 36. Heat Capacities of Some Carbonaceous and Graphite Materials

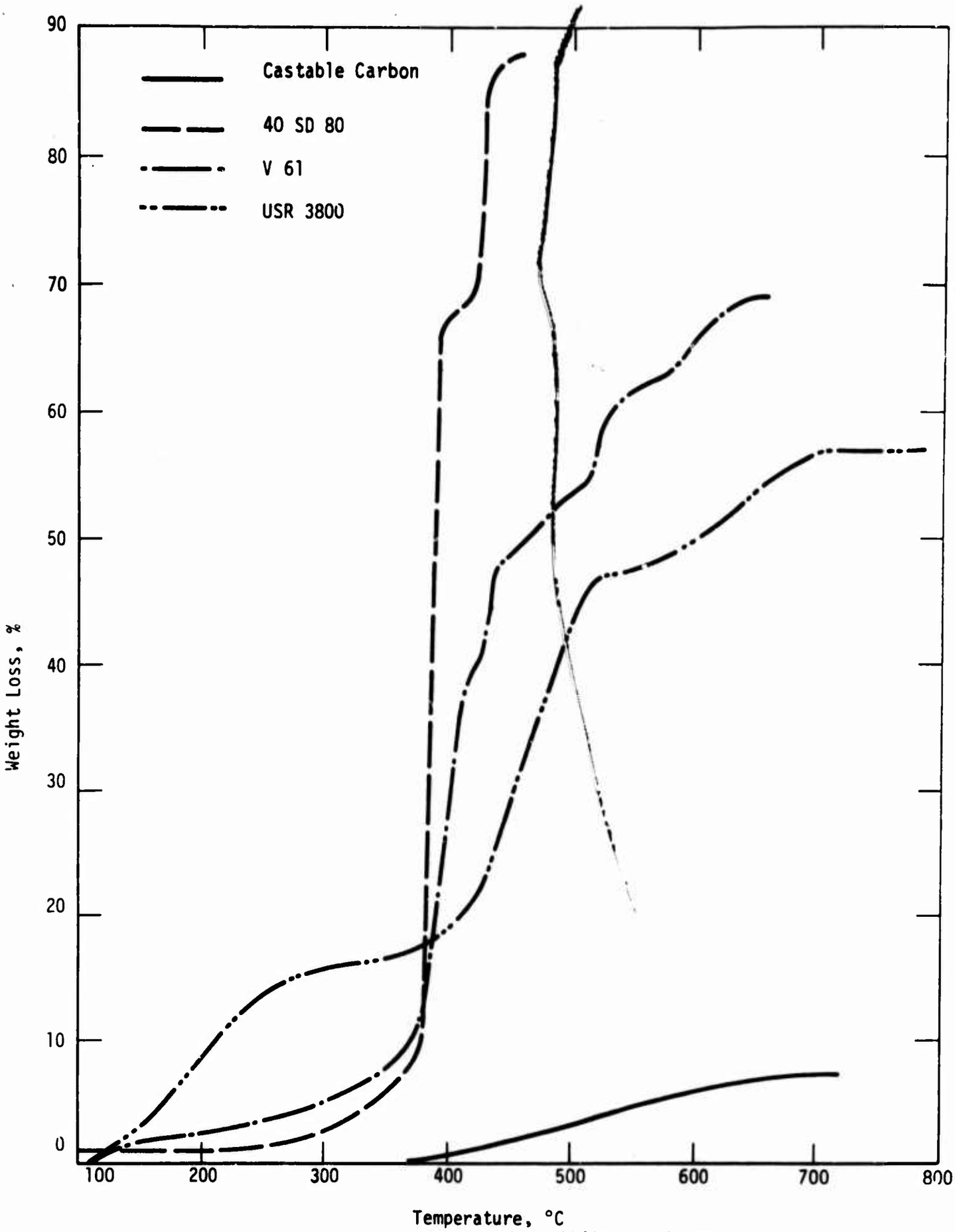

Figure 37. Thermogravimetric Analysis of Insulation Materials

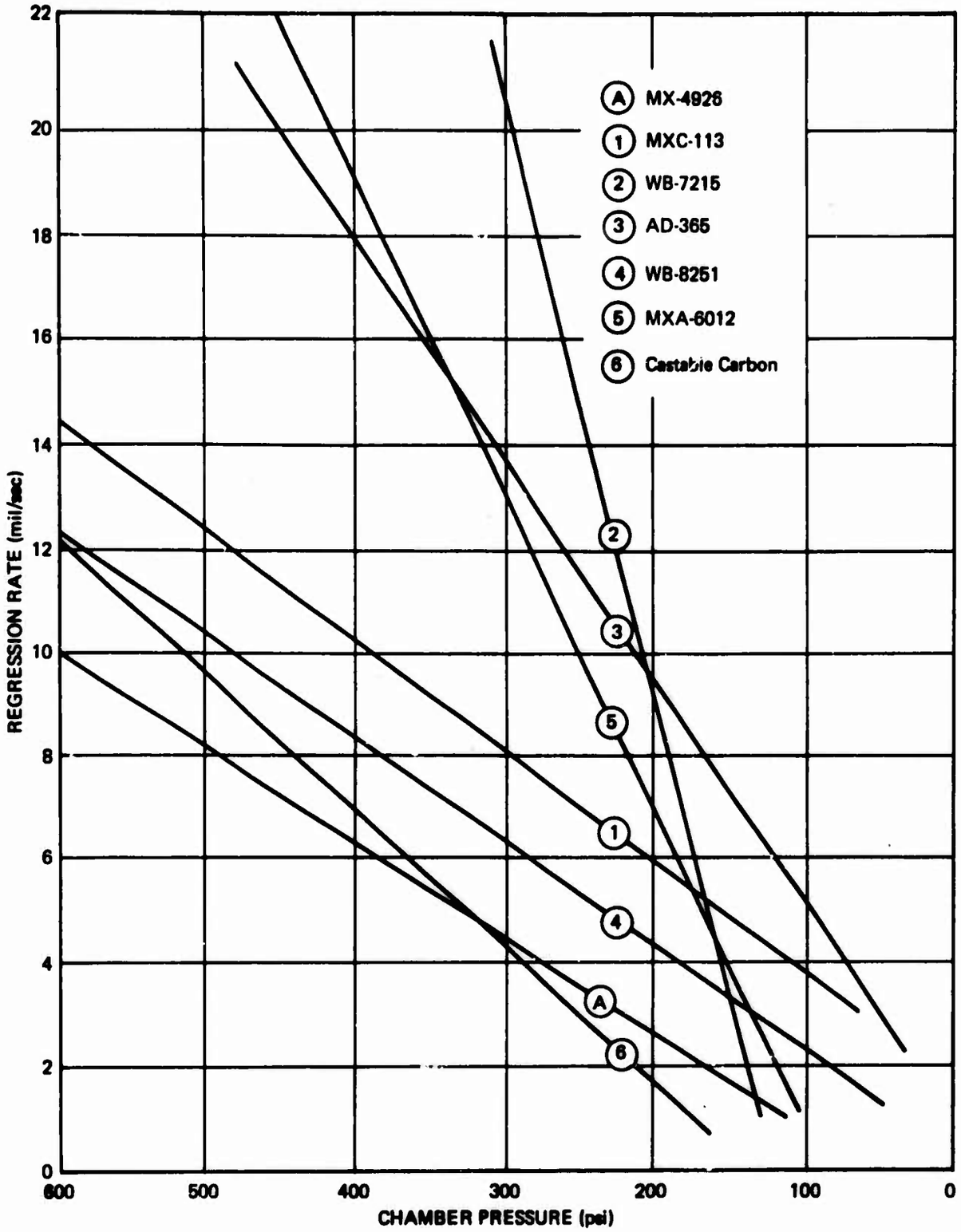

Figure 38. Erosion Data of AR Castable Carbon and Other Ablative Materials (from ref. 8)

Table 1

Results of Inspections on Castable Carbon by Monitors

Specimen No.	Gravimetric Density gm/cm³	Velocity in./μsec	Resistivity μ ohm cm	Liquid Absorption Measurements: Bulk Density gm/cm³	Open Porosity %	Closed Porosity[3] %	Remarks
CR-1-70	1.532[1]	0.1067					
CR-2-70	1.530[1]	0.1082					
CTE-3-70	Specimen not used for evaluation		430,500 425,600				Removed specimen and reversed ends
CR-1-1500	1.336[1]	Material defies evaluation - signal attenuated					
CR-2-1500	-----	Material defies evaluation - signal attenuated					
CR-1-4000	1.310	Material defies evaluation - signal attenuated					
CR-2-4000	1.286	Material defies evaluation - signal attenuated					
RI-1-4000	1.296	Material defies evaluation - signal attenuated					
RI-2-4000	1.288	Material defies evaluation - signal attenuated					
RI-3-4000	Specimen not used for evaluation						
CTE-1-4000	1.162[2]	Material defies evaluation - signal attenuated	12,390				Specimen very rough
CTE-2-4000	1.176[2]	Material defies evaluation - signal attenuated	12,079				Specimen very rough
CC-1-0 (4000° char)				1.386	24.9	12.6	Outside Material
CC-2-I (4000° char)				1.398	24.6	12.3	Inside Material

Notes:

1. Values corrected for thermocouple holes
2. Edges and corners chipped - values approximate.
3. Based on assumed true density of 2.22 gm/cm³

Table 2

Results of Inspections on Fibrous PG by Monitors

Specimen	Gravimetric Bulk Density gm/cm³	Velocity in./μsec	Resistivity μ ohm cm	Liquid Absorption Measurements		
				Bulk Density gm/cm³	Open Porosity %	Closed Porosity[1] %
As-Rec'd Sleeve:						
2	1.766	Specimen configuration not amenable to evaluation.				
3	1.797					
4	1.800					
5	1.770					
0.125-Inch High Rings from As-Rec'd Sleeve:						
2				1.887	3.2	15.4
3				1.810	2.2	16.2
4				1.810	1.9	16.5
5				1.814	2.0	16.3

Notes:

1. Based on assumed true density of 2.22 gm/cm³.

Table 3

Thermal Conductivity of Type 316 Stainless Steel Sleeve Measured in the Comparative Rod Apparatus with Type 316 Stainless Steel References
(Calibration using Type 316 Stainless Steel Adaptors)

Spec and Run	Mean Temp of Top Ref °F	ΔT through Top Ref °F	Thermal Conductivity of Top Ref $\frac{\text{Btu in.}}{\text{hr ft}^2\text{°F}}$	$\left(\frac{Q}{A}\right)^2$ through Top Ref $\frac{\text{Btu}}{\text{hr ft}^2}$	Mean Temp of Bottom Ref °F	ΔT through Bottom Ref °F	Thermal conductivity of Bottom Ref $\frac{\text{Btu in.}}{\text{hr ft}^2\text{°F}}$	$\left(\frac{Q}{A}\right)$ through Bottom Ref $\frac{\text{Btu}}{\text{hr ft}^2}$	Average $\lvert Q/A \rvert$ through Top and Bottom Ref $\frac{\text{Btu}}{\text{hr ft}^2}$	Average $\left(\frac{Q}{A}\right)$ through Spec (See Note 1)	Mean Spec Temp °F	ΔT through Specimen: Uncorrected °F	ΔT through Specimen: Corrected for Grafoil at interfaces - °F	Thermal Conductivity of Specimen $\frac{\text{Btu in.}}{\text{hr ft}^2\text{°F}}$
Spec 1 Run 1 Run 6071-15			l_1 = 0.750 in. (area of cross-section of reference = 0.7855 in.²) l_2 = 0.750 in. l_s = 1.1520 in. I. D. of sleeve = 0.8436 in. O. D. of sleeve = 1.0010 in. Length of sleeve = 0.9645 inch (Area of cross-section of sleeve = 0.2280 in.²)											
10:15	686	41.34	130.4	7188	379	47.80	111.2	7087	7138	24,591	534	237.68	225.35	125.8
2:15	1196	37.25	161.8	8036	908	41.66	144	7999	8018	27,623	1053	222.85	205.37	154.9
5:00	1623	26.85	183.0	6551	1410	29.56	172.5	6799	6675	22,996	1518	164.56	147.40	179.70
Spec 2 Run 1 Run 6071-20			I. D. of sleeve = 0.8436 in. O. D. of sleeve = 1.0010 in. Length of sleeve = 0.9642 in. (Area of cross-section of sleeve = 0.2280 in.²)											
5:00	656	37.50	128.7	6435	375	45.58	111.0	6746	6591	22,703	516	214.6	203.33	128.6
-	646	36.94	128.2	6314	375	44.90	111.0	6645	6480	22,324	514	209.1	198.14	129.7
10:15	1161	41.53	159.9	8854	867	43.67	141.8	8257	8556	29,476	1015	227.5	208.8	162.6
11:00	1159	39.77	159.7	8468	878	42.43	142.3	8050	8259	28.453	1019	218.3	200.6	163.3

Notes:

1. Corrected for cross-sectional area of sleeve. $(Q/A)_{sleeve} = \frac{Q}{A_{ref}} \times \frac{A_{ref}}{A_{sleeve}} = (Q/A)_{ref} \times \frac{0.7855}{0.2280} = (Q/A)_{ref} \times 3.4451$

2. $(Q/A)_{ref} = \frac{K_{ref} \times \Delta T_{ref}}{l_{ref}}$ for both top and bottom references. 3. $K_{spec} = \frac{Q}{A_{spec}} \times \frac{l_s}{\Delta T_{spec}}$

Table 4

Thermal Conductivity of Castable Carbon (uncharred)
Measured in the Comparative Rod Apparatus with Code 9606 Pyroceram References

Specimen and Time	Mean Temperature of Specimen °F	Thermal Conductivity of Specimen k_s Btu in./hr ft² °F	ΔT through Specimen °F	Mean Temperature of Lower Reference °F	Thermal Conductivity of Lower Reference k_1 Btu in./hr ft² °F	ΔT through Lower Reference ΔT_1 °F	Mean Temperature of Upper Reference °F	Thermal Conductivity of Upper Reference k_2 Btu in./hr ft² °F	ΔT through Upper Reference ΔT_2 °F
Specimen CR-1-70 (340°F) Run 1 Run 6071-5-3 Density: 1.532 gm/cm³		l_1 = 0.750 in. l_2 = 0.750 in. l_s = 0.750 in.		Initial Thickness: 0.9992 in. Initial Weight: 19.6642 gm Final Thickness: 0.9991 in. Final Weight: 19.6288 gm					
7:45 am	147	12.06	54.80	92	27.32	24.15	201	25.89	25.57
8:15 pm	147	12.17	54.90	92	27.32	24.60	201	25.89	25.57
Specimen CR-2-70 (340°F) Run 1 Run 6071-6-3 Density: 1.530 gm/cm³				Initial Thickness: 1.0007 in. Initial Weight: 19.6392 gm Final Thickness: 1.0006 in. Final Weight: 19.6260 gm					
1:00 pm	146	12.53	55.18	90	27.33	25.05	200	25.89	27.00
1:45 pm	146	12.47	55.82	90	27.33	25.45	201	25.69	26.90

Notes: 1. All measurements made with helium purge. Apparatus was evacuated prior to determination
2. Thermal conductivity (k_s) of specimen calculated from following equation

$$k_s = \left[\frac{k_1 \Delta T_1}{l_1} + \frac{k_2 \Delta T_2}{l_2}\right] \frac{l_s}{2\Delta T_s}$$

where

k = thermal conductivity
ΔT = temperature drop over gage length
l = gage length

and subscripts 1, 2, and s refer to lower reference, upper reference, and specimen, respectively.

Table 5

Thermal Conductivity of Castable Carbon (1500°F precharred)
Measured in the Comparative Rod Apparatus with Code 9606 Pyroceram References

Specimen and Time	Mean Temperature of Specimen °F	Thermal Conductivity of Specimen k_s Btu in./hr ft² °F	ΔT through Specimen °F	Mean Temperature of Lower Reference °F	Thermal Conductivity of Lower Reference k_1 Btu in./hr ft² °F	ΔT through Lower Reference ΔT_1 °F	Mean Temperature of Upper Reference °F	Thermal Conductivity of Upper Reference k_2 Btu in./hr ft² °F	ΔT through Upper Reference ΔT_2 °F
Specimen CR-1-1500 Run 1 Run 6071-9-2 Density: 1.336 gm/cm³		l_1 = 0.750 in. l_2 = 0.750 in. l_s = 0.750 in.		Initial Thickness: 1.0000 in. Final Thickness: 1.0005 in.			Initial Weight: 17.1620 gm Final Weight: 16.2277 gm		
9:15 am	180	7.54	72.30	122	26.89	9.90	243	25.42	11.56
2:40 pm	709	8.93	192.7	539	23.52	41.28	910	22.03	37.10
3:10 pm	709	8.85	192.8	541	23.51	40.30	908	22.04	36.58
6:10 pm	1160	10.30	145.2	1027	21.61	36.93	1325	20.61	35.82
7:45 pm	1422	11.54	182.3	1250	20.87	52.84	1633	19.70	53.60
8:05 pm	1421	11.35	185.6	1249	20.87	53.15	1632	19.70	53.45

Table 5 - Concluded

Specimen and Time	Mean Temperature of Specimen °F	Thermal Conductivity of Specimen k_s Btu in./hr ft² °F	ΔT through Specimen °F	Mean Temperature of Lower Reference °F	Thermal Conductivity of Lower Reference k_1 Btu in./hr ft² °F	ΔT through Lower Reference ΔT_1 °F	Mean Temperature of Upper Reference °F	Thermal Conductivity of Upper Reference k_2 Btu in./hr ft² °F	ΔT through Upper Reference ΔT_2 °F
Specimen CR-2-1500 Run 2 Run 6071-13-2		l_1 = 0.750 in. l_2 = 0.750 in. l_s = 0.750 in.		Initial Thickness: 1.0004 in. Final Thickness: ------- in.			Initial Weight: 15.7846 gm Final Weight: ------ gm		
5:30 pm	183	6.18	72.50	118	26.94	16.00	245	25.41	18.25
12:20 pm	864	9.58	227.0	537	23.10	94.00	1079	21.43	101.7
1:00 pm	869	9.64	225.2	643	23.05	95.15	1082	21.42	100.3
--	1356	11.55	196.4	1145	21.20	109.8	1562	19.90	111.0
--	1357	11.52	197.1	1146	21.20	109.3	1563	19.90	111.8

Table 6

Thermal Conductivity of Castable Carbon (4000°F precharred)
Measured in the Comparative Rod Apparatus with Code 9606 Pyroceram References

Specimen and Time	Mean Temperature of Specimen °F	Thermal Conductivity of Specimen k_s Btu in./hr ft² °F	ΔT through Specimen °F	Mean Temperature of Lower Reference °F	Thermal Conductivity of Lower Reference k_1 Btu in./hr ft² °F	ΔT through Lower Reference ΔT_1 °F	Mean Temperature of Upper Reference °F	Thermal Conductivity of Upper Reference k_2 Btu in./hr ft² °F	ΔT through Upper Reference ΔT_2 °F
Specimen CM-1-4000 Run 1 Run 6071-11-4 Density: 1.310 gm/cm³		l_1 = 0.750 in. l_2 = 0.750 in. l_s = 0.750 in.	Initial Thickness: 1.0010 in. Final Thickness: 1.0007 in.				Initial Weight: 16.7726 gm Final Weight: 16.7806 gm		
5:30 pm	979	104	22.03	889	22.10	101.6	1066	21.50	108.1
7:30 pm	1429	92.4	29.70	1312	20.64	136.0	1538	19.98	134.3
7:50 pm	1429	89.5	29.60	1315	20.63	129.4	1536	19.99	131.8

Table 7

Thermal Conductivity of Castable Carbon (4000°F precharred)
Measured in the Comparative Rod Apparatus with Type 316 Stainless Steel References

Specimen and Time	Mean Temperature of Specimen °F	Thermal Conductivity of Specimen k_s Btu in./hr ft² °F	ΔT through Specimen °F	Mean Temperature of Lower Reference °F	Thermal Conductivity of Lower Reference k_1 Btu in./hr ft² °F	ΔT through Lower Reference ΔT_1 °F	Mean Temperature of Upper Reference °F	Thermal Conductivity of Upper Reference k_2 Btu in./hr ft² °F	ΔT through Upper Reference ΔT_2 °F
Specimen CR-2-4000 Run 1 Run 6071-12-2 Density: 1.286 gm/cm³		l_1 = 0.750 in. l_2 = 0.750 in. l_s = 0.750 in.		Initial Thickness: 1.0003 in. Final Thickness: 1.0003 in.			Initial Weight: 16.4102 gm Final Weight: 16.4132 gm		
3:50 pm	1552	86.7	135.8	1363	170	71.2	1716	182	60.8
4:20 pm	1548	83.9	139.8	1359	170	71.3	1711	186	60.5

Notes: 1. All measurements made with helium purge. Apparatus was evacuated prior to determination
2. Thermal conductivity (k_s) of specimen calculated from following equation

$$k_s = \left[\frac{k_1 \Delta T_1}{l_1} + \frac{k_2 \Delta T_2}{l_2}\right] \frac{l_s}{2\Delta T_s}$$

where

k = thermal conductivity
ΔT = temperature drop over gage length
l = gage length

and subscripts 1, 2, and s refer to lower reference, upper reference, and specimen, respectively.

Table 8

Thermal Conductivity of Castable Carbon (4000°F Precharred)
Measured in Radial Inflow Apparatus

Specimen and Run	Time	Outer Face Temp. °F	Outside Hole Temp. °F	Inside Hole Temp. °F	Specimen ΔT °F	Heat to Calorimeter Btu/hr	Mean Temperature °F	Thermal Conductivity Btu in./hr ft² °F
Spec:	on		Front to Back					
RI-1-4000	9:15	1800	1555	1388		536		
Run 2	Read		1562	1394		500		
Run 6047-34-A5	10:25		1570	1400		509		
Density:			1571	1389		491		
1.296			1584	1406				
gm/cm³			1592	1412				
		Average	1572	1398	174	509	1485	84.3
			Side to Side					
			1560	1396				
			1567	1403				
			1574	1408				
			1576	1422				
			1580	1432				
			1596	1438				
		Average	1576	1417	159	509	1497	92.2
			Front to Back					
	Read	3375	3240	2850	390	918		
	11:25		3240	2860	380	924		
			3250	2880	370	905		
			3290	2885	405	891		
			3295	2880	415			
		Average			392	910	3067	66.9
			Side to Side					
		3405	3230	2850	380			
			3230	2850	380			
			3240	2850	390			
			3305	2920	385			
			3320	2920	400			
		Average			387	910	3072	67.7

Table 8 - Continued

Specimen and Run	Time	Outer Face Temp. °F	Outside Hole Temp. °F	Inside Hole Temp. °F	Specimen ΔT °F	Heat to Calorimeter Btu/hr	Mean Temperature °F	Thermal Conductivity Btu in./hr ft^2 °F
			Front to Back					
	Read 12:40	4466	4340	3800	540	1220		
			4320	3800	520	1183		
			4350	3800	550	1183		
						1200		
						1164		
						1171		
		Average			530	1187	4068	64.5
			Side to Side					
		4476	4330	3820	510			
			4340	3820	520			
		Average			515	1187	4078	66.4

Table 8 - Continued

Specimen and Run	Time	Outer Face Temp. °F	Outside Hole Temp. °F	Inside Hole Temp. °F	Specimen ΔT °F	Heat to Calorimeter Btu/hr	Mean Temperature °F	Thermal Conductivity Btu in./hr ft² °F
Spec:	on		Front to Back					
RI-1-4000	9:15	-	3795	3340	455	1109		
Run 3	Read		3805	3340	465	1089		
Run 6047-39-A5	10:45		3805	3355	450	1070		
			3780	3330	450	1076		
Density:			3810	3360	450			
1.296 gm/cm³		Average			454	1086	3572	68.9
			Side to Side					
		-	3805	3355	450			
			3800	3380	420			
			3810	3380	430			
			3780	3330	450			
			3810	3360	450			
		Average			440	1086	3581	71.1
	Read		Front to Back					
	12:00		4390	3850	540	1207		
			4400	3860	540	1207		
			4390	3850	540	1195		
			4360	3840	520	1199		
						1193		
		Average			535	1200	4113	64.6
			Side to Side					
		-	4390	3850	540			
			4400	3870	530			
			4390	3880	510			
		Average			527	1200	4130	65.6

Table 8 - Continued

Specimen and Run	Time	Outer Face Temp. °F	Outside Hole Temp. °F	Inside Hole Temp. °F	Specimen ΔT °F	Heat to Calorimeter Btu/hr	Mean Temperature °F	Thermal Conductivity Btu in./hr ft² °F
			Front to Back					
	Read 1:30	-	4720	4150	570	1272		
			4700	4140	560	1290		
			4700	4130	570	1273		
			4670	4090	580	1266		
						1283		
		Average			570	1277	4413	64.5
			Side to Side					
		-	4720	4180	540			
			4730	4180	550			
			4740	4160	580			
			4700	4130	570			
		Average			560	1277	4443	65.7

Table 8 - Continued

Specimen and Run	Time	Outer Face Temp. °F	Outside Hole Temp. °F	Inside Hole Temp. °F	Specimen ΔT °F	Heat to Calorimeter Btu/hr	Mean Temperature °F	Thermal Conductivity Btu in./hr ft² °F
Spec RI-2-4000 Run 1 Run 6047-36-A5 Density: 1.288 gm/cm³	on 9:00 Read 10:15	1870	Front to Back					
			1665	1480		583		
			1675	1488		563		
			1680	1490				
			1687	1480		562		
			1690	1482				
			1688	1480				
		Average	1681	1483	198	566	1582	82.3
		1880	Side to Side					
			1672	1482				
			1681	1490				
			1685	1492				
			1684	1498				
			1686	1500				
			1682	1497				
		Average	1682	1493	189	566	1586	86.2
	Read 11:30	2890	Front to Back					
			2770	2440	330	832		
			2780	2435	345	824		
			2775	2445	330	770		
			2820	2460	360	742		
		Average			341	792	2616	66.9
		2900	Side to Side					
			2755	2435	320			
			2765	2440	325			
			2760	2430	330			
			2800	2420	380			
		Average			339	792	2601	67.3

Table 8 - Continued

Specimen and Run	Time	Outer Face Temp. °F	Outside Hole Temp. °F	Inside Hole Temp. °F	Specimen ΔT °F	Heat to Calorimeter Btu/hr	Mean Temperature °F	Thermal Conductivity Btu in./hr ft² °F
			Front to Back					
	Read 12:40	4000	3870	3390	480	1149		
			3870	3400	470	1143		
			3860	3390	470	1112		
			3850	3390	460	1098		
		Average			470	1126	3628	69.0
			Side to Side					
		4000	3870	3370	500			
			3860	3360	500			
			3880	3360	520			
		Average			507	1126	3617	63.98
	Read 1:45		Front to Back					
		4486	4320	3760	560	1402		
			4320	3760	560	1377		
			4350	3770	580	1374		
			4310	3800	510	1346		
		Average			553	1375	4049	71.6
			Side to Side					
		4496	4360	3750	610			
			4360	3795	565			
			4360	3800	560			
			4350	3745	605			
		Average			585	1375	4065	67.7

Table 8 - Concluded

Specimen and Run	Time	Outer Face Temp. °F	Outside Hole Temp. °F	Inside Hole Temp. °F	Specimen ΔT °F	Heat to Calorimeter Btu/hr	Mean Temperature °F	Thermal Conductivity Btu in./hr ft² °F
			Front to Back					
	Read 2:45	5055	4860	4260	600	1577		
			4890	4280	610	1573		
			4880	4270	610	1567		
			4870	4260	610			
		Average			608	1572	4571	74.5
			Side to Side					
			4900	4280	620			
			4910	4300	610			
			4920	4290	630			
			4920	4260	660			
		Average			630	1572	4598	71.9

Notes:

1. Measurements made in helium, apparatus was not evacuated prior to run.

2. Specimen mean temperatue is the average of temperatures read for outside and inside holes of specimen.

3. Specimen thermal conductivity (K_s) calculated by the relation:

$$K_s = \frac{\ln(R_o/R_i)}{2\pi L} \quad \frac{Q}{\Delta T}$$

where

R_o = radius of outside hole = 0.437 inch
R_i = radius of inside hole = 0.233 inch
Q = heat flow - Btu/hr
ΔT = specimen temperature gradient (outside hole (°F) inside hole (°F)) - °F
l = 1/2 inch calorimeter gage length

Table 9

Thermal Conductivity of Fibrous PG Sleeve in the Axial ("a-b") Direction
Measured in the Comparative Rod Apparatus with Type 316 Stainless Steel References

Spec Run and Time	Mean Temp of Top Ref °F	ΔT through Top Ref °F	Thermal Conductivity of Top Ref $\frac{\text{Btu in.}}{\text{hr ft}^2\text{°F}}$	$\left(\frac{Q}{A}\right)^2$ through Top Ref $\frac{\text{Btu}}{\text{hr ft}^2}$	Mean Temp of Bottom Ref °F	ΔT through Bottom Ref °F	Thermal conductivity of Bottom Ref $\frac{\text{Btu in.}}{\text{hr ft}^2\text{°F}}$	$\left(\frac{Q}{A}\right)$ through Bottom Ref $\frac{\text{Btu}}{\text{hr ft}^2}$	Average Q/A through Top and Bottom Ref $\frac{\text{Btu}}{\text{hr ft}^2}$	Average $\left(\frac{Q}{A}\right)$ through Spec See Note 1	Mean Spec Temp °F	ΔT through Specimen: Uncorrected °F	ΔT through Specimen: corrected for Grafoil at interface - °F	Thermal[1] Conductivity of Specimen $\frac{\text{Btu in.}}{\text{hr ft}^2\text{°F}}$
Spec CR-1 Ring 4 Run 1 Run 6071-21 Density: 1.774 gm/cm³			l_1 = 0.750 in. (Area of cross-section of reference = 0.7855 in.²) l_2 = 0.750 in. l_s = 1.0117 in. I. D. of sleeve = 0.8470 in. (Area of cross-section of sleeve = 0.2219 in.²) O. D. of sleeve = 1.000 in.					Initial length: 0.8242 in. Final length: 0.8252 in.				Initial weight: 5.2638 gm Final weight: 5.2646 gm		
1:30	652	51.60	128.2	8,820	435	56.67	115.0	8,689	8,754	30,987	544	130.86	115.74	270.9
3:30	1126	53.38	158	11,235	859	62.70	140.5	11,745	11,490	40,672	994	170.75	146.32	281.2
6:20	1650	45.32	182	10,998	1410	45.25	172.0	10,377	10,687	37,830	1529	159.75	132.28	289.3
Spec CR-2 Ring 4 Run 1 and 2 Run 6071-29			l_1 = 0.750 in. l_2 = 0.750 in. l_s = 1.0130 in.					Initial length: 0.8255 in. Final length: 0.8255 in.				Initial weight: 5.3807 gm Final weight: 5.3789 gm		
8:30	602	46.68	125.5	7,811	409	52.77	113.0	7,952	7,881	27,897	507	115.6	102.5	275.7
4:40	1196	57.02	161.5	12,278	900	68.32	142.0	12,935	12,606	44,623	1045	187.9	160.43	281.8
2:40	1227	41.57	163.5	9,062	1018	47.22	Run 2 151.0	9,507	9,284	32,864	1124	134.93	114.25	291.4
6:50	1593	37.05	182	8,991	1391	40.95	172.0	9,391	9,191	32,534	1493	133.93	110.44	298.4

Table 9 - Concluded

Spec Run and Time	Mean Temp of Top Ref °F	ΔT through Top Ref °F	Thermal Conductivity of Top Ref $\frac{\text{Btu in.}}{\text{hr ft}^2\text{°F}}$	$(\frac{Q}{A})^2$ through Top Ref $\frac{\text{Btu}}{\text{hr ft}^2}$	Mean Temp of Bottom Ref °F	ΔT through Bottom Ref °F	Thermal conductivity of Bottom Ref $\frac{\text{Btu in.}}{\text{hr ft}^2\text{°F}}$	$(\frac{Q}{A})$ through Bottom Ref $\frac{\text{Btu}}{\text{hr ft}^2}$	Average (Q/A) through Top and Bottom Ref $\frac{\text{Btu}}{\text{hr ft}^2}$	Average $(\frac{Q}{A})$ through Spec See Note 1	Mean Spec Temp °F	ΔT through Specimen: Uncorrected °F	ΔT through Specimen: Corrected for Grafoil at interface-°F	Thermal[3] Conductivity of Specimen $\frac{\text{Btu in.}}{\text{hr ft}^2\text{°F}}$
Spec CR-1 Ring 4 Run 2 Run 6071-37 Density: 1.774 gm/cm³	$l_{ref} = l_{ref} = 0.750$ in. (Area of cross-section of reference = 0.7855 in.²) $l_s = 1.0117$ in. I. D. of sleeve = 0.847 in. (Area of cross-section of sleeve = 0.2219 in.²) O. D. of sleeve = 1.000 in.											Initial length: 0.8252 in. Final length: 0.8252 in.		Initial weight: 5.2624 gm Final weight: 5.2618	
2:45	625	22.06	365	10,736	423	18.67	410	10,206	10,471	37,065	523	159.0	140.9	266
3:00	627	22.00	365	10,707	425	18.95	410	10,359	10,533	37,285	525	158.2	140.0	269
5:10	1071	23.02	273	8,379	909	19.47	305	7,918	8,148	28,842	989	120.85	103.77	281
5:30	1073	22.32	272	8,095	914	19.50	303	7,878	7,986	28,269	992	119.50	102.76	278
6:55	1637	50.40	195	13,104	1368	42.10	223	12,518	12,811	45,348	1501	186.65	153.74	298
7:15	1648	51.20	195	13,312	1376	42.80	222	12,669	12,990	45,982	1509	189.32	155.95	298
				Note: Armco Iron References used for this run										

Notes:

1. $\frac{Q}{A_{spec}} = \frac{Q}{A_{ref}} \times \frac{A_{ref}}{A_{spec}} = \frac{Q}{A_{ref}} \times \frac{0.7855}{0.2219} = \frac{Q}{A_{ref}} \times (3.5398)$

2. $\frac{Q}{A_{ref}} = \frac{K_{ref}\Delta T_{ref}}{l_{ref}}$ Both for top and bottom references

3. $K_{spec} = \frac{Q}{A_{spec}} \times \frac{l_s}{\Delta T_{spec}}$

Table 10

Electrical Resistivity of Fibrous PG Sleeve
(Measured in the Comparative Rod Apparatus)

Specimen, Run and Other Information	Specimen Mean Temp °F	Closed Circuit — Open Circuit E.M.F. mv	Current through Circuit amps	Electrical Resistivity μ ohm cm	Remarks
Spec CR-1	81	11.752	5.0	1605.3	
Ring 4		2.348	1.0	1603.7	
(Previously exposed		2.341	1.0	1598.9	Direction of current reversed
to 1500°F)		11.663	5.0	1593.1	Direction of current reversed
Run 1			Average	1600.2	
Run 6071-43					
I.D. = 0.8470 in.	487	12.326	5.0	1683.7	
O.D. = 1.000 in.		2.439	1.0	1665.8	
Length: 0.8252 in.			Average	1674.7	
Gage Length					
(Across which	1000	10.622	5.0	1450.9	
potential was		2.130	1.0	1454.8	
measured) =		2.127	1.0	1452.7	Direction of current reversed
0.8252 in.		10.695	5.0	1460.9	Direction of current reversed
Area of			Average	1454.8	
cross-section					
0.2219 in.^{2}	1002	10.718	5.0	1464.0	
		2.150	1.0	1468.4	
		2.125	1.0	1451.4	Direction of current reversed
		10.747	5.0	1468.0	Direction of current reversed
			Average	1463.9	
Spec CR-2	510	2.1115	1.0	1442.2	
Ring 4		11.1190	5.0	1518.8	Direction of current reversed
(Previously exposed			Average	1480.5	
to 1500°F)					
Run 1	1000	10.252	5.0	1400.4	
Run 6071-45		11.6515	5.0	1591.5	Direction of current reversed
I.D. = 0.8470 in.			Average	1495.6	
O.D. = 1.000 in.					
Length = 0.8255 in.					
Gage Length =					
0.8255 in.					
Area of cross-					
section = 0.2219 in.^{2}					

Table 11

Thermal Conductivity of Fibrous Pyrolytic Graphite Sleeve in the "c" Direction
(Measured in the Radial Inflow Apparatus with Optical Method)

Specimen and Run Number	Time	Average Outer Face Temp °F	Average Inner Wall Temp °F	Specimen Temp Gradient ΔT °F	Specimen Mean Temp °F	Heat Flow to Calorimeter Btu/hr	Average Thermal Conductivity Btu in./hr ft²°F	Environmental Condition
Specimen RI-1C	on					101		Apparatus evacuated twice and all data obtained in helium atmosphere
Ring #3	11:15					113		
Run 1	Read					106		
Run 6047-44-A5	12:50					105		
Initial O.D.:						107		
1.000 in.	Average	2118	2028	90	2069	106	9.59	
Initial I.D.:								
0.824 in.	Read					348		
Initial weight:	2:30					333		
12.9962 gm						335		
Initial bulk density:						323		
1.797 gm/cm³						322		
	Average	3231	2981	250	3106	332	11.79	
	Read					592		
	3:35					578		
						537		
						540		
						562		
	Average	3960	3649	311	3804	562	16.02	
Specimen RI-1C	on					54		Apparatus evacuated twice prior to run
Ring #3	8:00					54		
Run 2	Read					53		
Run 6047-46-A5	10:30					51		
						54		Vacuum 3 x 10^{-5} torr
	Average	1988	1935	53	1962	53	8.86	
	Read					119		
	12:00					120		
						110		
						118		
						116		
	Average	2117	2020	97	2068	116	10.80	Helium atmosphere
	Read					365		Helium atmosphere
	2:30					371		
						369		
						356		
						356		
	Average	3196	2950	246	3073	364	13.12	
	Read					846		
	4:05					838		
						820		
						846		
						829		
	Average	4187	3792	395	3990	836	18.76	Helium atmosphere

Thermal Conductivity of the Sleeve (K_s) Calculated from the following Equation:

$$K_s = \frac{\ln (R_o/R_i)}{2\pi L} \quad \frac{Q}{\Delta T}$$

where

K_s = thermal conductivity of the sleeve
R_o = outside radius of the sleeve
R_i = inside radius of the sleeve
Q = heat to calorimeter
ΔT = temperature gradient across the specimen wall

L = 1/2 inch gage length

Table 12

Thermal Expansion of Castable Carbon (4000°F precharred)
Measured in the Graphite Dilatometer

Specimen and Run No.	Temp. °F	Time	Observed Total Elongation (10^{-3} in.)	Observed Unit Elongation (10^{-3} in./in.)	Unit Correction for Dilatometer Motion (10^{-3} in./in.)	Corrected Specimen Unit Elongation (10^{-3} in./in.)
Specimen CTE-1 - 4000	75	9:55	0.00	0.00	0.00	0.00
Run 1	980	10:55	2.47	0.82	0.83	1.65
Run 6047-29-127E	1763	11:55	4.89	1.63	2.07	3.70
Initial length:	2311	12:30	6.81	2.27	2.98	5.25
2.9970 in.	3008	1:30	9.14	3.05	4.51	7.56
Final length:	4010	2:20	12.10	4.04	6.68	10.72
2.9840 in.	4496	3:00	10.09	3.37	7.73	11.10
Initial weight:	5045	3:35	0.96	0.32	9.04	9.36
13.6953 gm	75	8:00	-15.02	-5.01	0.00	-5.01
Final weight:						
13.6153 gm						

Table 12 - Concluded

Specimen and Run No.	Temp. °F	Time	Observed Total Elongation (10^{-3} in.)	Observed Unit Elongation (10^{-3} in./in.)	Unit Correction for Dilatometer Motion (10^{-3} in./in.)	Corrected Specimen Unit Elongation (10^{-3} in./in.)
Specimen CTE-2 -4000	73	8:35	0.00	0.00	0.00	0.00
Run 1	510	9:15	1.15	0.38	0.30	0.68
Run 6047-28-123-K1	1761	10:15	4.96	1.66	2.02	3.68
Initial length:	2584	11:15	8.00	2.67	3.48	6.15
2.9960 in.	3615	12:15	11.74	3.92	5.46	9.38
Final length:	4435	1:15	10.67	3.56	7.20	10.76
2.9850 in.	5004	2:00	3.91	1.31	8.49	9.80
Initial weight:	75	8:00	-12.86	-4.29	0.00	-4.29
13.2650 gm						
Final weight:						
13.1678 gm						

Table 13

Enthalpy of Castable Carbon (Uncharred) Measured in an Adiabatic Calorimeter

Specimen	Run	Initial Cup Temp. °F	Final Cup Temp. °F	Change in Cup Temp. °F	Initial Sample Temp. °F	Initial Wt. of Sample gm	Final Wt. of Sample gm	Enthalpy $h=\frac{K}{W_s(t_2-t_1)}$ Btu/lb	Enthalpy Btu/lb Above 85°F Ref.	Enthalpy Btu/lb Above 32°F Ref.
HC-1-70										
6047-2	1	73.884	80.812	6.928	507.667	7.3280	7.3078	114.13	113.00	122.00
HC-2-70										
6047-1	1	77.137	89.101	11.964	528.333	12.7853	12.6459	113.88	114.94	123.94

Table 14

Enthalpy of Castable Carbon (1500°F Precharred) Measured in an Adiabatic Calorimeter

Specimen	Run	Initial Cup Temp. °F	Final Cup Temp. °F	Change in Cup Temp. °F	Initial Sample Temp. °F	Initial Wt. of Sample gm	Final Wt. of Sample gm	Enthalpy $h=\frac{K}{W_s(t_2-t_1)}$ Btu/lb	Enthalpy Btu/lb Above 85°F Ref.	Enthalpy Btu/lb Above 32°F Ref.
BC-1-1500										
6047-2	1	80.349	87.710	7.361	511.50	8.8681	8.7596	101.16	101.80	109.80
6047-3	2	76.639	98.826	22.188	1014.50	8.7596	8.5334	313.01	317.71	325.71
BC-2 -1500										
6047-3	1	76.783	83.909	7.126	512.667	8.1767	8.0796	106.18	105.90	113.90
6047-4	2	73.870	94.130	20.260	1003.0	8.0796	7.7926	312.99	316.13	324.13

Table 15

Enthalpy of Castable Carbon (1500°F Precharred)
Measured in an Ice Calorimeter

Specimen	SRI Run Number	Drop Temperature °F	Initial Weight Grams	Final Weight Grams	Enthalpy from Drop Temperature to 32°F Btu/lb
HC-3 -1500					
6047-8	1	1013	13.0747	12.9615	307.4
6047-11	2	1531	12.9615	12.7987	543.6
HC-4 -1500					
6047-10	1	989	17.4138	17.2618	290.4
6047-11	2	1540	17.2618	17.1005	561.3

Table 16

Enthalpy of Castable Carbon (4000°F Precharred)
Measured in an Ice Calorimeter

Specimen	SRI Run Number	Drop Temperature °F	Initial Weight Grams	Final Weight Grams	Enthalpy from Drop Temperature to 32°F Btu/lb
HC-1-4000					
6047-12	1	1531	11.3095	11.2843	545.1
6047-13	2	2528	11.2843	11.1791	980.2
6047-14	3	3574	11.1791	11.0613	1538.2
6047-15	4	3989	11.0613	10.9450	1729.3
6047-17	5	4933	11.9450	10.8675	2262.6
HC-2-4000					
6047-12	1	1543	10.2053	10.1793	525.0
6047-13	2	2528	10.1793	10.1006	1009.7
6047-14	3	3594	10.1006	9.9835	1523.7
6047-16	4	4020	9.9835	9.8764	1759.5
6047-17	5	4984	9.8764	9.8202	2309.0

Table 16 - Concluded

	SRI Run Number	Drop Temperature °F	Initial Weight Grams	Final Weight Grams	Enthalpy from Drop Temperature to 32°F Btu/lb
HC-3 -4000					
6047-18	1	3023	8.8404	8.7953	1222.5
6047-20	2	4557	8.7953	8.6792	2022.3

Table 17

Enthalpy of Fibrous PG Sleeve Measured in an Adiabatic Calorimeter

Specimen	Run	Initial Cup Temp. °F	Final Cup Temp. °F	Change in Cup Temp. °F	Initial Sample Temp. °F	Initial Wt. of Sample gm	Final Wt. of Sample gm	Enthalpy $h=\frac{K}{W_s(t_2-t_1)}$ Btu/lb	Enthalpy Btu/lb Above 85°F Ref.	Enthalpy Btu/lb Above 32°F Ref.
Ring #2 Spec HC-1										
6047-5	1	73.609	79.894	6.285	525.0	6.7021	6.7005	112.92	111.62	120.62
6047-6	2	72.682	88.304	15.622	1007.0	6.7005	6.6795	281.55	282.54	291.54
Spec HC-2										
6047-5	1	81.739	87.000	5.261	529.0	5.9271	5.9247	106.90	107.38	116.38
6047-6	2	80.899	94.188	13.289	998.0	5.9247	5.8920	271.52	274.26	283.26

Table 18

Enthalpy of Fibrous PG Sleeve Measured in an Ice Calorimeter

Specimen	SRI Run Number	Drop Temperature °F	Initial Weight Grams	Final Weight Grams	Enthalpy from Drop Temperature to 32°F Btu/lb
Ring #2 HC-3					
6047-21	1	1599	4.8523	4.8456	528.6
6047-23	3	2543	4.8270	4.8103	969.7
6047-24	4	3013	4.8103	4.7905	1244.4
6047-25	5	4010	4.7905	4.7716	1835.9
6047-26	6	2014	4.7716	4.7578	737.8
Ring #5 HC-5					
6047-19	1	997	------	11.3591	260.3

Table 18 - Continued

Specimen	SRI Run Number	Drop Temperature °F	Initial Weight Grams	Final Weight Grams	Enthalpy from Drop Temperature to 32°F Btu/lb
Ring #2 HC-4					
6047-22	1	1594	4.5403	4.5324	519.8
6047-23	2	2553	4.5324	4.5183	976.4
6047-24	3	3033	4.5183	4.5050	1298.7
6047-25	4	3559	4.5050	4.4791	1585.1
6047-26	5	4050	4.4791	4.4659	1915.5

Table 19. Properties of Atlantic Research Castable Carbon Measured by Aerojet (Reference 7).

Temperature (°F)	Conductivity (Btu-in/hr-ft^2/°F)	Diffusivity (cm^2/sec)	Heat Capacity (cal/gm-°C)	Density (gm/cc)
74	16.491	0.0172	-	-
100	-	-	-	1.674
150	16.140	0.0151	0.216	-
200	-	-	-	1.625
250	16.086	0.0148	0.234	-
300	-	-	0.241	1.599

APPENDIX A

A COMPARATIVE ROD APPARATUS FOR MEASURING THERMAL CONDUCTIVITY TO 2000°F

A COMPARATIVE ROD APPARATUS FOR MEASURING THERMAL CONDUCTIVITY TO 2000°F

Southern Research Institute's comparative rod apparatus is used to measure thermal conductivities of a wide variety of materials from -300°F to 2000°F. This apparatus, shown schematically in Figure 1, consists basically of two cylindrical reference pieces of known thermal conductivity stacked in series with the cylindrical specimen. Heat is introduced to one end of the rod, composed of the references and specimen, by a small electrical heater. A cold sink or heater is employed at the opposite end of the rod as required to maintain the temperature drop through the specimen at the preferred level. Cylinders of zirconia may be inserted in the rod assembly to assist in controlling the temperature drop. Radial losses are minimized by means of radial guard heaters surrounding the rod and consisting of three separate coils of 16, 18 or 20-gage Kanthal wire wound on a 2 or 4-inch diameter alumina core. The annulus between the rod and the guard heaters is filled with diatomaceous earth, thermatomic carbon, bubbled alumina or zirconia powder. Surrounding the guard is an annulus of diatomaceous earth enclosed in an aluminum or transite shell.

The specimens and references (see Figure 2) are normally 1-inch diameter by 1-inch long. Thermocouples located 3/4 inch apart in radially drilled holes measure the axial temperature gradients. Thermocouples located at matching points in each guard heater are used to monitor guard temperatures, which are adjusted to match those at corresponding locations in the test section.

In operation, the apparatus is turned on and allowed to reach steady state. The guard and rod heaters are adjusted to minimize radial temperature gradients between the rod and guard sections consistent with maintaining equal heat flows in the references. Temperatures are measured on a Leeds and Northrup Type K-3 potentiometer, and the temperature gradients calculated. A typical temperature profile in the test section is shown in Figure 3.

The thermal conductivity of the specimen is calculated from the relation

$$K_s = \frac{K_1 \Delta T + K_2 \Delta T}{2\Delta T_s} \cdot \frac{\Delta X_s}{\Delta X_r}$$

where K_1 and K_2 are the thermal conductivities of the upper and lower references; ΔT_1, ΔT_2 and ΔT_s are the temperature differences in the upper and lower references and specimen, respectively; ΔX_s and ΔX_r are the distances between thermocouples in the specimen and references.

Note that for purely axial heat flow, the products $K_1\Delta T_1$ and $K_2\Delta T_2$ should be equal. Due to imperfectly matched guarding and other factors, this condition is seldom attained in practice; therefore, the average of the two values is used in the calculations. Their difference is maintained as small as possible, usually within 5 percent of the smaller.

For identical specimens, the radio $\Delta X_s/\Delta X_r$ should be unity but may vary due to the uncertainty in hold locations. To prevent introducing an additional error in calculations, ΔX is determined as follows: the depth of the hole is measured by inserting a snugly fitting drill rod in the hole, measuring the projecting length and subtracting it from the total length of the rod. The slope, or angle the hole makes with the perpendicular to the specimen axis, is determined by making measurements to the face of the hole and the outer end of the drill rod with respect to a datum plane, using a dial gage. From these measurements, the location of the bottom of the hole can be calculated.

Generally, measurements with the comparative rod apparatus are performed in an inert helium environment. The apparatus can also be operated in vacuum and at gas pressures of up to 100 psig. We have had experience operating under all conditions.

The primary reference materials which we use are Code 9606 Pyroceram and Armco iron for measurements on materials with low and high thermal conductivities, respectively. Primary standard reference sets are kept and are used to calibrate other references made from the same materials. The standards of Code 9606 Pyroceram were made from a batch of material which NBS purchased shortly after their measurements on a sample of Code 9606 Pyroceram. The curve which Flynn presented for the thermal conductivity of the Pyroceram is given in Figure 4.[1] Note that the curve is in good

---

[1] Robinson, H. E. and Flynn, D. R., Proceedings of Third Conference on Thermal Conductivity, pages 308-321, 1963 (with author's permission)

agreement with the recommended values from NSRDS-NBS 8[2]. The standards of Armco iron were made from the stock which was used in the round-robin investigations from which Powell[3] developed the most probable values for Armco iron. The curve used for the Armco iron standards is shown in Figure 5. Powell estimated the uncertainty to be within ±2 percent over the temperature range from 0° to 1000°C. Note in Figure 5 that numerous evaluations of Armco iron from other batches of material have agreed within ±3 percent (coefficient of variation about curve) with Powell's original data.

In addition to Code 9606 Pyroceram and Armco iron, several other materials have been used as references. These include copper for high conductivity specimens, 316 stainless steel for specimens of intermediate thermal conductivity and Teflon or Pyrex for low conductivity materials.

Copper references have been calibrated against Armco iron and excellent agreement with literature data has been obtained. Thermal conductivity values obtained from calibrations of 316 stainless steel against Pyroceram, Armco iron and a set of 316 stainless steel standards are presented in Figure 6. Note the consistency of the data obtained with the three different sets of references. The coefficient of variation of the data shown in Figure 6, about the curve value, was ±3.3 percent. These data indicate the internal consistency of the stainless steel and the reference materials. Note that the thermal conductivity values for 316 stainless steel presented in Figure 6 lie between values reported by several steel manufacturers and Lucks and Deem.[4]

The calibrations indicate that for materials with moderate to high thermal conductivities the apparatus operates with a precision of about ±3 percent and a total uncertainty of about ±5 percent at temperatures above 0°F if temperatures between the guard and test section are closely matched. Below 0°F, the precision achieved to date has been about ±7 percent with a total uncertainty of about ±10 percent. We anticipate that the precision and uncertainty at cryogenic temperatures can be improved by additional calibrations.

---

[2] Powell, R. W., C. Y. Ho and P. E. Liley, Thermal Conductivity of Selected Materials, NSRDS-NBS 8, Department of Commerce, November 25, 1966.

[3] Powell, R. W., Proceedings of Third Conference on Thermal Conductivity, pages 322-341, 1963.

[4] WADC TR58-476, "The Thermophysical Properties of Solid Materials", Armour Research Foundation, November, 1960.

Some additional data obtained on the comparative rod apparatus are shown in Figures 7 and 8. Figure 7 shows thermal conductivity data for ATJ graphite, with grain, using Armco iron as the referene material. These data show excellent agreement with earlier data obtained here and by other sources [5-7]. The maximum scatter of the comparative rod points was about 5 percent.

Figure 8 shows data for thermocouple grade constantan obtained on the comparative rod apparatus using Armco iron references and on Southern Research Institute's high temperature radial inflow apparatus. Note the excellent agreement. These data also show close agreement with data obtained by Silverman[4] on an alloy of very similar composition.

---

[5] ASD-TDR-62-765, "The Thermal Properties of Twenty-Six Solid Materials to 5000°F or Their Destruction Temperatures," Southern Research Institute, August, 1962.

[6] Pears, C. D., Proceedings of Third Conference on Thermal Conductivity, 453-479, 1963.

[7] NSRDS-NBS 16, "Thermal Conductivity of Selected Materials", Part 2, by C. Y. Ho, R. W. Powell and P. E. Liley, National Bureau of Standards, 1968.

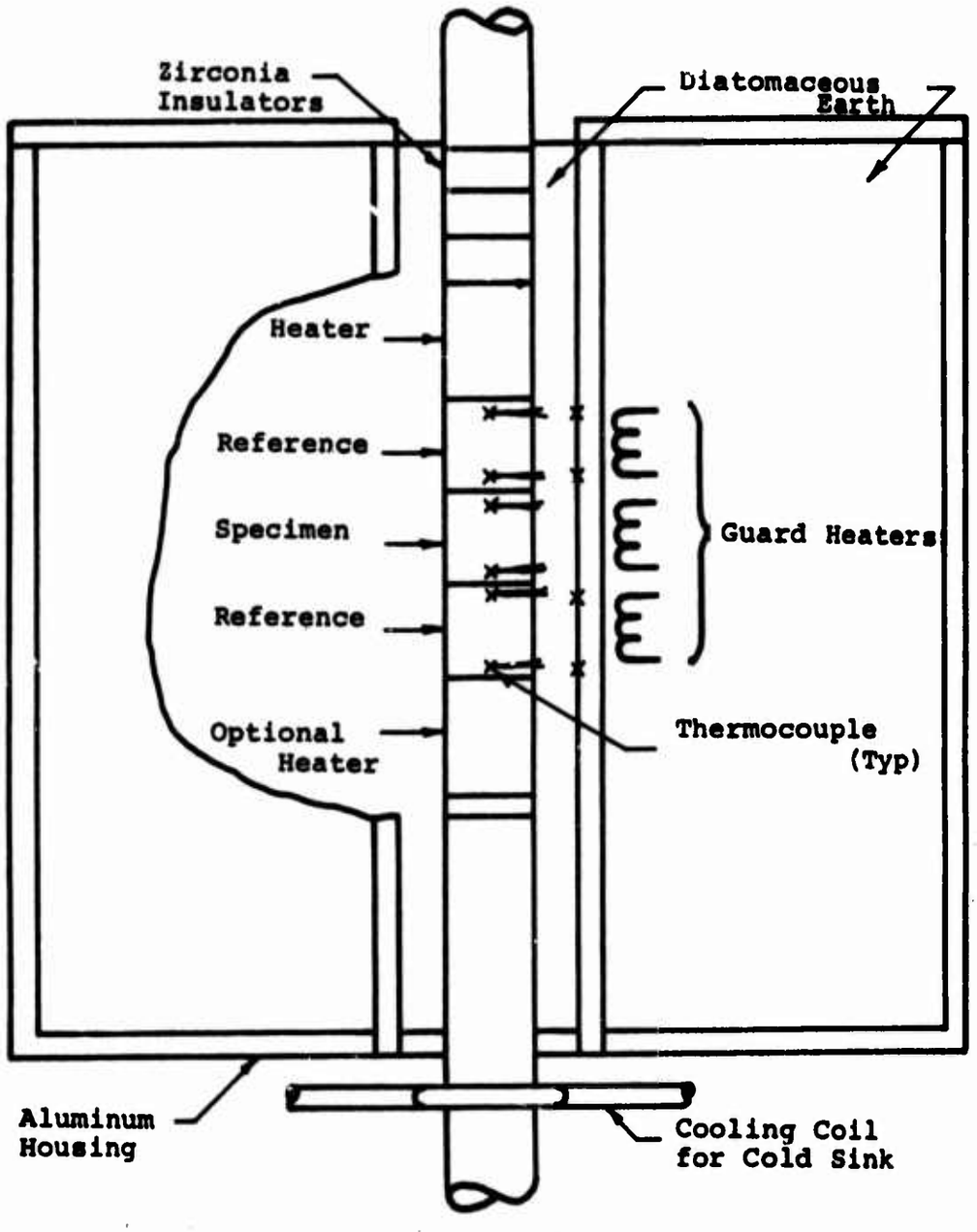

Figure 1. Schematic of Comparative Rod Thermal Conductivity Apparatus

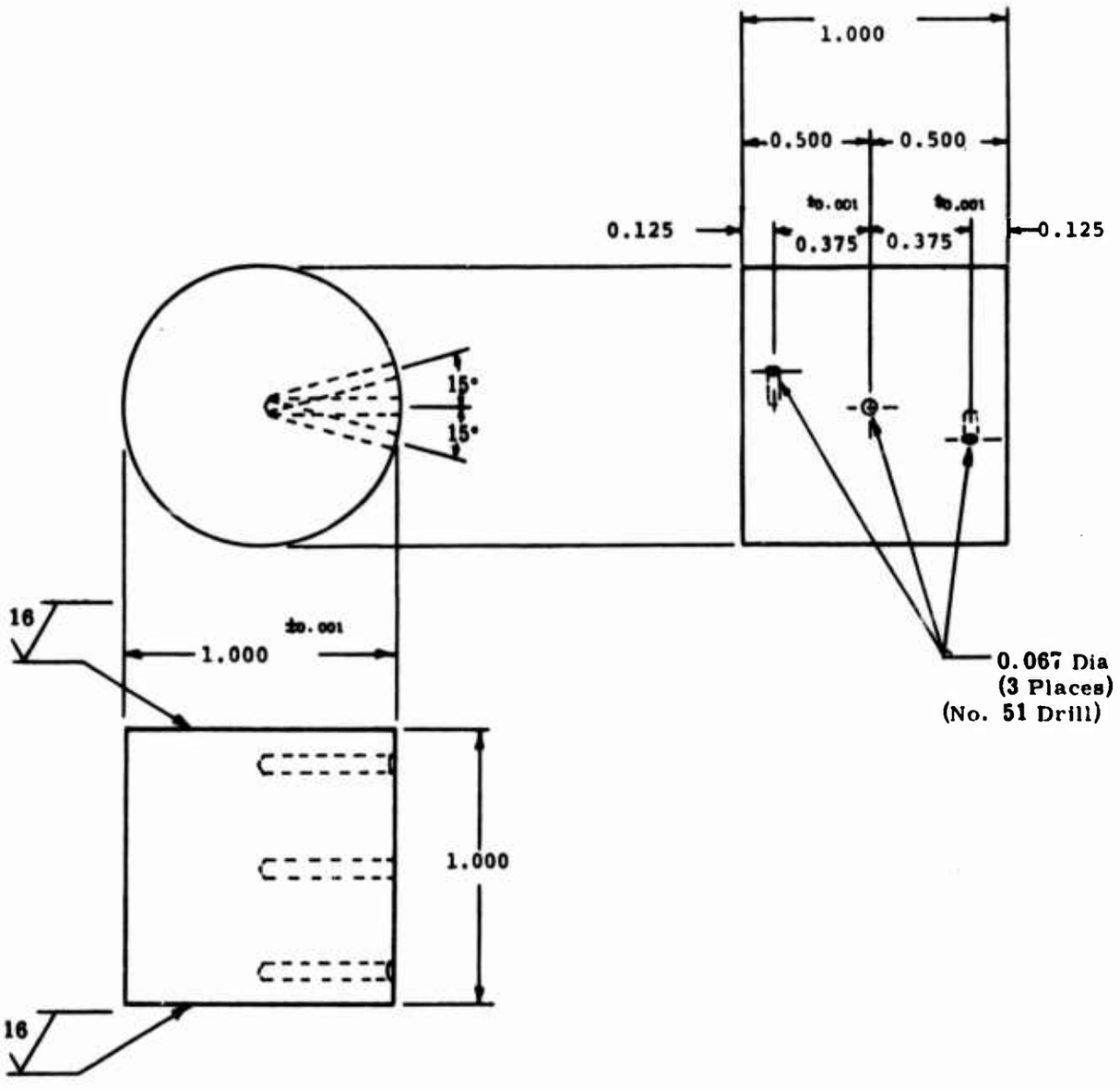

Note: All dimensions ±0.005 except where noted

Figure 2. Drawing of Specimen for Thermal Conductivity Measurements in Comparative Rod Apparatus to 1800°F

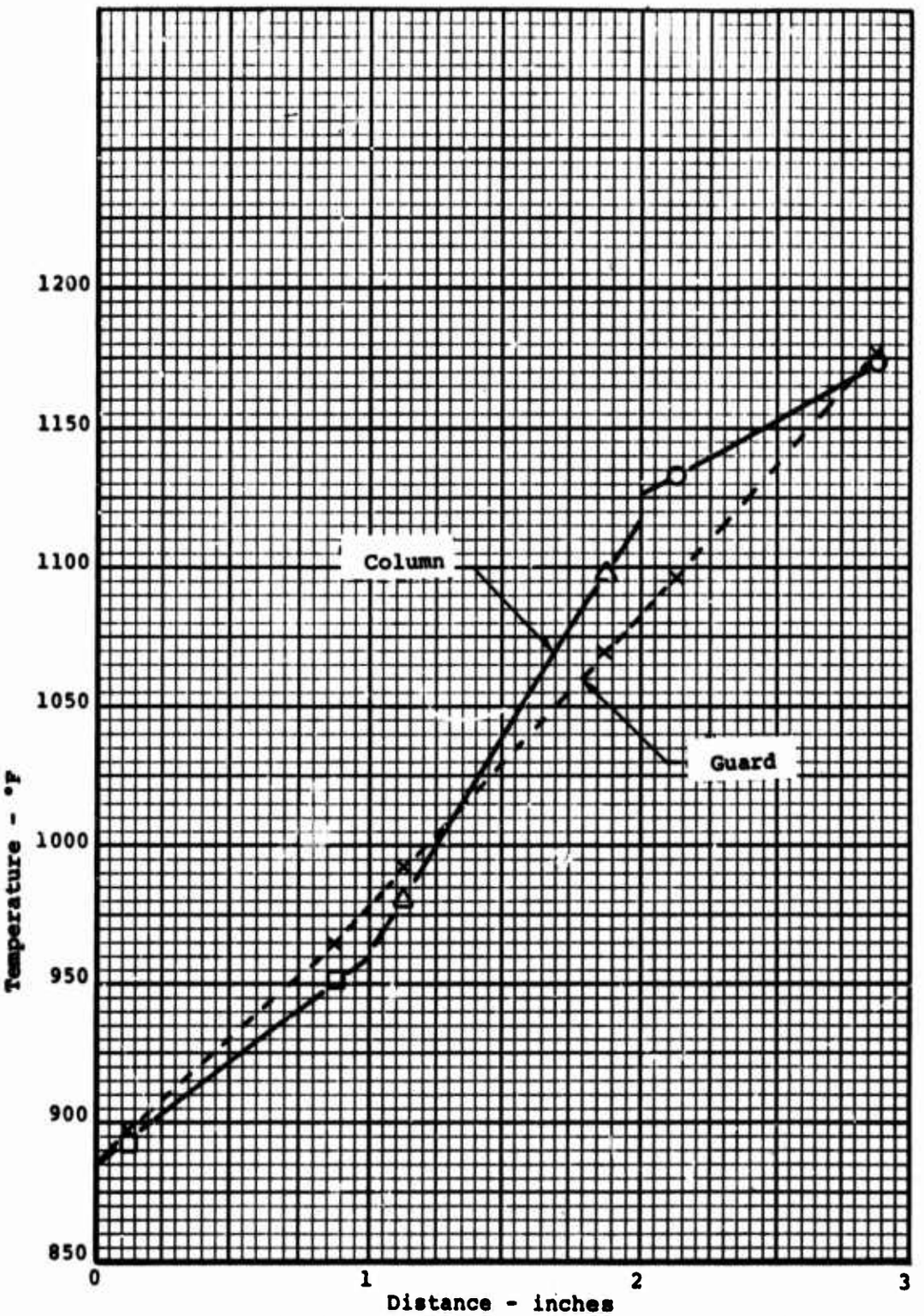

Figure 3. Typical Temperature Profile in Test Section

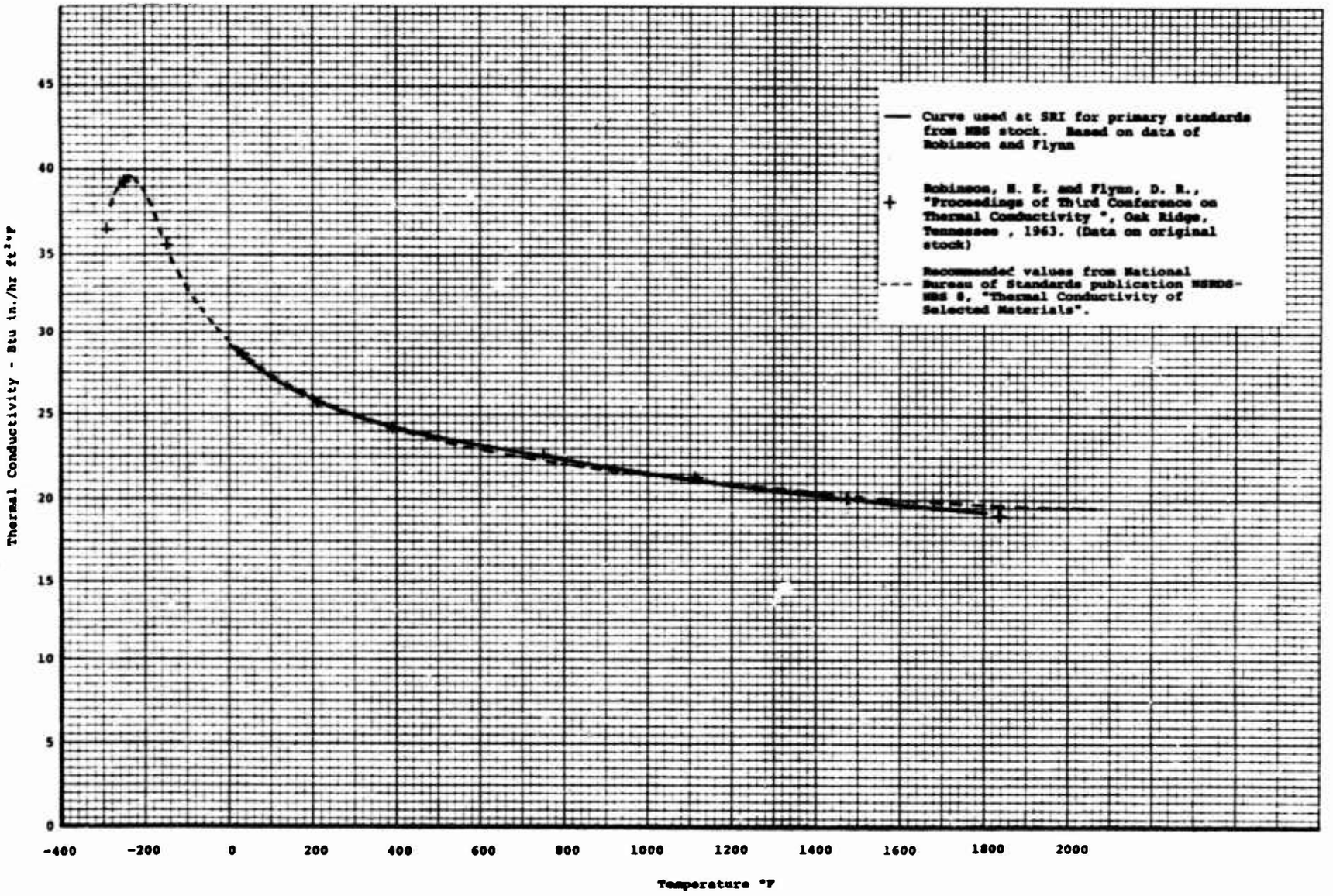

Figure 4. The Thermal Conductivity of Primary SRI Standards from NBS Stock of Code 9606 Pyroceram

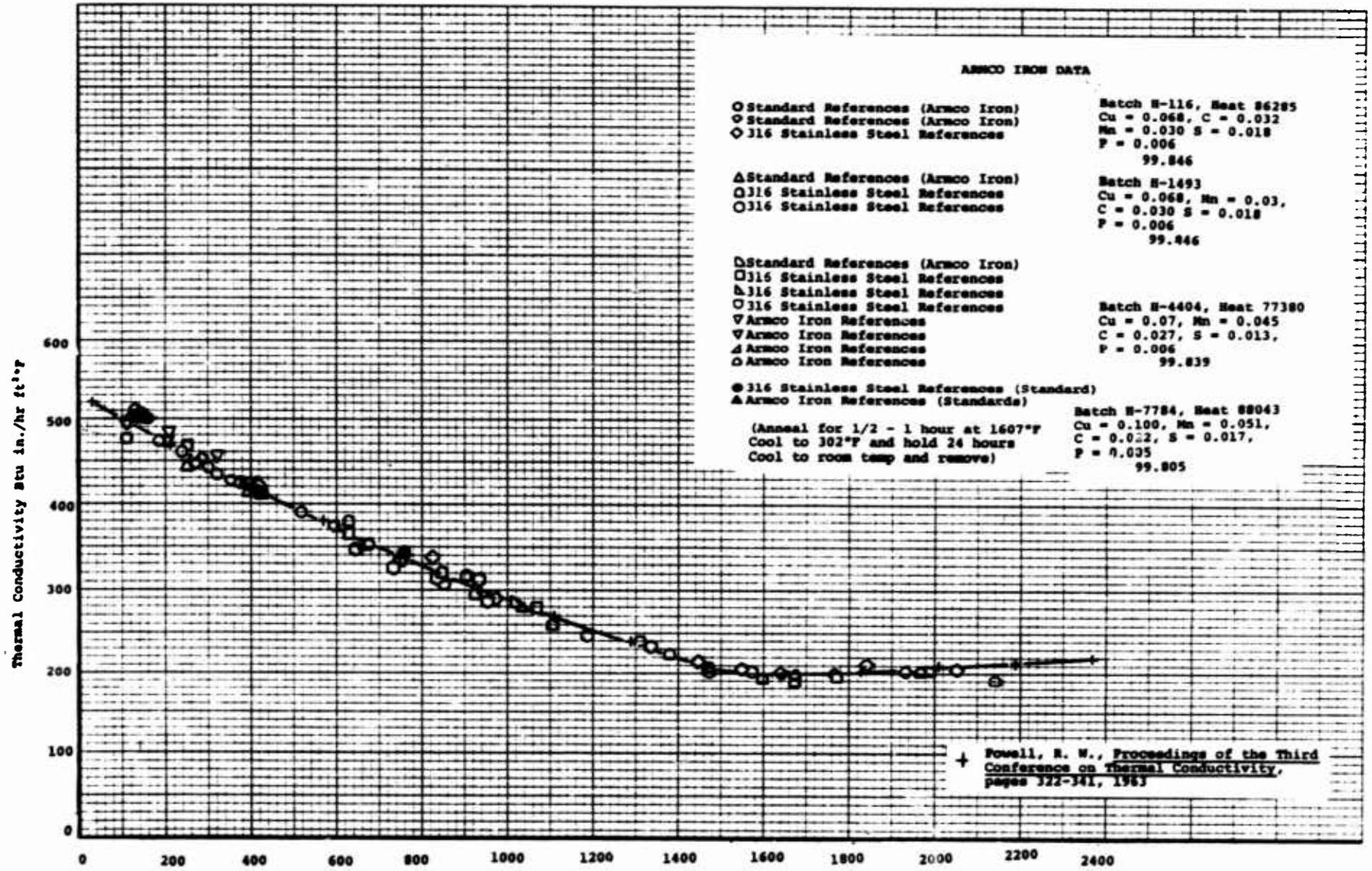

Figure 5. The Thermal Conductivity of Armco Iron

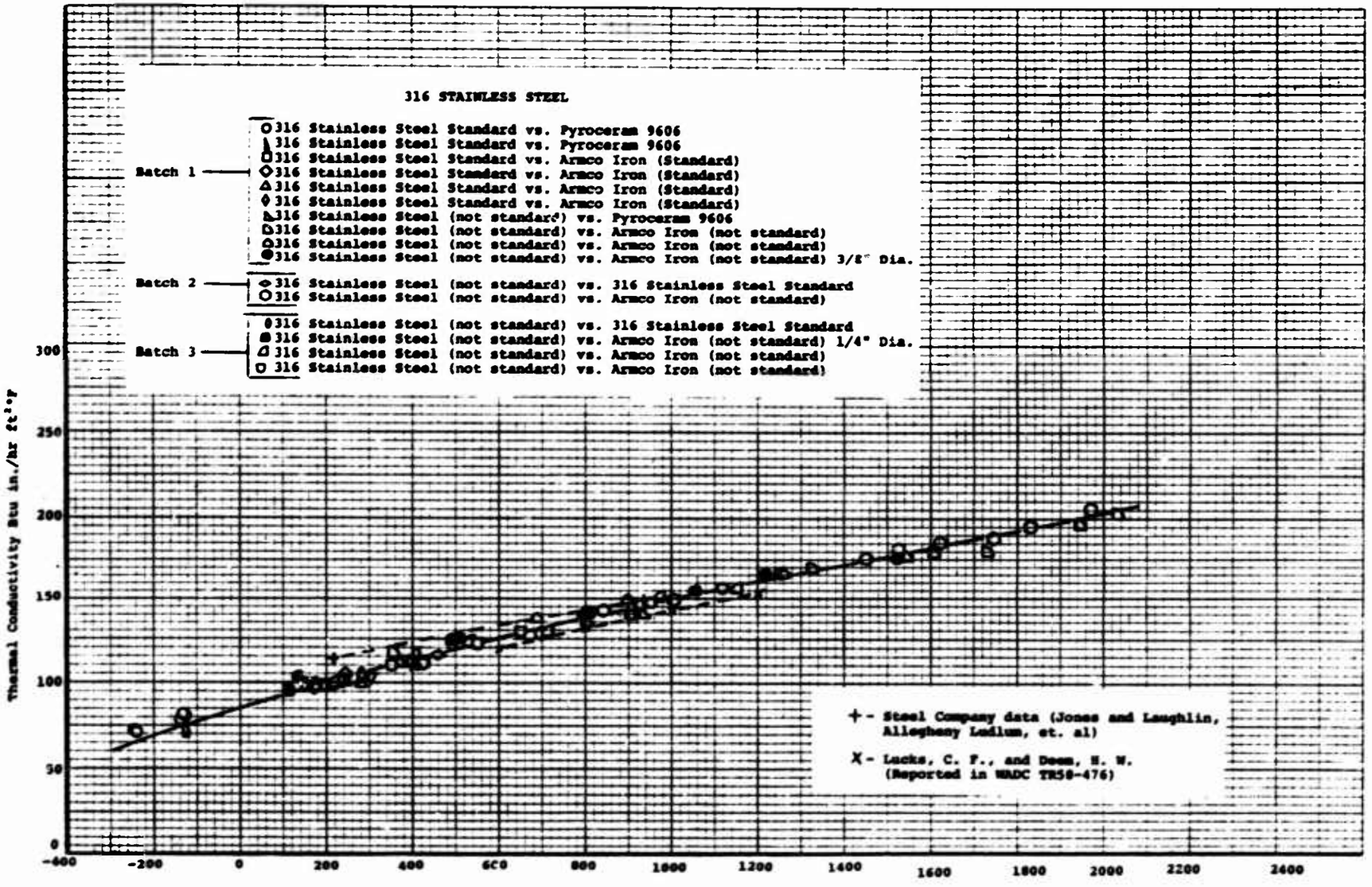

Figure 6. The Thermal Conductivity of 316 Stainless Steel

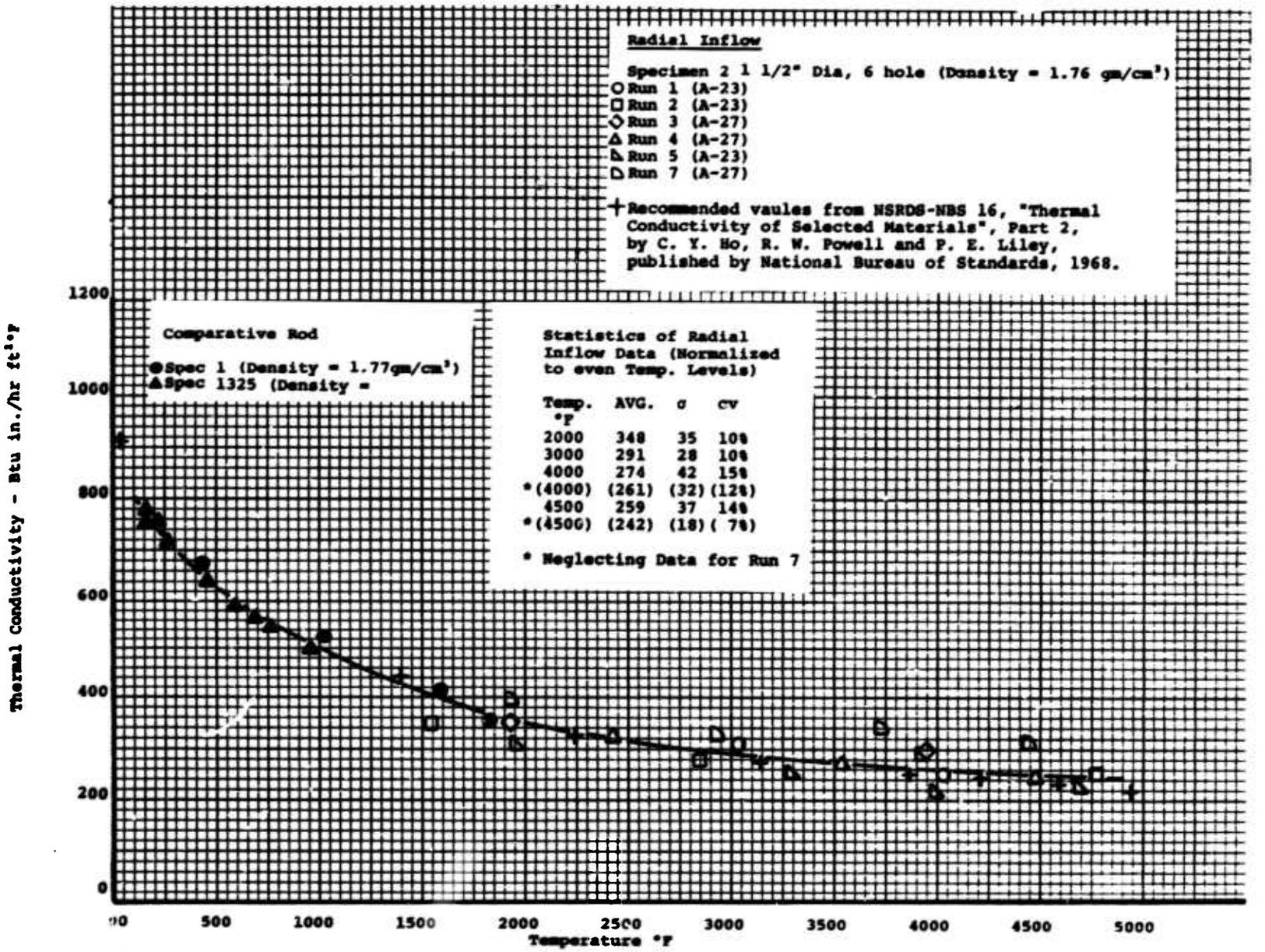

Figure 7. The Thermal Conductivity of ATJ Graphite, With Grain

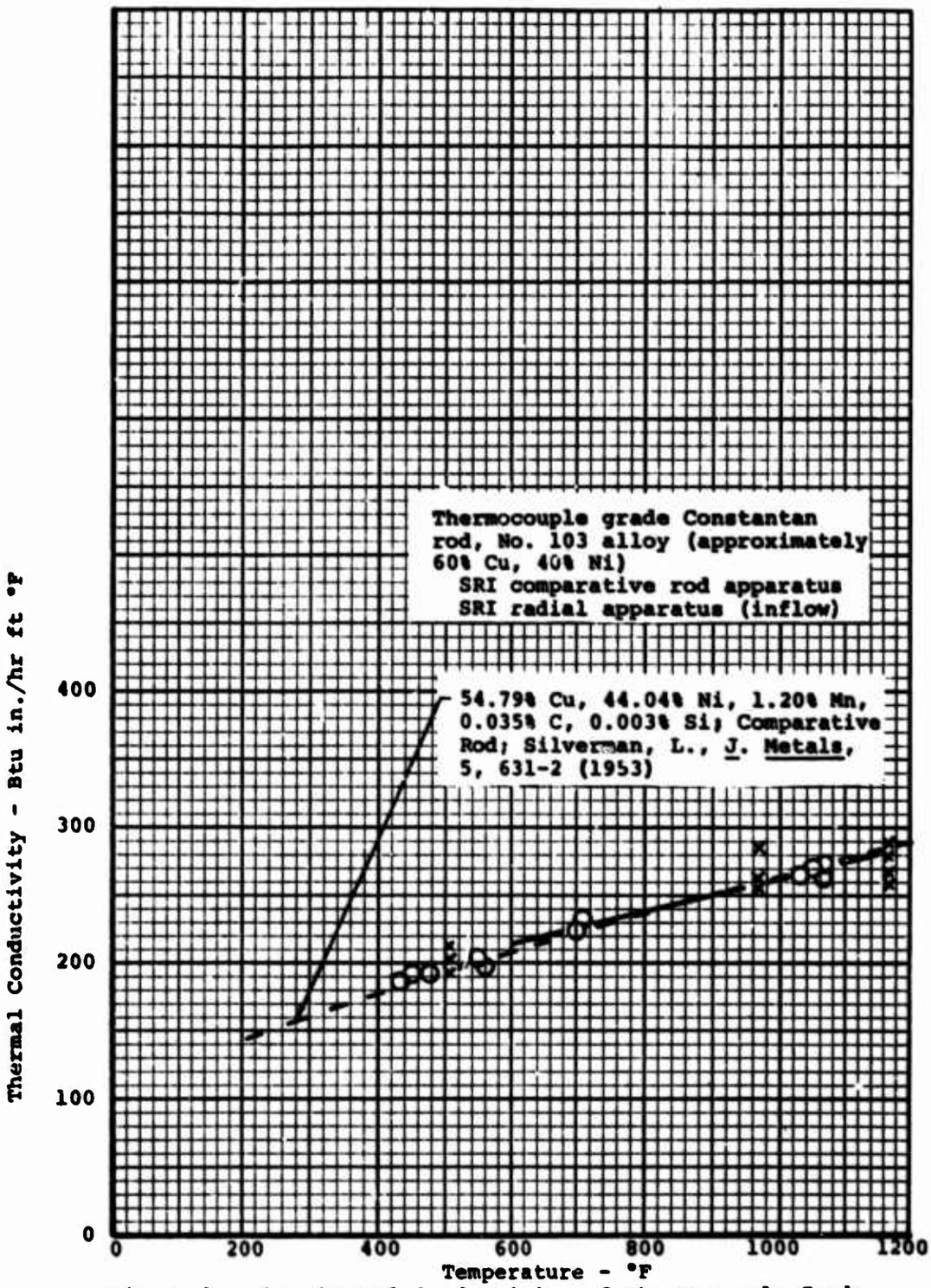

Figure 8. The Thermal Conductivity of Thermocouple Grade Constantan Rod

APPENDIX B

THERMAL CONDUCTIVITY TO 5500°F
BY RADIAL INFLOW METHOD

THERMAL CONDUCTIVITY TO 5500°F BY RADIAL INFLOW METHOD

The thermal conductivity is determined with a radial heat inflow apparatus that utilizes a central specimen 1" long. This apparatus is normally employed for measurements over the temperature range from 1500°F to 5500°F. Comparative rod apparatus is used at temperatures below 1500°F where radiant heating is less effective. The radial inflow apparatus gives a direct measurement of the thermal conductivity rather than a measurement relative to some standard reference material. A picture of the apparatus ready to be installed in the furnace is shown in Figure 1. The furnace and associated equipment for the thermal conductivity work is shown in Figure 2. In addition to the specimen, the apparatus consists primarily of (1) a water calorimeter that passes axially through the center of the specimen, (2) guards made from the same specimen material at both ends of the specimens to reduce axial heat losses, (3) sight tubes that allow the temperature at selected points in the specimen to be determined either by thermocouples or optical pyrometer, and (4) an external radiant heat source (see Figure 3). The water calorimeter provides a heat sink at the center of the specimen to create a substantial heat flow through the specimen and allows the absolute value of the heat flow to be determined. Thermocouples mounted 1/2" apart in the calorimeter water stream measure the temperature rise of the water as it passes through the gage portion of the specimen. By metering the water flow through the calorimeter, it is possible to calculate the total radial heat flow through the 1/2" gage section of the specimen from the standard relationship $Q = MC\Delta T$. M is the weight of water flowing per hour, C is the specific heat of water, and ΔT is the temperature rise of the water as it passes through the gage section.

The standard specimen configuration is shown in Figure 4. The specimen is 1.062"O.D. x 0.250"I.D. x 1" long. Holes 0.073" in diameter are drilled on radii of 0.233 and 0.437 inch to permit measurement of the radial temperature gradient. In specimens which are anisotropic in the diametral plane (for example, certain graphites) a second pair of holes is drilled 90° to the first pair. The diameters joining each pair of holes is located to coincide with the principal planes of anisotropy in the material.

A 1/2" long upper guard and a 1/2" long lower guard of specimen material are placed above and below the 1" long specimen to maintain a constant radial temperature gradient throughout the entire specimen length and thereby prevent axial heat flow in the specimen. The outer ends of the specimen guards are insulated with graphite tubes filled with thermatomic carbon. These tubes also hold the specimen in alignment. The combined effect of specimen guards and thermatomic carbon insulation permits a

minimum axial temperature gradient within the specimen. This gradient is not detectable by optical pyrometer readings. Visual inspection of the specimens after runs have verified that no large axial temperature gradient exists in the specimen. The guards, made of specimen material, display axial distortion of the isothermal lines for approximately 1/4" from the outer ends before reaching an apparent constant axial temperature.

When sufficient material is available the alternate specimen configuration shown in Figure 5 is employed. This specimen, being 1.5" in diameter, provides a larger gage length (0.357") between temperature wells and allows the installation of three holes on each radius without excessively distorting the radial temperature profiles. Thus this specimen configuration permits a more precise measurement of the average temperature at each radial location. As with the smaller specimen, the location of the temperature wells must be altered for transversely anisotropic specimens.

The annulus between the specimen inside diameter and the 7/32" outside diameter of the calorimeter tube is packed with either copper granules, graphite or zirconia powder. This packing provides a positive method for centering the calorimeter within the specimen and promotes good heat transfer between specimen and calorimeter.

Temperatures up to 2000°F are measured with Chromel/Alumel thermocouples inserted into the specimen through the sight tubes. At high temperatures, the temperatures are measured through the vertical sight tubes using a right-angle mirror device and optical pyrometer.

In Figures 1 and 3 showing a typical conductivity calorimeter apparatus ready for insertion into a furnace for a run, a water-cooled copper section can be seen at the top of the unit. This section provides permanent sight tubes to within about 2 1/2" of the guard specimen, in addition to a permanent mount for the right-angle mirror device used with the optical pyrometer. Within the short zone between the water-cooled section and the top guard, thin-walled graphite sight tubes are fitted. The remainder of the annulus is filled with thermatomic carbon insulation.

During thermal conductivity runs, the following data are recorded: (1) power input, (2) specimen face temperature, (3) specimen temperatures in the gage section at the two radii, (4) temperature of the calorimeter water at two points 1/2" apart axially within the specimen center, and (5) water flow rate through the calorimeter. At least 5 readings are made at each general temperature range to determine the normal data scatter and to minimize the error that might be encountered in a single reading.

All thermocouple readings are measured on a Leeds and Northrup K-3 null balance potentiometer used in conjunction with a galvanometer of 0.43 microvolts per mm deflection sensitivity. All optically measured temperatures are read with a Leeds and Northrup Type 8622 optical pyrometer. The flow rate of the calorimeter water is measured with a Fischer and Porter Stabl-Vis Flowrater.

The thermal conductivity values are computed from the relation

$$K = \frac{QL}{\Delta T A_{lm}}$$

where Q is the heat flow to the calorimeter within the specimen gage section, A_{lm} is the log mean area for the specimen gage length, ΔT is the specimen temperature change across the specimen gage length, and L is the gage length over which the specimen ΔT is measured.

The heat flow Q is determined by the calorimeter. A_{lm} and L are calculated directly for the particular specimen configuration. ΔT is determined directly from the observed temperature difference across the specimen gage length.

Based on an extensive error analysis and calibrations on homogeneous isotropic materials of known thermal conductivities, such as Armco iron and tungsten, the precision (coefficient of variation) in the measurements has been established at ±7 percent over the temperature range. For multiple runs on samples having similar properties, the uncertainty in a smooth curve through the data can be established to within ±7 percent. A detailed error analysis has been presented in a paper by Mann and Pears.[1]

Data obtained here on several high temperature materials are presented in Figures 6, 7 & 8. Figure 6 is a plot of data obtained here on tungsten. The specimen for these determinations were fabricated from stacks of 0.060 inch washers cut from hot rolled sheet stock. Also plotted are values reported by other investigators including "recommended values" given by Powell, Ho and Liley[2] based on a compilation of 103 sets of data. Agree-

---

[1]Mann, W. H. Jr., and C. D. Pears, "A Radial Heat Flow Method for the Measurement of Thermal Conductivity to 5200°F", presented at the Conference on Thermal Conductivity Methods, Battelle Memorial Institute, October 26-28, 1961.

[2]Powell, R. W., C. Y. Ho and P. E. Liley, "Thermal Conductivity of Selected Materials" NSRDS-NBS 8, National Standard Reference Data Series - National Bureau of Standards - 8, 1966, pp.11, 54-59.

ment between our data and the recommended values is excellent throughout the temperature range.

Figure 7 shows data obtained here on ATJ graphite, with grain. This material is premium grade, medium grain graphite having a density range of 1.73 to 1.78 gm/cm^3. The crosses (+) shown in the figure are "recommended values" given by Ho, Powell and Liley.[3] Again agreement is excellent.

Figure 8 shows data obtained on AXM-5Q1. These data were obtained under a program sponsored by the Air Force Materials Laboratory to develop high temperature thermal conductivity standards. Measurements were made on this material by four laboratories in addition to Southern Research Institute. The bands shown in Figure 8 represent the range of data reported by the other participating organizations. A complete presentation and discussion of the data is given in AFML-TR-69-2[4].

[3]Ho, C. Y., R. W. Powell and P. E. Liley, "Thermal Conductivity of Selected Materials, Part 2," NSRDS-NBS16 National Standard Reference Data Series-National Bureau of Standards-16, 1968, pp.89-128.

[4]AFML-TR-69-2, "Development of High Temperature Thermal Conductivity Standards" submitted by Arthur D. Little, Inc., under contract AF33(615)-2874, 1969, pp.115-127.

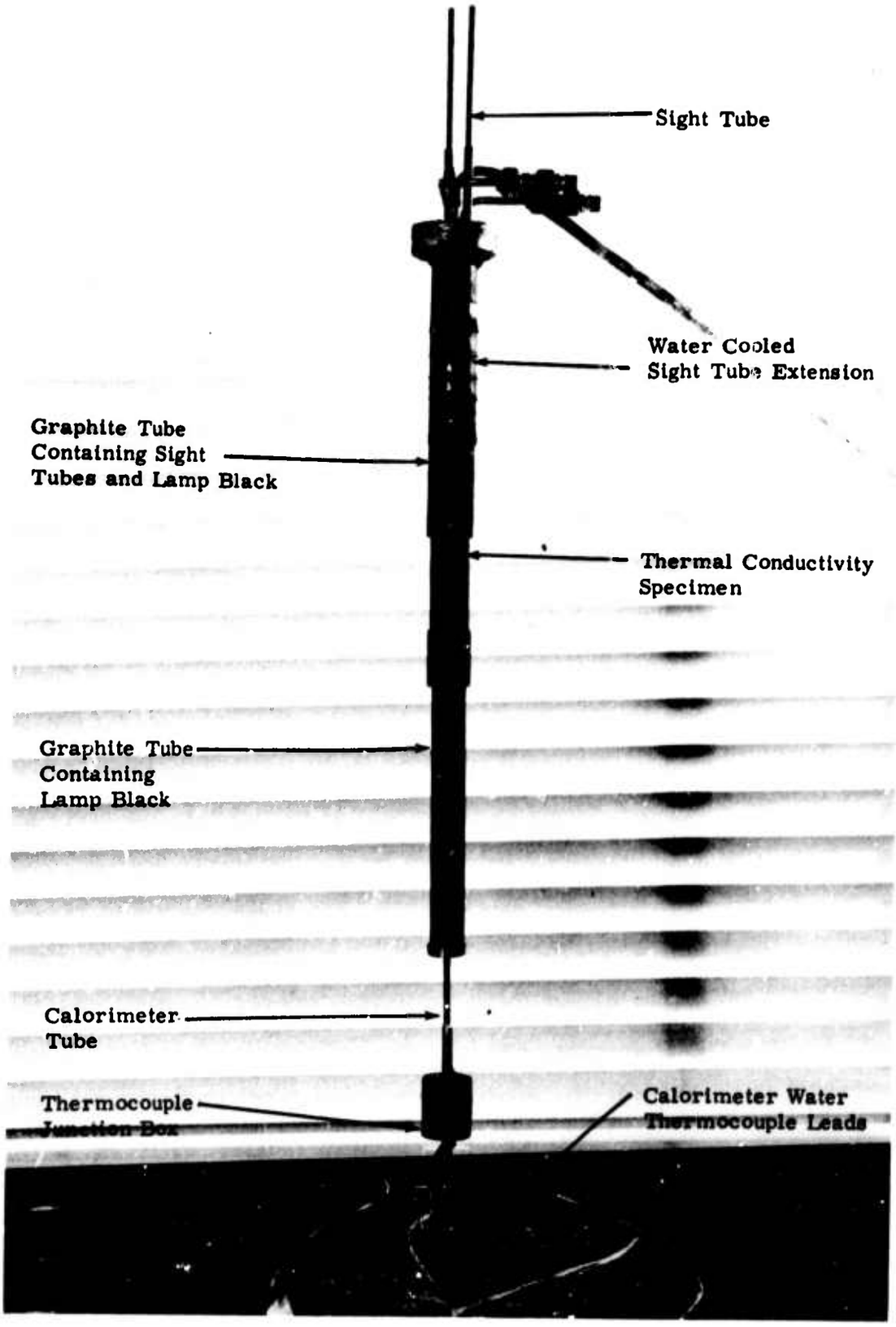

Figure 1. Picture of the Radial Thermal Conductivity Apparatus

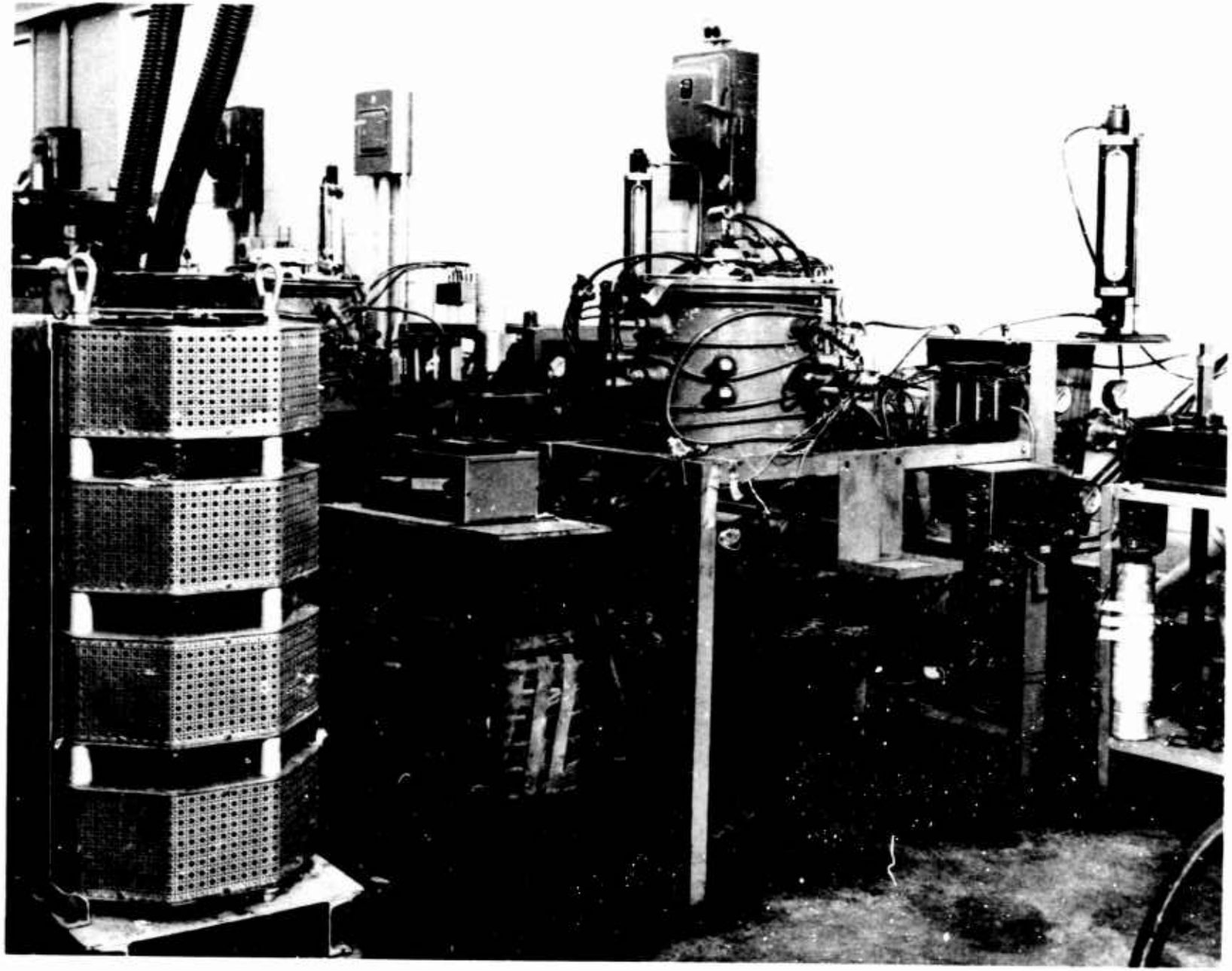

Figure 2. Furnace with Thermal Conductivity Apparatus Installed

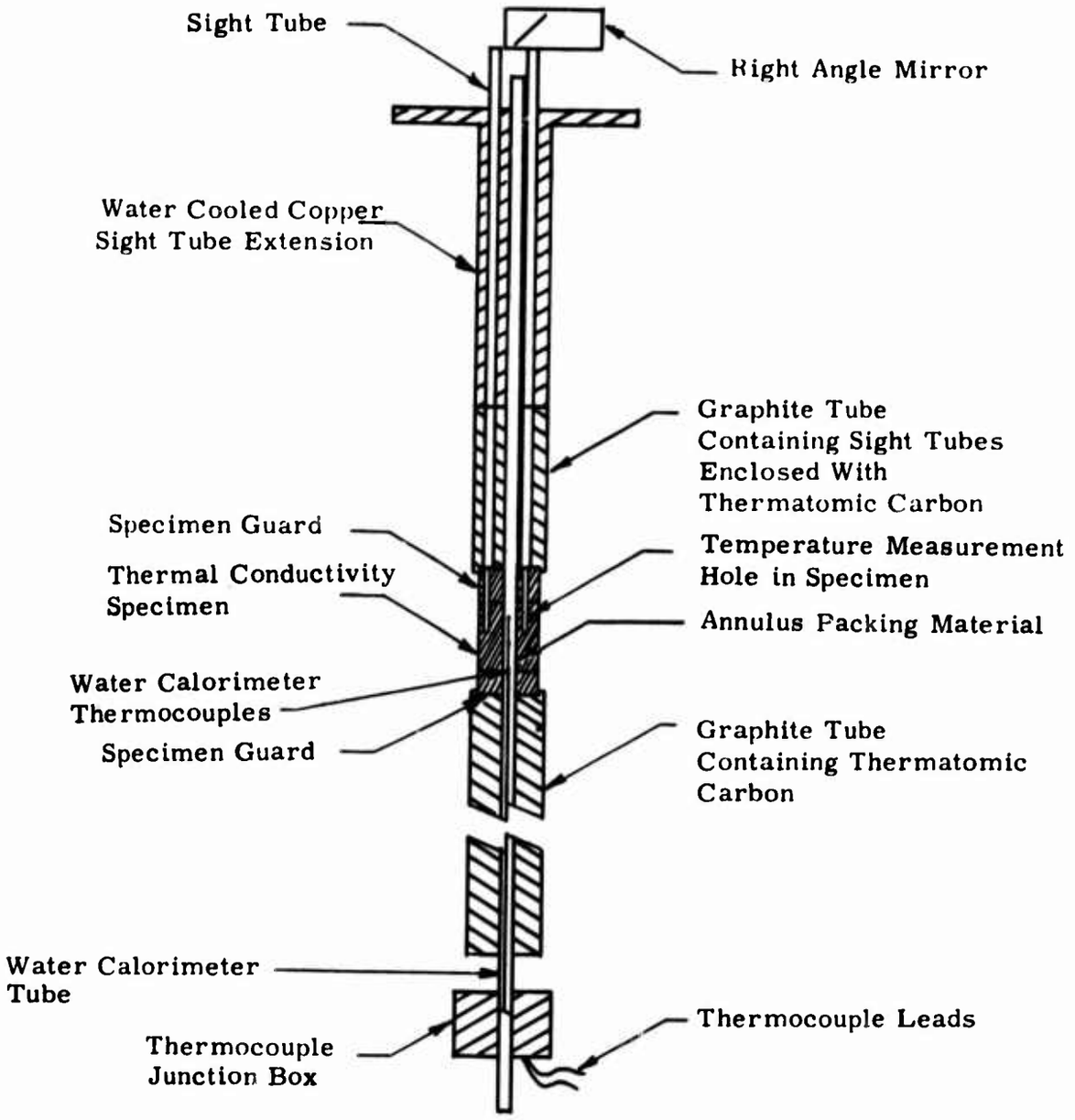

Figure 3. Cross-section Schematic of the Thermal Conductivity Apparatus

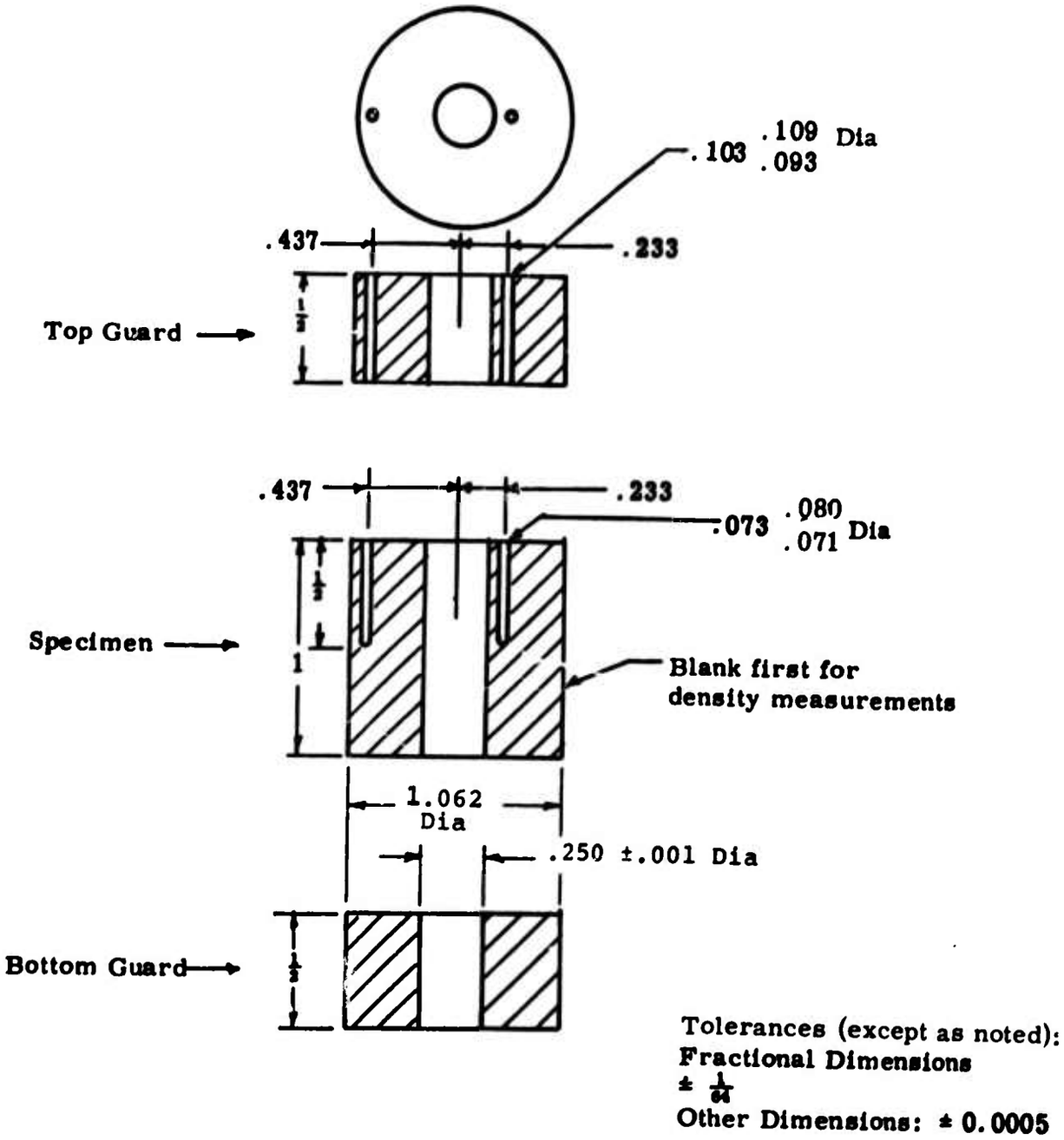

Figure 4. 1.06 Diameter Thermal Conductivity Specimen for Radial Inflow Apparatus

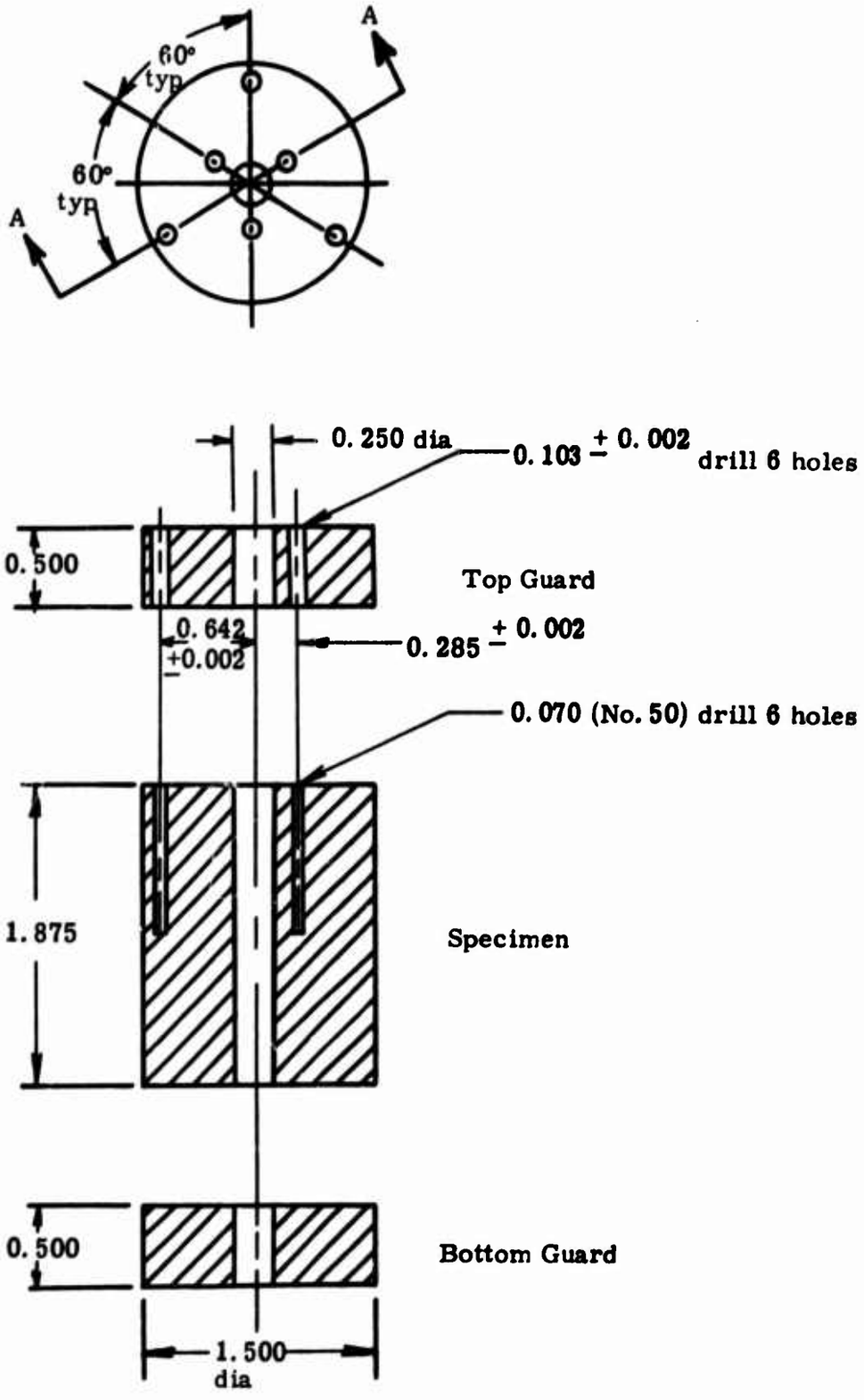

Figure 5. Dimensions of 1.50 Inch Diameter Specimen and Guards Used for Radial Inflow Thermal Conductivity Measurements

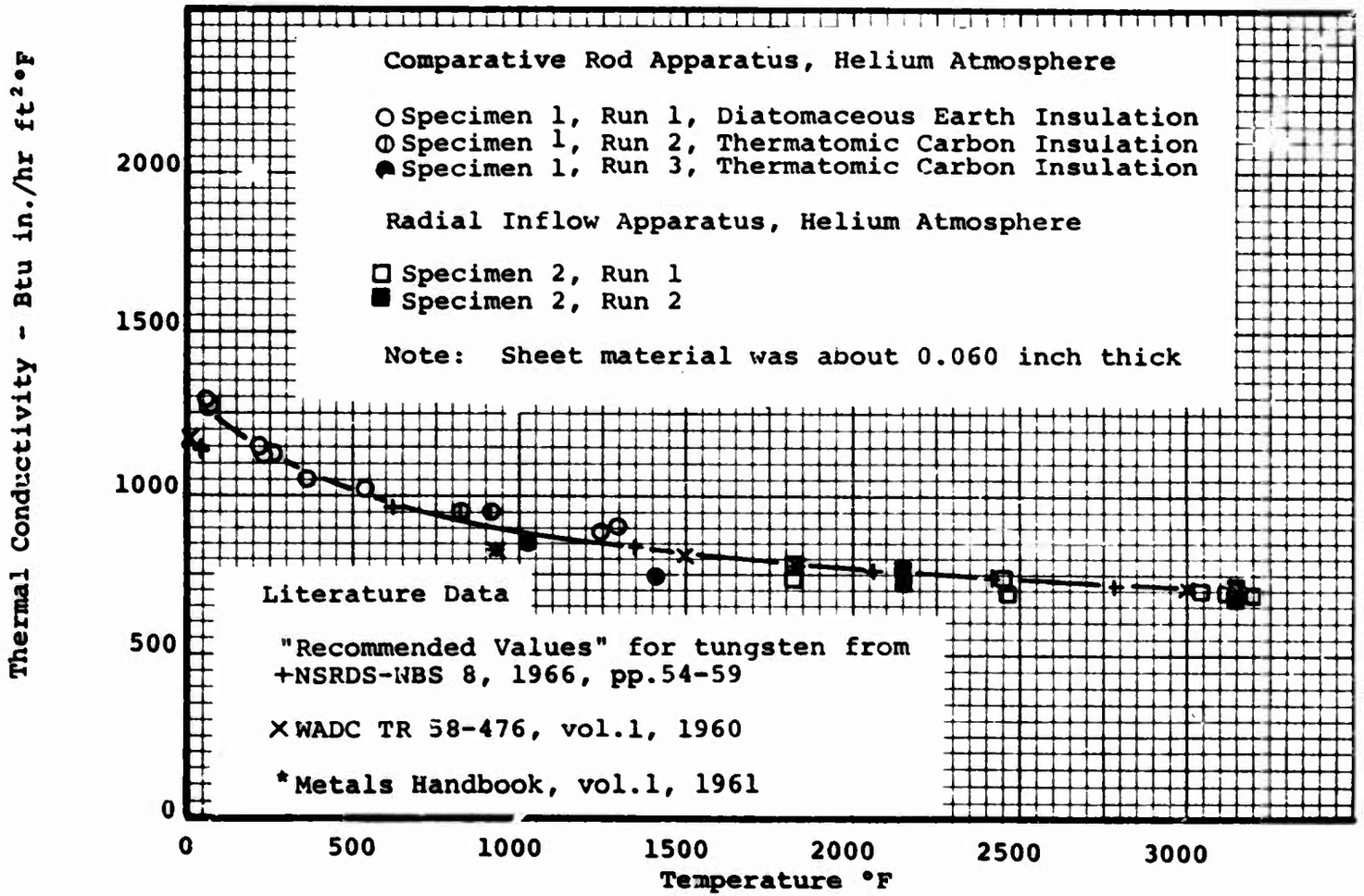

Figure 6. The Thermal Conductivity of Tungsten Sheet Parallel to the Plane of the Sheet

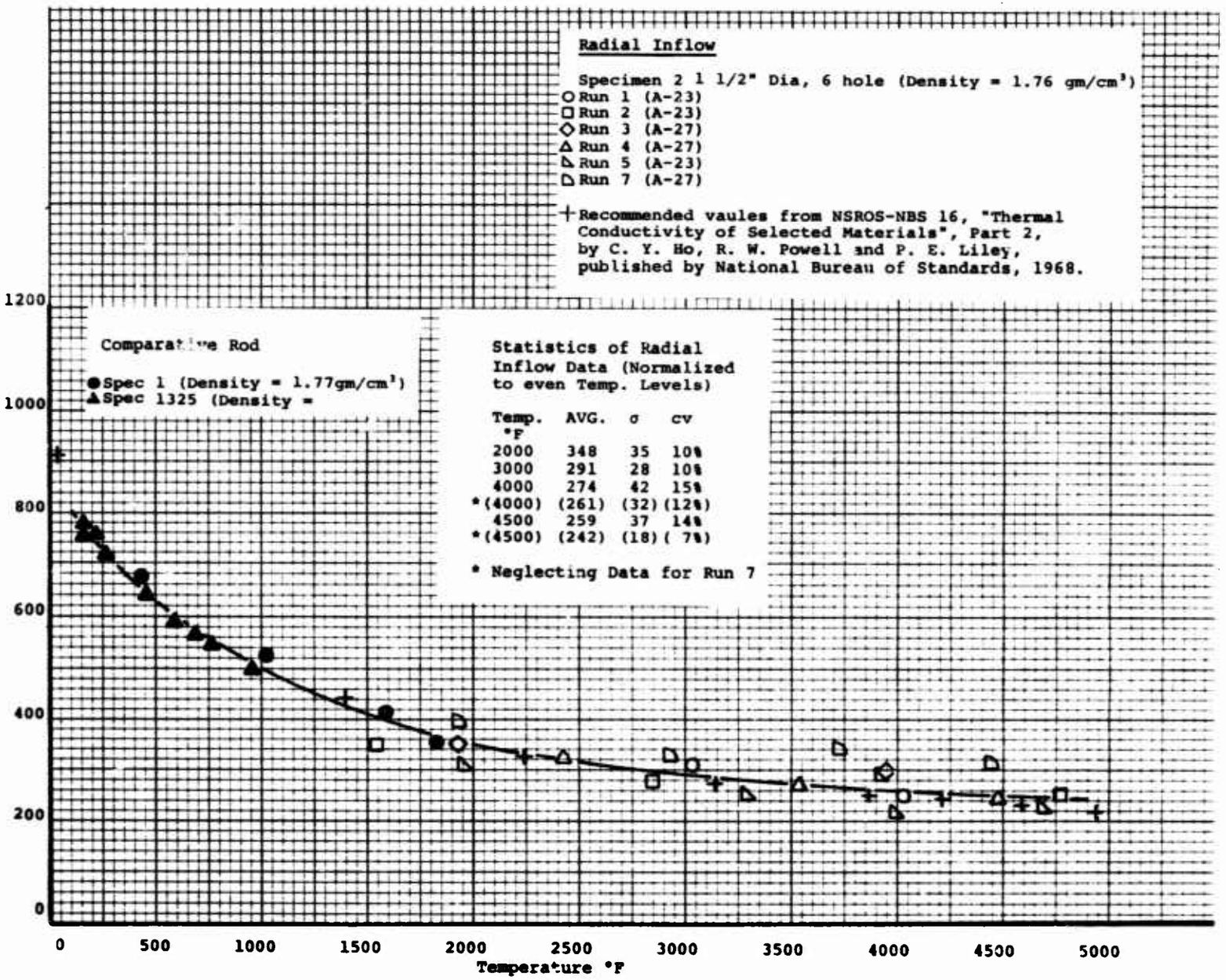

Figure 7. The Thermal Conductivity of ATJ Graphite, With Grain

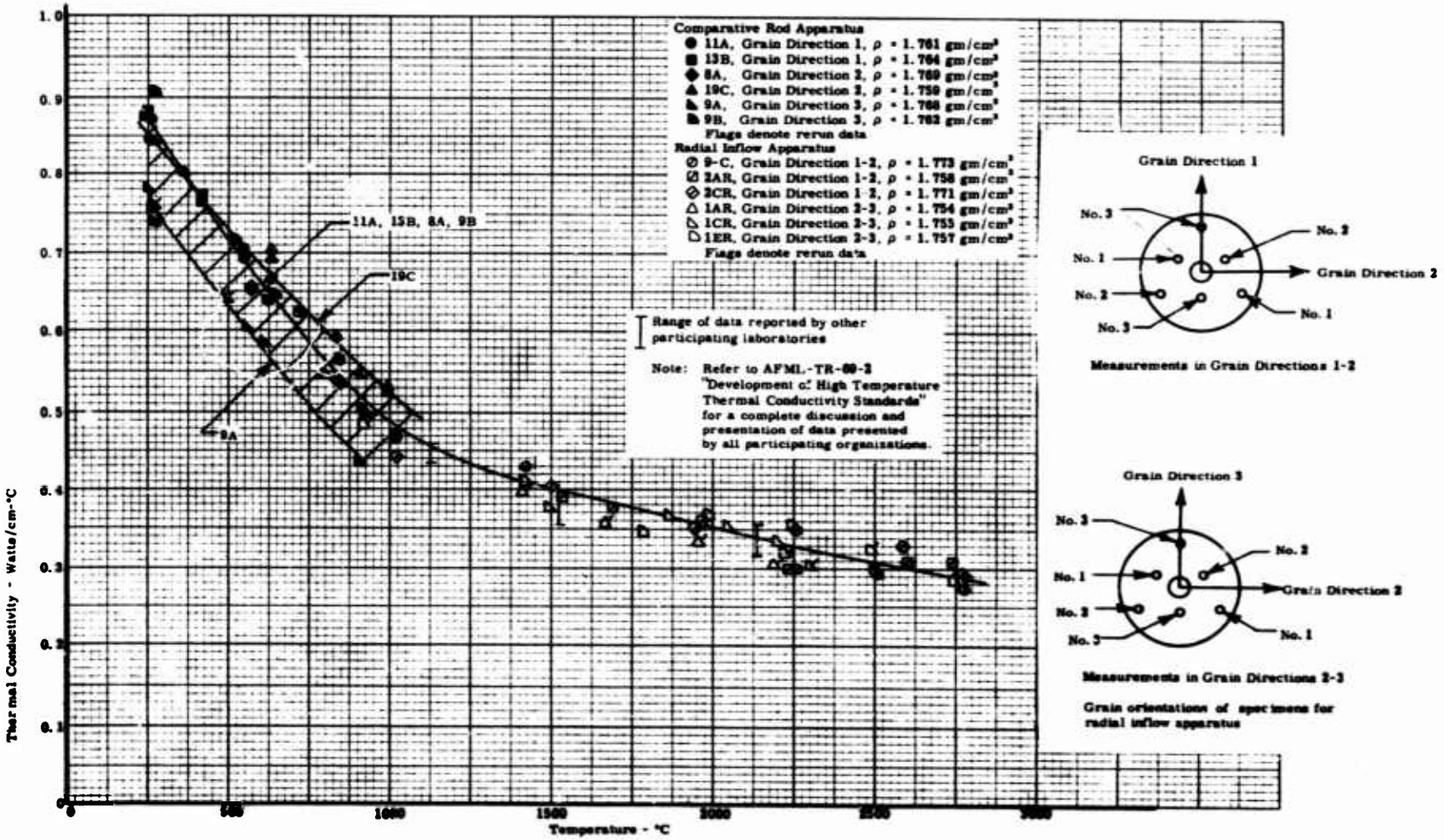

Figure 9. The Thermal Conductivity of AXM-5QI Graphite

APPENDIX C

THERMAL EXPANSION TO 5500°F

THERMAL EXPANSION TO 5500°F

Thermal expansion is measured in a graphite tube dilatometer developed by Southern Research Institute for performance to 5500°F, see Figure 1. The specimen required is about $\frac{1}{2}$" diameter and 3" long, although the exact size can vary somewhat if it appears desirable from the standpoint of specimen availability. Specimens $\frac{3}{4}$" in diameter and only $\frac{1}{4}$" thick can be evaluated, but with a reduced precision. Discs can be stacked to provide more length in many cases. Of course, specimens can always be pinned together from smaller pieces to provide both length and columnar strength.

In the dilatometer, the specimen rests on the bottom of the cylinder with a graphite extension rod resting on the specimen to extend to the top of the cylinder. When required, tungsten pads are inserted at the ends of the specimen to eliminate graphite diffusion from the dilatometer parts into the specimen. This entire assembly is inserted into one of the 5000°F furnaces described in another brochure.

The motion of the specimen is measured by a dial gage attached to the upper end of the cylinder with the stylus bearing on the extension rod. The system accurately indicates total motions of 0.0001" - or less than 0.00004" per inch of specimen.

Either a helium or an argon environment can be employed. Nitrogen has been used on occasion. The equipment will permit operation at hard vacuums, but this procedure is rarely used.

A CS graphite, which has a fairly low expansion relative to other grades of graphite, is used as the material for the dilatometer. Prior to calibrations, the dilatometers are heat soaked to a temperature several hundred degrees above the maximum temperature to which they would be exposed during normal service. Dimensional stability is confirmed by measuring the lengths of the dilatometer tube and rod after each run. Past experience has shown that following the initial heat soak the expansion is reproducible in subsequent repeated cycles to lower temperatures. Reproducibility is also confirmed by repeated runs on standards.

To calibrate the dilatometers we have developed in-house primary and secondary standards of ATJ graphite. ATJ graphite was selected as a standard because of our vast experience with it, its stability after repeated exposure to high temperatures, and its relatively low expansion.

The true expansion of the primary standard was determined by a direct optical technique using a traveling Gaertner telescope. The total error in the telescope readings, based on calibration data, was estimated to be 0.2×10^{-3} in./in. For the direct optical measurements, the 3.5 in. long specimen was heated in a graphite furnace, and the expansion was determined by sighting on "knife" edges machined on the ends of the specimen. Typically a total of 11 runs have been made in two different furnaces both in vacuum and helium environments. The two environments are used to check effects of refraction as reported in the literature. The same standard was then machined to the configuration of a regular dilatometer specimen and several runs were made in our precision quartz dilatometers. The optical expansion data were fitted to a quadratic equation over the temperature range from 2500°F to 5000°F using the method of least squares and statistically analyzed to determine the uncertainty (primarily the scatter). Below 2500°F, the quartz dilatometer data were fitted by hand since the uncertainty of this apparatus has been well established, and the imprecision is small ($<0.1 \times 10^{-3}$ in./in.). A typical plot of all data points with the curve fit is shown in Figure 2.

A check of the expansion of the standard was obtained by making runs on round robin specimens of various graphites and synthetic sapphire which had been previously evaluated by others, including the National Bureau of standards. Our data on these specimens agreed within a 2.5 percent random difference with the data reported by the other laboratories.

After establishing the expansion of the ATJ standard, several graphite dilatometers were then calibrated by making runs on this standard. These dilatometers were used to establish the expansion of secondary standards (also ATJ graphite) which are used to calibrate new dilatometers and to make periodic checks on dilatometers currently in service. This use of secondary standards thus minimizes the wear and tear on the primary standard and prolongs its life.

Table 1 lists the uncertainties in the dilatometer measurements in 10^{-3} in./in. Observe that most of the uncertainty is in the expansion of the standard and includes both random and systematic uncertainties. Other sources of uncertainty, resulting from such factors as dial gage and temperature measurement, are small amounting to less than 0.2×10^{-3} in./in. at any temperature. The precision in the dilatometer measurements is quite good and amounts to about 0.1×10^{-3} in./in. From Table 1, it can be seen that the maximum total uncertainty, which occurs at a temperature of 4500°F, is $\pm 0.45 \times 10^{-3}$ in./in. For a low expansion graphite, such as ATJ, this amounts to an uncertainty of ±4.5 percent at 4500°F (see Figure 2). For graphites having higher expansions, the percentage uncertainty would be lower.

1/70-200

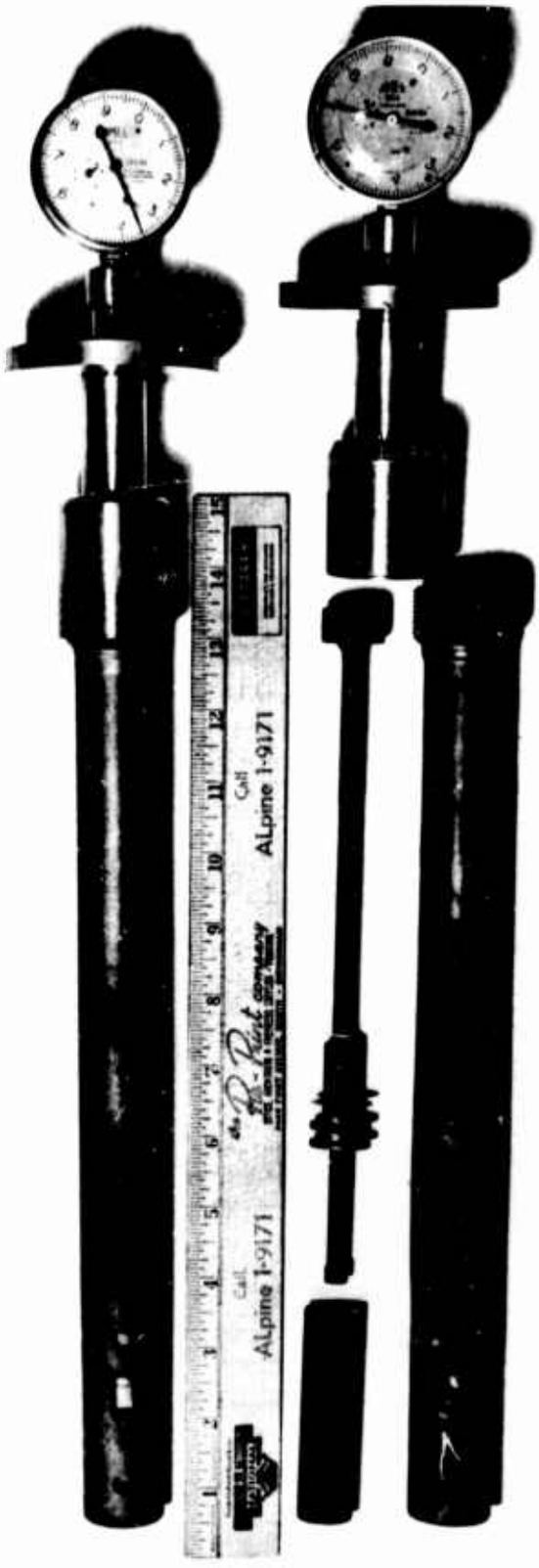

Figure 1. Picture of the Graphite Dilatometer Tubes for Measuring Thermal Expansion to 5500°F

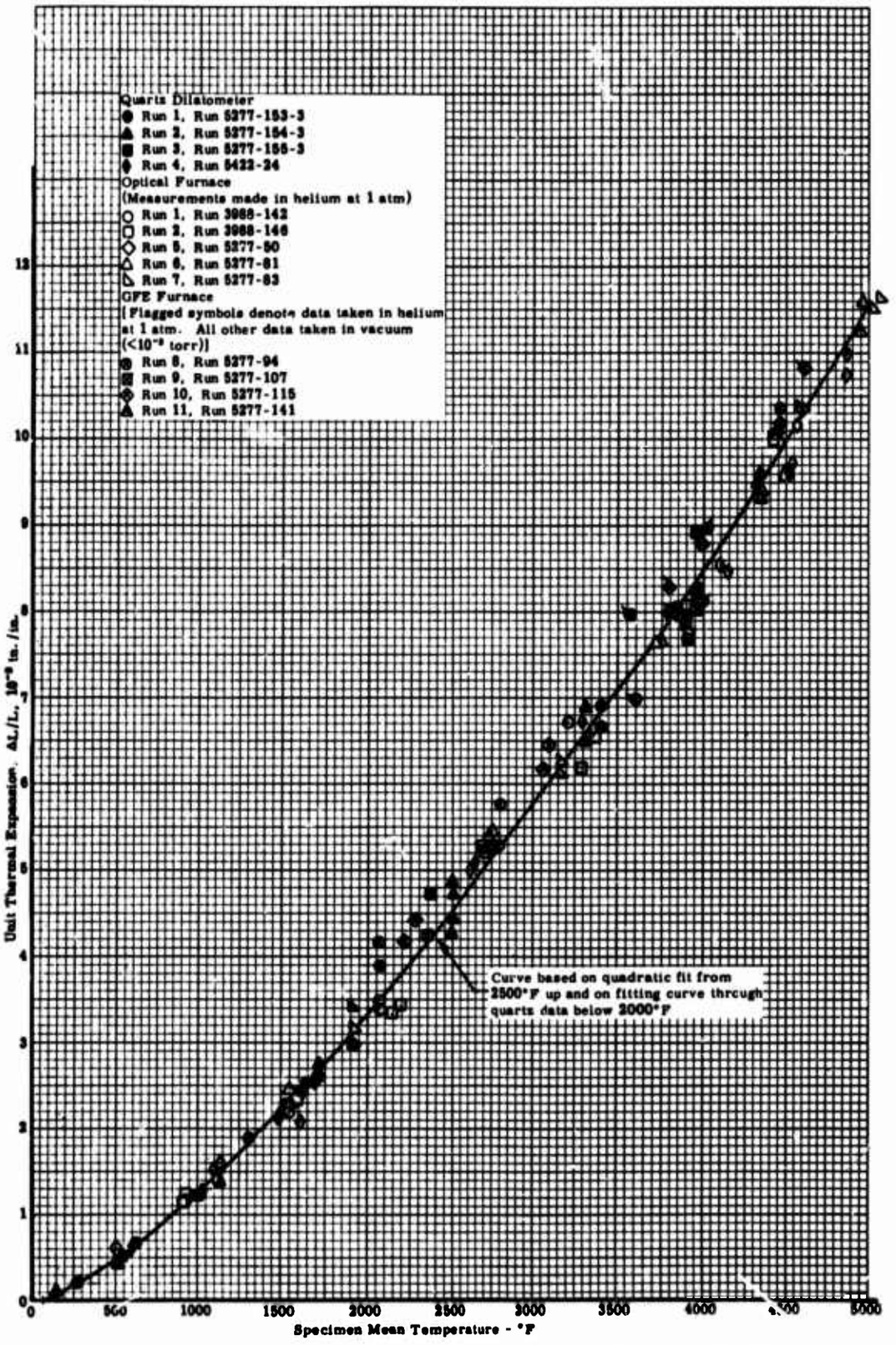

Figure 2. The Thermal Expansion of ATJ Graphite (wg) Standard No. 5 by In-house Optical Calibration

Table 1

Uncertainty in Thermal Expansion Measurements
Made in Graphite Dilatometers

Temperature °F	Uncertainty in Expansion of Standard in 10^{-3} in./in.		Random Uncertainty in Dilatometer Measurements in 10^{-3} in./in.	Total Uncertainty in Dilatometer Measurements from all Sources in 10^{-3} in./in.	
	Random Uncertainty (See Note 1)	Systematic Uncertainty (See Note 2)		+	−
500	±0.04	0	±0.03	0.05	0.05
1000	±0.04	0	±0.03	0.05	0.05
1500	±0.05	0	±0.04	0.07	0.07
2000	±0.17	+0.03	±0.05	0.21	0.18
2500	±0.11	+0.20	±0.07	0.33	0.13
3000	±0.12	+0.21	±0.08	0.35	0.14
3500	±0.19	-0.02	±0.10	0.21	0.23
4000	±0.14	-0.09	±0.12	0.18	0.27
4500	±0.14	±0.25	±0.14	0.45	0.45
5000	±0.19	-0.12	±0.16	0.25	0.37

Notes: 1. 95% confidence limits.
2. Represents deviation between average measured value and least squares curve through all data.

APPENDIX D

HEAT CAPACITY TO 1000°F

HEAT CAPACITY TO 1000°F

The heat capacity to 1000°F is determined from data obtained in an adiabatic calorimeter. In this apparatus the heated specimen is dropped into a thermally guarded, calibrated cup, and the enthalpy is measured as a function of the increase in temperature of the cup. The heat capacity is the slope of the enthalpy versus temperature curve. A picture of the apparatus is shown in Figure 1.

A tubular furnace and a cold box are used to bring the specimens to temperature. By pivoting this equipment on a common post near the calorimeter, the samples are transferred to a position directly over the calorimeter cup. At this position the specimen is released from a suspension assembly that is triggered externally. Thermocouples located near the specimen are used to measure specimen temperature. The normal specimen size is about 1" x 1" x 1".

Elevated specimen temperatures are maintained by a manual setting of a variable voltage transformer, which controls the power input to the furnace. Cold sample temperatures are obtained by filling the cold box with dry ice and, when required, injecting liquid nitrogen vapors. The cold box consists of two concentric cylinders enclosed in a housing. The smaller cylinder (3" diameter by 16" high) is constructed of $\frac{1}{4}$" mesh hardware cloth. The larger cylinder is made of galvanized sheet metal (15" diameter and 16" high). The annulus is partially filled with dry ice.

Specimens of the materials are heated or cooled to the desired temperature, and following a stabilization period, are dropped into the calorimeter cup. Adiabatic conditions are maintained during each run by manually adjusting the cup guard bath temperature.

The covered cup of the drop-type adiabatic calorimeter is approximately $2\frac{1}{2}$" in diameter by 2" deep. Three thermocouple wells are located in the bottom wall of the cup. The cup is mounted on cork supports, which rest in a silver-plated copper jacket. The jacket is immersed in a bath of ethylene glycol which is maintained at the temperature of the cup by means of a heater and copper cooling coils immersed in the liquid. Chilled trichloroethylene is circulated through the coils to cool the bath below ambient temperature when cold enthalpy measurements are made. A double-bladed stirrer maintains uniform bath temperature.

In the calorimeter six copper-constantan thermocouples, differentially connected between calorimeter cup and jacket, indicate temperature difference between cup and bath. The six thermocouples enable a difference of 0.03°F to be detected. This difference is maintained to within 0.15°F. During the runs, absolute temperature measurements of the cup are determined by means of the three thermocouple junctions, series connected, in the bottom of the calorimeter cup. All of the thermocouple readings are taken with instruments which permit readout to within 0.1°F; however, the system uncertainty is about 0.5°F.

The enthalpy of the specimen at any initial temperature is calculated from the following equation:

$$h = \frac{K}{W_s} (t_2 - t_1) \qquad (1)$$

where

h = enthalpy above t_2
K = calorimeter constant, 0.2654 Btu/°F
W_s = sample weight in lbs
t_1 = initial cup temperature in °F
t_2 = final cup temperature in °F

The calorimeter constant of 0.2654 Btu/°F was determined by measuring the enthalpy of an electrolytic copper specimen of known specific heat.

The enthalpy is referred to a common base temperature of 85°F using the following linear interpolation:

$$h_{85} = h \frac{(t_3 - 85)}{(t_3 - t_2)} \qquad (2)$$

where

h_{85} = enthalpy above the reference temperature of 85°F in Btu/lb
t_3 = initial sample temperature in °F

The base of 85°F is used because this is usually near the actual final cup temperature.

The enthalpy-temperature curve established is used to determine heat capacity (specific heat) by measuring its slope at different temperatures. This is done both graphically and by analytical methods which first fit the enthalpy data to an equation of the following type:

$$h_{BS} = aT + bT^2 + cT^{-1} + d \qquad (3)$$

The temperature (T) employed usually is in degrees Rankine. While this equation may not provide the best definition of the enthalpy data over the entire temperature range, it does anticipate the theoretical behavior and is consistent with methods recommended in WADC TR 57-308 and by K. K. Kelley.[1] The derivative of this equation, the heat capacity, is used with the constant "c" adjusted so that the analytical solution agrees with the value determined graphically at 150°F. This technique is similar to that of Kelley in forcing the heat capacity equation through a known value. The equations are developed using a digital computer.

The accuracy of the apparatus has been confirmed by measuring the enthalpy of sapphire and other standard specimens and comparing the results to literature values. The results of the comparison on sapphire are shown in Table 1. From these and other data the overall uncertainty of the apparatus was established at $\pm$ 3%.

---

1. Kelley, K.K., "Contributions to Data on Theoretical Metallurgy," Vol. XIII High Temperature Heat Content, Heat Capacity, and Enthalpy Data for Elements and Inorganic Compounds, Bulletin 584, U.S. Bureau of Mines, Nov. 1958.

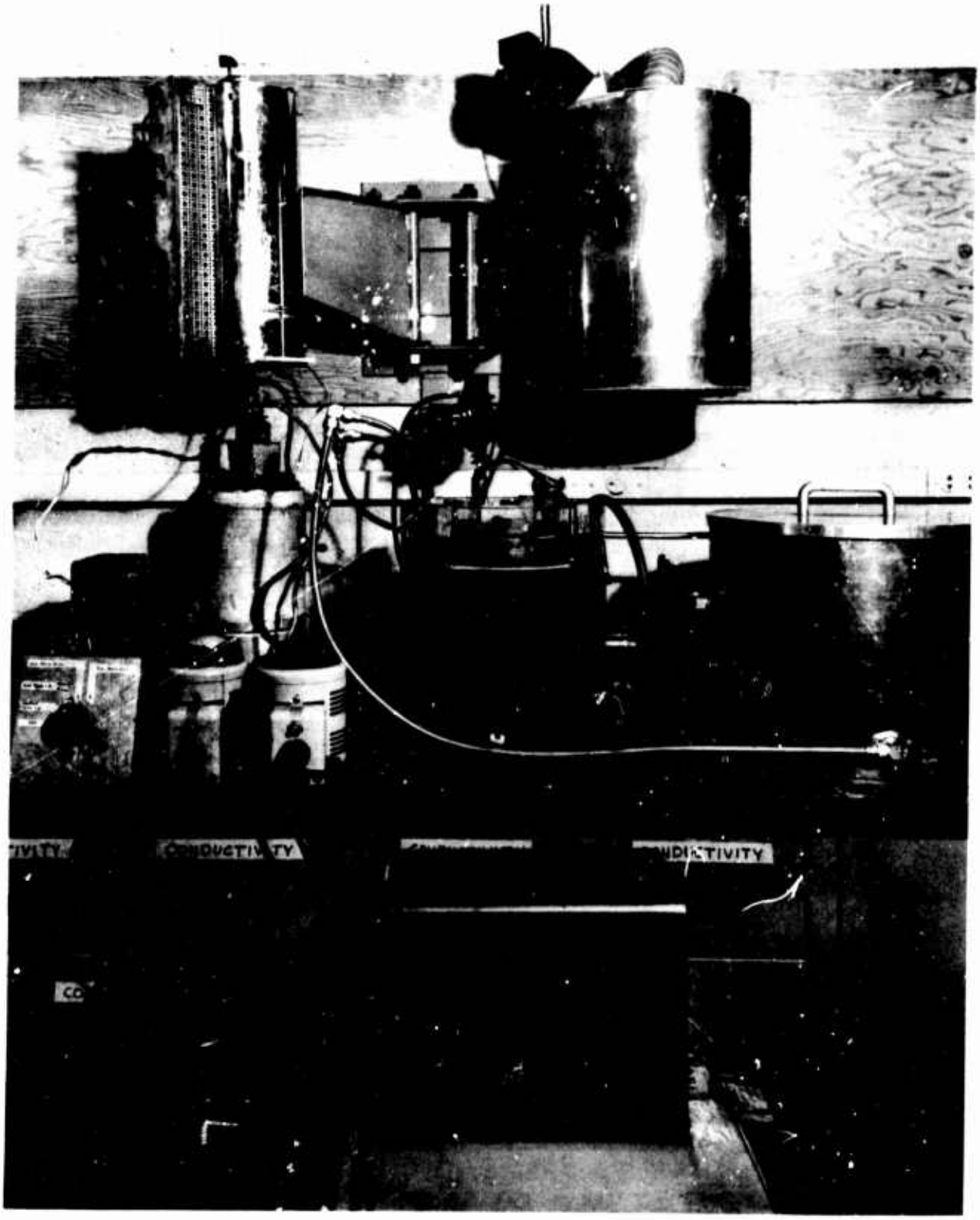

Figure 1. Heat Capacity Apparatus

Table 1

Comparison of the Specific Heat of Sapphire Obtained by the Adiabatic Calorimeter to Several Other Sources

SRI Adiabatic Calorimeter		SRI Ice Calorimeter		Armour Research Foundation		Linde Company		International Critical Tables	
Temp. °F	Specific Heat Btu/lb °F	Temp. °F	Specific Heat Btu/lb °F	Approx. Temp. °F	Specific Heat Btu/lb °F	Approx. Temp. °F	Specific Heat Btu/lb °F	Temp. °F	Specific Heat Btu/lb °F
490	0.233	497	0.210	500	0.263	500	0.2125		
996	0.240	1008	0.241	1000	0.280	1000	0.2265	922	0.239

APPENDIX E

HEAT CAPACITY TO 5500°F

HEAT CAPACITY TO 5500°F

The apparatus used for heat capacity employs the drop technique in which the specimen is heated in a furnace and then dropped into an ice calorimeter. The calorimeter contains a cup surrounded by a frozen ice mantle. Water at an inlet temperature of 32°F is circulated through an annulus surrounding the mantle in order to absorb heat leak from the surroundings. The entire system is insulated with glass wool. The enthalpy of the specimen is sensed as a change in volume of the water-ice system of the calorimeter as the ice melts. The annulus containing the flooded ice mantle communicates with the atmosphere through a mercury column in order that the change in volume can be read directly in a burette. An assembly drawing of the calorimeter is shown in Figure 1 and a picture of the calorimeter is shown in Figure 2. A picture of the ice mantle is shown in Figure 3. The specimen nominally is $\frac{3}{4}$" dia x $\frac{3}{4}$" long.

The specimen is placed in either a graphite or stainless steel basket and heated in the furnace in a controlled atmosphere such as helium. The specimen and basket are dropped into the calorimeter and the volume change due to the resultant melting of ice is measured. The flutter valve immediately above the cup and the diaphragm valve immediately below the furnace are major features of the apparatus since the first blocks off radiation losses from the specimen up the drop tube, and the second blocks radiation gains from the furnace down the drop tube just prior to dropping. The volume changes due to the baskets are measured and correction curves are established. Separate basket calibration minimizes the radiation error accompanying drop techniques. These errors are reported to be only about 0.5%.[1] Our theoretical calculations indicate even smaller errors from this source.

The heat necessary to melt enough ice to cause a volume change of 1 cc has been established by the U. S. National Bureau of Standards[2] at 3.487 Btu. This value is reported as the theoretical one for any ice calorimeter. Figure 4 shows a typical curve of mercury displacement

---

1. Furukawa, G. T., Douglas, McCoskey, and Ginnings, "Thermal Properties of Aluminum Oxide from 0° to 1200°K."

2. Ginnings, D. C. and R. J. Corruccini, "An Improved Ice Calorimeter," NBS Research Journal, Vol. 38, 1947, p 583.

versus time for one drop using a synthetic sapphire specimen. The correction for the stainless steel basket is subtracted from the measured mercury displacement and the result used to calculate specimen enthalpy above 32°F. The heat capacity, which is by definition the slope of the enthalpy versus temperature curve, is determined both graphically and analytically. The analytical approach is to fit the enthalpy data to an equation of the form

$$h_{32} = aT + bT^2 + cT^{-1} + d \qquad (1)$$

using a least squares technique. The derivative of this equation, the heat capacity, is computed with the constant "c" adjusted so that the analytical solution agrees with the graphical solution at 5000°F. [3] This technique is similar to that of Kelley in forcing the heat capacity equation through a known value. [4] The equations are developed using a digital computer.

A compilation of all errors has indicated that the apparatus is accurate to well within 5% uncertainty over the entire temperature range. Comparison of Southern Research Institute data on copper, Linde synthetic sapphire, and ATJ graphite all have confirmed this value.

---

3. Pears, C. D., and J. G. Allen, "The Thermal Properties of Twenty-six Solid Materials to 5000°F or Their Destruction Temperatures," ASD-TDR-62-765.

4. Kelley, K. K., "Contributions to Data on Theoretical Metallurgy," Vol. XIII, High Temperature Heat Content, Heat Capacity and Enthalpy Data for the Elements and Inorganic Compounds, USBM 584, Nov. 1958.

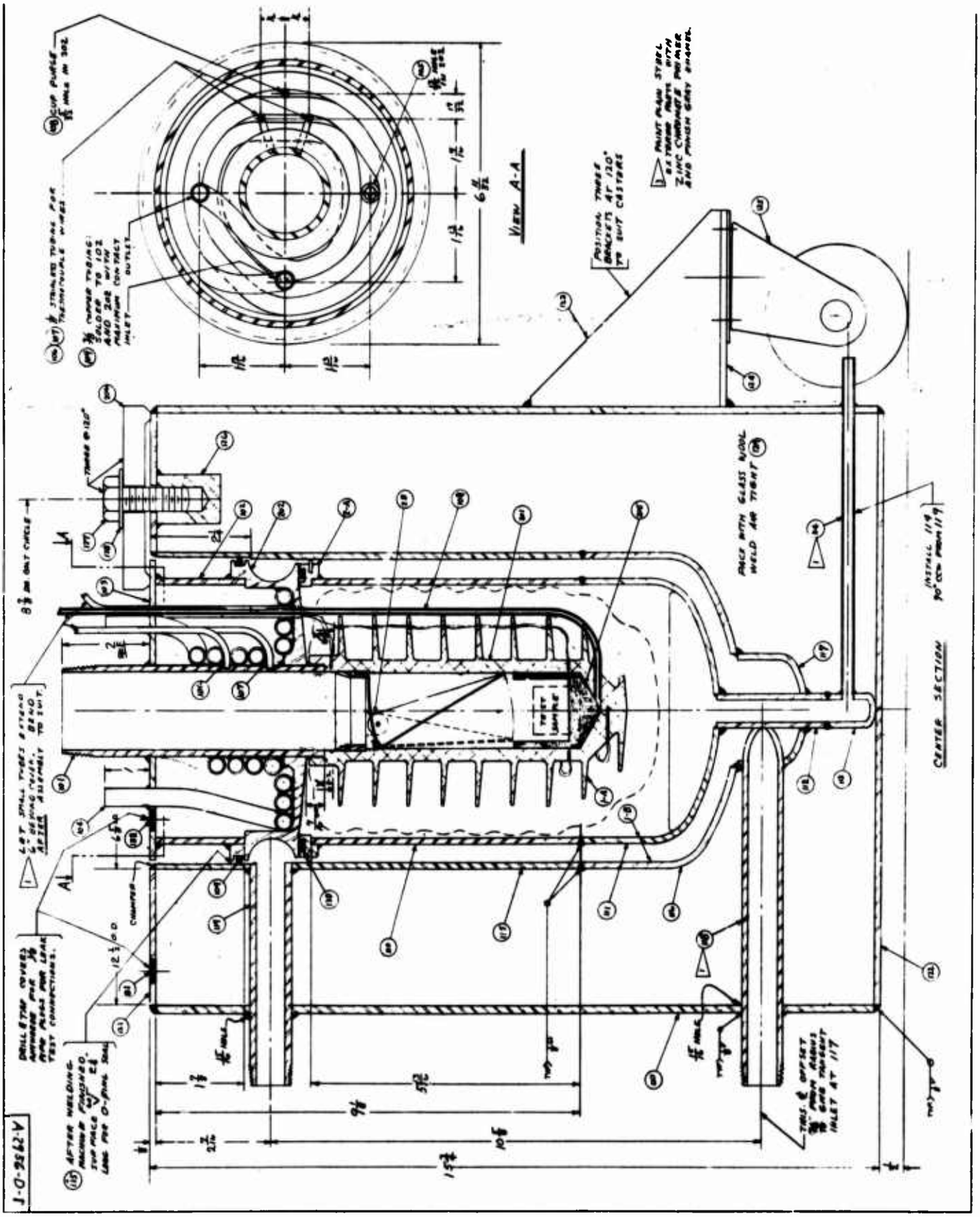

Figure 1. Ice Calorimeter, Drop Type - Specimens to 5500°F

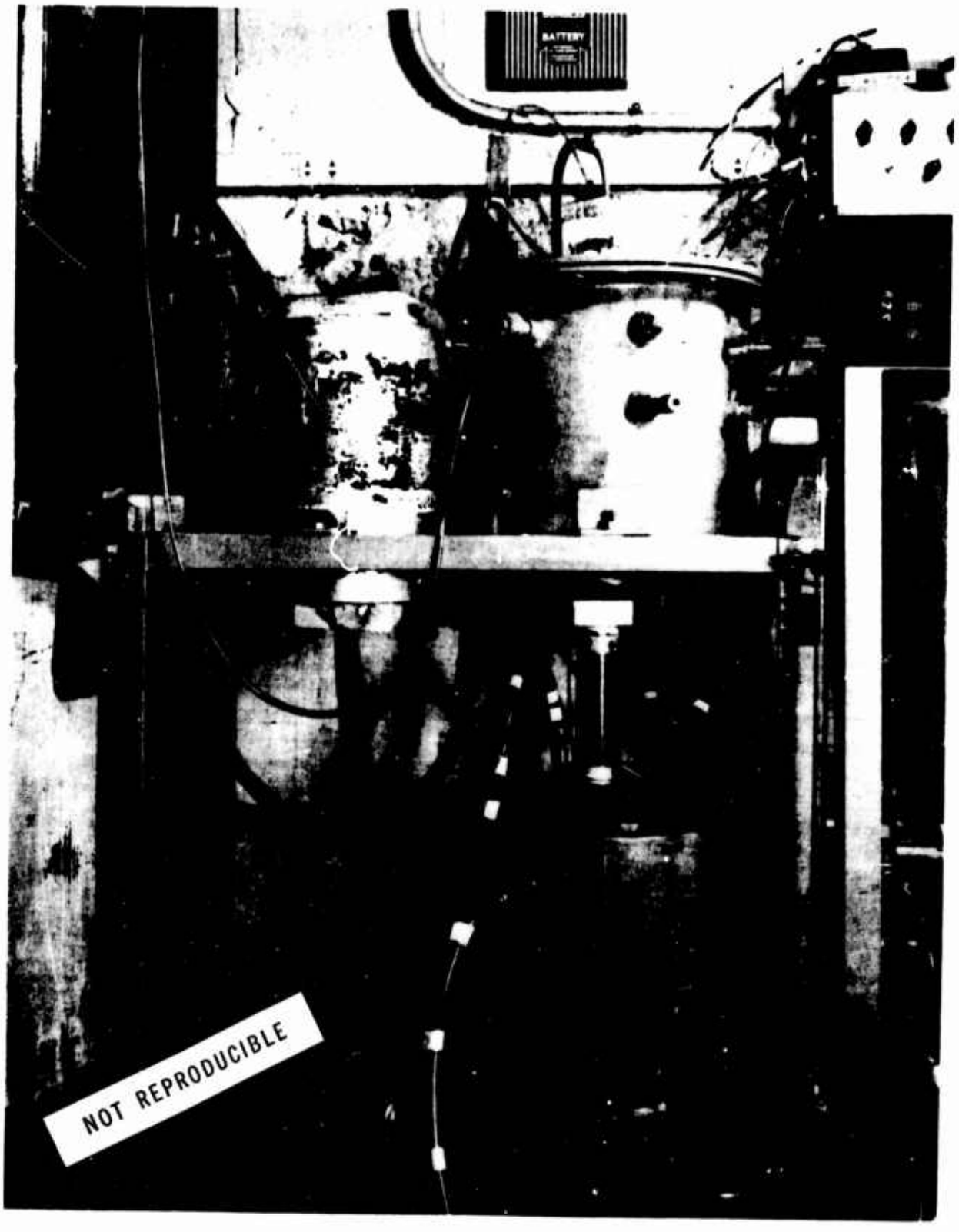

Figure 2. Picture of Heat Capacity Equipment with Drop Shield Tube in Place

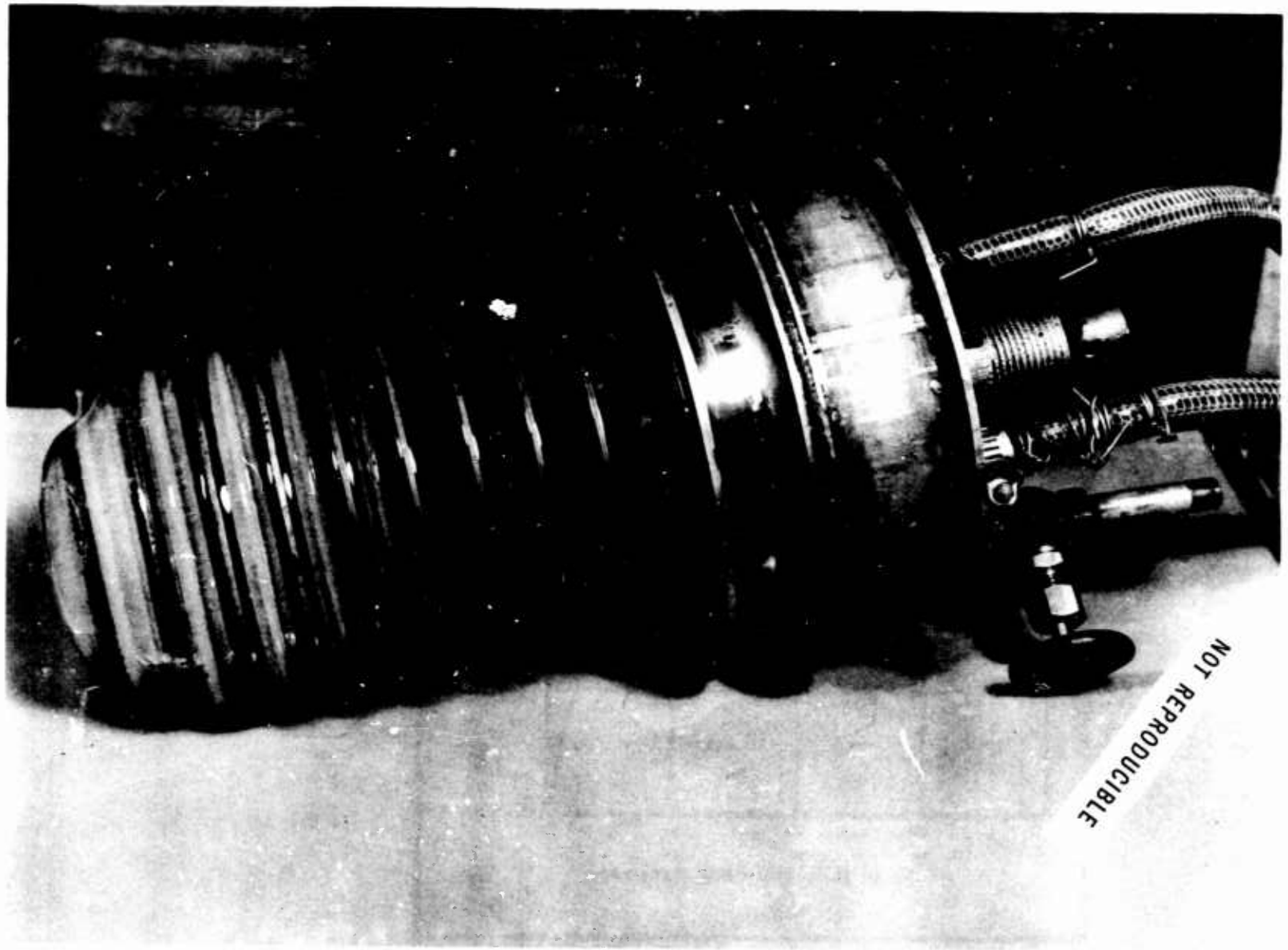

Figure 3. Picture of Ice Mantle in Heat Capacity Ice Calorimeter

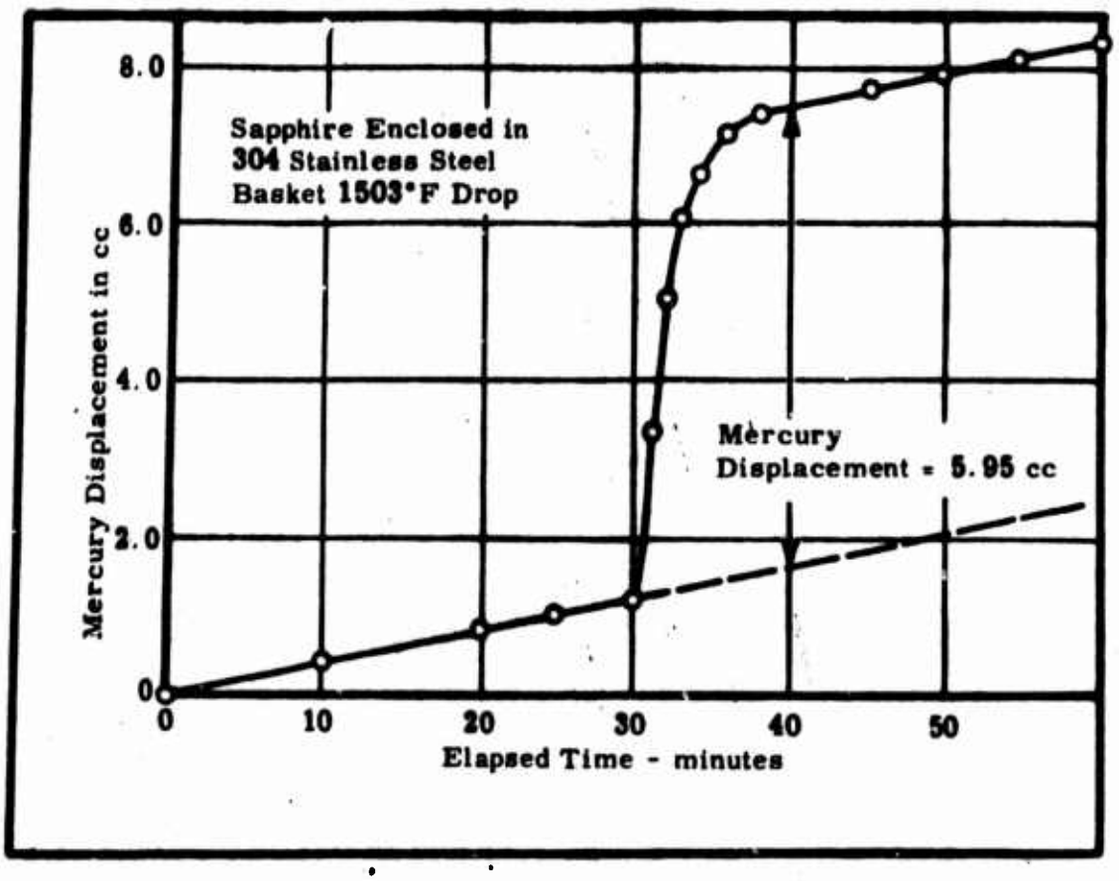

Figure 4. Mercury Displacement Due to Sapphire and 304 Stainless Steel Basket